



**HAL**  
open science

# Nuclear effects in high-energy proton-nucleus collisions: transverse momentum broadening of energetic parton systems and soft anomalous dimension matrices

Florian Cougoulic

► **To cite this version:**

Florian Cougoulic. Nuclear effects in high-energy proton-nucleus collisions: transverse momentum broadening of energetic parton systems and soft anomalous dimension matrices. High Energy Physics - Phenomenology [hep-ph]. Ecole nationale supérieure Mines-Télécom Atlantique, 2018. English. NNT : 2018IMTA0086 . tel-02011152

**HAL Id: tel-02011152**

**<https://theses.hal.science/tel-02011152>**

Submitted on 7 Feb 2019

**HAL** is a multi-disciplinary open access archive for the deposit and dissemination of scientific research documents, whether they are published or not. The documents may come from teaching and research institutions in France or abroad, or from public or private research centers.

L'archive ouverte pluridisciplinaire **HAL**, est destinée au dépôt et à la diffusion de documents scientifiques de niveau recherche, publiés ou non, émanant des établissements d'enseignement et de recherche français ou étrangers, des laboratoires publics ou privés.

# THÈSE DE DOCTORAT DE

L'ÉCOLE NATIONALE SUPÉRIEURE MINES-TELECOM ATLANTIQUE  
BRETAGNE PAYS DE LA LOIRE - IMT ATLANTIQUE  
COMUE UNIVERSITÉ BRETAGNE LOIRE

ÉCOLE DOCTORALE N°596  
*Matière, Molécules, Matériaux*  
Discipline: *Physique*  
Spécialité : *Constituants élémentaires et physique théorique*

Par

**Florian COUGOULIC**

**Nuclear effects in high-energy proton-nucleus collisions:  
transverse momentum broadening of energetic parton systems  
and soft anomalous dimension matrices.**

Thèse présentée et soutenue à Nantes, le 21 septembre 2018  
Unité de recherche : SUBATECH UMR 6457  
Thèse N° : 2018IMTA0086

## Rapporteurs avant soutenance :

François ARLEO    Chargé de Recherche HDR, LLR - École Polytechnique  
Yuri KOVCHegov    Professeur, The Ohio State University

## Composition du Jury :

Président :	François ARLEO	Chargé de Recherche HDR, LLR - École Polytechnique
Examineurs :	Yuri KOVCHegov	Professeur, The Ohio State University
Dir. de Thèse :	Ginès MARTINEZ	Directeur de Recherche, SUBATECH
Co-dir. de Thèse :	Stéphane PEIGNÉ	Chargé de Recherche, SUBATECH

## Invités :

Stéphane MUNIER    Chargé de Recherche HDR, CPhT - École Polytechnique  
Stefan KEPPELER    Akademischer Oberrat, Universität Tübingen



<b>1</b>	<b>Introduction</b>	<b>1</b>
1.1	Symmetry in Physics . . . . .	1
1.1.1	Symmetry in relativity and the Poincaré group . . . . .	1
1.1.2	Internal symmetries: global and local . . . . .	2
1.2	QCD at high energies . . . . .	3
1.2.1	Degrees of freedom at high energies . . . . .	3
1.2.2	A gentle confinement, local parton-hadron duality . . . . .	5
1.2.3	Factorization theorems . . . . .	6
1.3	Medium-induced effects . . . . .	7
1.3.1	Before hadron-hadron collisions . . . . .	7
1.3.2	My motivations to study medium-induced effects . . . . .	8
1.4	Plan of the manuscript . . . . .	12
<b>a</b>	<b>Prelude: Color considerations in hadron-hadron collisions</b>	<b>13</b>
a.1	Unobserved degree of freedom . . . . .	13
a.2	Radiation spectrum . . . . .	15
a.3	Soft anomalous dimension matrix . . . . .	17
<b>2</b>	<b>B.a. ba of QCD and Nuclear effects at high energies</b>	<b>21</b>
2.1	A bit of history . . . . .	21
2.2	QCD . . . . .	23
2.2.1	Lagrangian formulation . . . . .	23
2.2.2	A few words on renormalization . . . . .	25
2.3	Collinear factorization and nuclear parton distribution function . . . . .	27

2.3.1	Collinear factorization in DIS	27
2.3.2	Nuclear parton distribution function	30
2.3.3	Collinear factorization in other processes	30
2.4	Saturation	31
2.4.1	Physical picture of saturation	32
2.4.2	Color Glass Condensate	33
2.4.3	Relation to my study	33
<b>b</b>	<b>Interlude: birdtracks for beginners</b>	<b>35</b>
b.1	Feynman diagrams	35
b.2	Getting started with birdtracks	36
b.2.1	Quarks and the fundamental representation	36
b.2.2	Irreducible representation and Fierz identity	37
b.2.3	Interaction vertices and ajoint representation	38
b.3	Simple computations using birdtracks	39
b.3.1	Color conservation	39
b.3.2	Casimir operators	40
b.3.3	Simplification tips	41
<b>3</b>	<b>Nuclear broadening</b>	<b>45</b>
3.1	Color structure of the $p_t$ -broadening process	45
3.1.1	Scattering process and multipole picture	45
3.1.2	Color space at the cross section level	47
3.1.3	Vector space and basis choice.	48
3.2	Kinetic equation and evolution kernel	51
3.2.1	Scattering potential and single parton case	51
3.2.2	Validity and limitations	54
3.2.3	Asymptotic parton pair	55
3.2.4	Asymptotic parton system	59
3.3	A random walk in color space	64
3.3.1	Compact pair limit	64
3.3.2	Compact pair limit - color transitions	65
3.3.3	Compact pair limit - Same initial and final color states	68
<b>4</b>	<b>Nuclear broadening in dijet production</b>	<b>71</b>
4.1	Broadening distribution in realistic cases	71

4.1.1	Requiring a color transition between initial and final color states . . .	72
4.1.2	Particular case: same initial and final color states . . . . .	74
4.1.3	Result for broadening distribution . . . . .	77
4.2	Colorimetry . . . . .	77
4.2.1	Broadening distribution . . . . .	78
4.2.2	Daydreaming or actual applications? . . . . .	79
<b>5</b>	<b>A study on anomalous dimension matrices</b>	<b>81</b>
5.1	Soft anomalous dimension matrix . . . . .	81
5.1.1	Review of the Dokshitzer-Marchesini method . . . . .	83
5.2	Relation to the broadening evolution kernel and calculation of Q for stan- dard partons . . . . .	84
5.2.1	Evolution Kernel . . . . .	84
5.2.2	Calculation of Q for standard partons . . . . .	86
5.2.3	An unexpected symmetry . . . . .	89
5.3	Calculation of Q for generalized partons . . . . .	90
5.3.1	Generalized parton and soft anomalous dimension matrix . . . . .	90
5.3.2	Quark-quark, again! . . . . .	91
5.3.3	The story of two symmetric diquarks . . . . .	94
5.3.4	Algorithm . . . . .	97
5.3.5	Application scope and results . . . . .	99
5.4	Negative dimension Theorem and anomalous dimension matrices . . . . .	101
5.4.1	Setup . . . . .	101
5.4.2	Fully symmetric times fully symmetric case . . . . .	102
<b>A</b>	<b>Appendix: Complementary algebra</b>	<b>107</b>
A.1	Young Diagrams and their use in QCD . . . . .	107
A.1.1	Permutation Group and Young diagrams . . . . .	107
A.1.2	Pocket formula for Dimensions and Quadratic Casimir . . . . .	108
A.1.3	Derivation using Young operator . . . . .	109
A.2	Color triviality . . . . .	117
<b>B</b>	<b>Appendix: Technicalities</b>	<b>123</b>
B.1	Phase . . . . .	123
B.2	Hessian matrix . . . . .	125

*CONTENTS*

---

<b>C Résumé en Français</b>	<b>127</b>
<b>References</b>	<b>135</b>
<b>Acronyms</b>	<b>137</b>

*Last edit: November 26, 2018*

## 1.1 Symmetry in Physics

*“Symmetry is what we see at a glance; based on the fact that there is no reason for any difference,...”*

Blaise Pascal, Pensées.

The notion of symmetry is a familiar one. Cut an apple along its horizontal plane and you will see a central pentamerous pattern; but if you cut the same apple along its vertical plane and you will see a chiral symmetry. Visit Parthenon of Athens and imagine its original shape symmetric along a vertical axis. Appreciate *“Morning On The Seine”* or *“Pathway in Monet’s Garden at Giverny”* from Claude Money and their respective balancing along an horizontal or vertical symmetry axis. Symmetry appears in many fields: Biology, Architecture, Painting, and more...

Modern physics also includes this notion and it comes with different forms. On the one hand, the space-time geometry of a system may present some symmetries. Those are symmetries regarding the space-time coordinates or the arbitrary in the choice of referential. On the other hand, a system can have **degrees of freedom (dof)** different from space-time coordinates such as quantum numbers.

### 1.1.1 Symmetry in relativity and the Poincaré group

For any theatre play, a proper theatre stage is needed... This is also true for particle physics where the stage is the four dimensions space-time (Minkowski space-time)! As a *“relativistic”* **Quantum Field Theory (QFT)** the **Standard Model of Particule Physics (SMPP)** verify the two following principles of *special relativity*:

- All fundamental laws of physics have the same form in two distinct **inertial reference frames (ir-frames)**.
- There exists a constant  $c$  in every **ir-frame** associated to the speed of light in an empty space-time.



The first principle is related to three transformations, namely: translations in space or time, spatial rotations and boosts between two **ir-frames**. A system of coordinates in a given **ir-frame** will transform into another system of coordinates, and physical laws are the same in different **ir-frames**.

Those three transformations form a group<sup>1</sup> called the ‘‘Poincaré group’’ and any type of field (bispinor, vector,...) in **QFT** has definite transformation laws under this group. A consequence is the key element of **QFT**, ‘‘the Lagrangian density’’, only contains scalars with respect to the Poincaré group transformations as a memento of the underlying symmetries of space-time.

## 1.1.2 Internal symmetries: global and local

Having a proper theatre stage, one can look at how actors will interact during the play... One can consider transformations acting on a quantum field that does not affect space-time coordinates but other **dof**.

### Global symmetry

As an illustration, let us consider a complex spin-zero field that depends on space-time coordinates and an overall phase:  $\psi(x, \theta) = e^{i\theta}\phi(x)$ . Also, let us introduce a transformation  $T$  that rotates the phase  $\theta$  into  $\theta + \delta$ . A Lagrangian density  $\mathcal{L}$  usually involves fields and their derivatives with respect to space-time.  $\mathcal{L}$  (defined as a Poincaré scalar) being symmetric under the group of transformation  $T$ , means  $\mathcal{L}$  being a scalar with respect to all transformations  $T$  of this group. One can easily see that terms such as  $\psi^*\psi$  or  $(\partial\psi^*) \cdot (\partial\psi)$  are invariant as

$$T[\delta] : \psi \rightarrow \psi' = e^{i\delta}\psi \quad T[\delta] : \psi^* \rightarrow \psi'^* = e^{-i\delta}\psi^*$$

The same holds for any term of  $\mathcal{L}$  involving derivatives of the field as long as  $\delta$  is independent of space-time. In this case, the Lagrangian is said to have a global symmetry under the group of transformations  $T$ .

### Local symmetry

In contrast with global transformations discussed in the previous paragraph, one can consider local transformations acting on a field differently at different points in space-time. If the Lagrangian density is a scalar (i.e., is left invariant) under such transformations, the Lagrangian has a *local* symmetry or *gauge* symmetry. The impact of gauge symmetry is drastic as it introduces gauge fields that will mediate interactions between particles of the free field theory. The form of the interaction is dictated by the symmetry group and this concept is at the core of the **SMPP**.

With the same notations, one can consider that the parameter of the transformation  $T$  becomes locally space-time dependent:  $\delta$  becomes  $\delta(x)$ . Applying such a transformation to the field  $\psi(x, \theta) = e^{i\theta}\phi(x)$ , any term in the Lagrangian density that involves a derivative of the field will transform according to:

$$T[\delta(x)] : \partial_\mu\psi \rightarrow (\partial_\mu\psi)' = e^{i\delta}(\partial_\mu + \partial_\mu\delta)\psi$$

---

<sup>1</sup>With respect to the composition of transformation.

At first glance, the additional contribution  $[\partial_\mu \delta(x)] e^{i\delta(x)}\psi$ , will break the symmetry of the free Lagrangian density built in the previous paragraph. However the symmetry can be recovered by introducing of a gauge field  $A_\mu(x)$  that transforms as  $A_\mu(x) \rightarrow A_\mu(x)' = A_\mu(x) - \partial_\mu \delta$ , and by substituting the usual derivative  $\partial_\mu$  by the covariant derivative  $D_\mu = \partial_\mu + iA_\mu$ . Using this procedure, a Lagrangian density being invariant under local transformations is recovered.

A miracle has happened: starting from a non-interacting field theory with a given *global internal symmetry* in the first paragraph, and asking for *gauge symmetry* instead leads to a theory where the gauge field mediate interactions.

In this sense, it is natural that the study of particle interactions in modern physics and in particular within the SMPP is related to the study of symmetry.

## 1.2 QCD at high energies

The strong interaction part of the SMPP is a QFT called “Quantum ChromoDynamics (QCD)”. To introduce this theory, I will follow the same steps as in the previous section.

Matter constituents of the theory are quark fields. As fields of spin 1/2, they transform under Poincaré group transformations as bispinors and are solutions to the Dirac equation. Those fields carry an internal dof called the color quantum number that takes integers value from 1 to  $N_c$  (in practice  $N_c = 3$ ). The gauge symmetry associated to this dof is with respect to the Lie group  $SU(N_c)$ . The associated gauge field is the gluon field. Quark fields (resp gluon-field) transform in the fundamental (resp adjoint ) representation of  $SU(N_c)$ .

In short from [1], “Take free quarks, supply them with colour degrees of freedom, demand invariance with respect to the “repainting” quark fields arbitrarily in each point in space-time — and you get the unique QCD Lagrangian describing interacting quarks and gluon.”

QCD is an awkward theory which it is still not fully understood but at the same time admitted as the theory of the strong interaction. On the one hand, we lack an understanding of confinement, and on the other hand the predictive power of the theory has been verified by experiments on numerous occasions. This two folded situation transposes directly on the way nuclear effects are approached.

### 1.2.1 Degrees of freedom at high energies

Before discussing QCD, I let us remember a result of Quantum ElectroDynamics (QED). If one performs the analysis of Feynman diagrams involving loops in the photon propagator, one has to integrate over high momentum modes of the electron field and produce ultraviolet divergences. To cure the theory constructed from the *bare* Lagrangian, renormalization is necessary (see [2, 3]). A major consequence of this renormalization is that the initial *bare coupling* is replaced by an effective *running coupling* related to the physical coupling  $\alpha$  measured in experiments. In the renormalization procedure the shape of the coupling  $\alpha$  as a function of the momentum scale  $\mu$  is given by perturbative calculations. However, the theory does not give the absolute normalization of the coupling, and it

should be measured from experiments. In the following sketch the dashed line indicate the measured coupling at low momentum scale  $\mu \rightarrow 0$ , this is essentially non perturbative. The increase of the curve to higher momenta is dictated by renormalization, through [perturbation Theory \(PT\)](#). The large momentum where the coupling diverge is called the Landau pole  $\Lambda_{QED}$ .

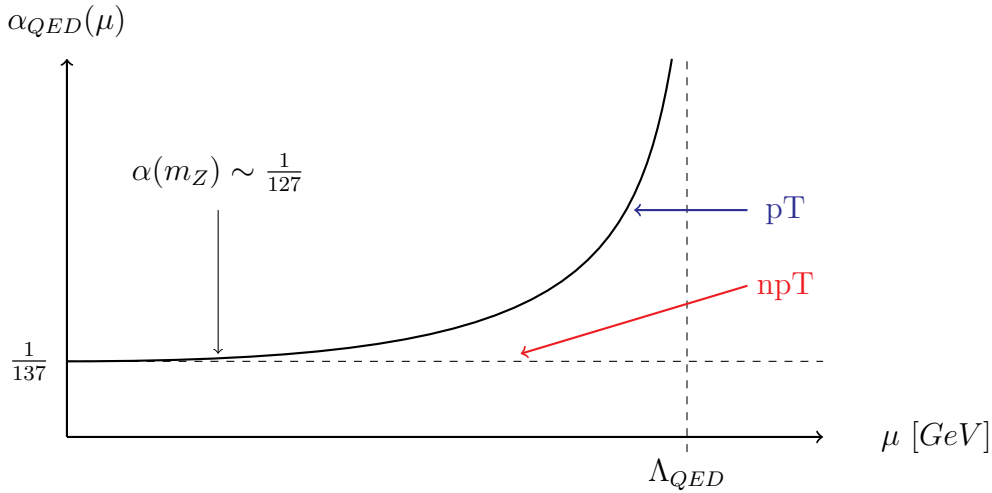


**Figure 1.1:** A sketch of the *QED* running coupling.

In contrast to the [QED](#) running coupling (Fig. 1.1), the [QCD](#) running coupling  $\alpha_s$  behaves differently (see Fig. 1.2). On the one hand, as the momentum scale tends to infinity, the coupling tends to zero. This property of [QCD](#) is called *asymptotic freedom*. On the other hand, the perturbative prediction for the coupling diverges at the Landau pole  $\Lambda_{QCD}$ . This apparent illness of the perturbative calculation means that one cannot use naively perturbation theory in this region. [QCD](#) is separated into [perturbative QCD](#) (pQCD) and [non-perturbative QCD](#) (npQCD) depending on strength of the coupling:  $\alpha_s \ll \mathcal{O}(1)$  or  $\alpha_s \sim \mathcal{O}(1)$ .

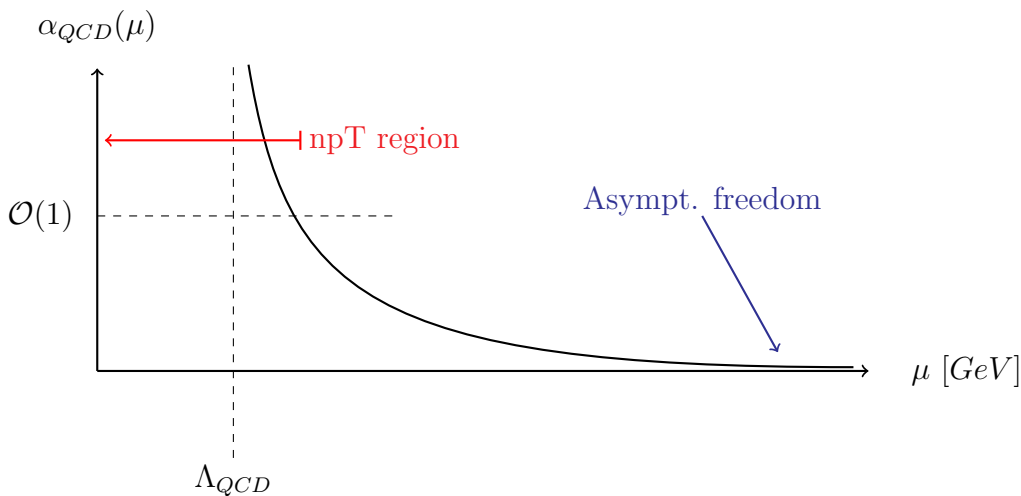


**Figure 1.2:** A sketch of the *QCD* running coupling

Nowadays, pQCD is the only analytic method at disposal to address the strong interaction. To fully understand QCD, one can

1. wait for our mathematician colleagues to formulate tools in view of handling non-perturbative and perturbative parts of QCD at the same time;
2. ingeniously use pQCD and structure observables into measurable quantities and calculable quantities; eventually arrive at a description of QCD in terms of pQCD following Gribov's program [4].

**Problem:** At high energy, one can use asymptotic freedom and pQCD to describe parton dynamics, however partons are not observed by experiments, only hadrons are. It is not obvious that such approach is relevant. The problem is the following: “How do one computes high energy cross section?” To this end, the strategie in QCD depends on the considered observable: one can either use local parton-hadron duality or factorization.

### 1.2.2 A gentle confinement, local parton-hadron duality

*“Quarks/gluons are the Truth but hadrons are the Reality.”*

Yu. L. Dokshitzer [5].

The first strategy is to look for observables that are less sensitive to our ignorance about confinement. Such observables are called **Collinear and Infrared Safe (CIS)** and this status is granted if they can be calculated from *partons* without any collinear or infrared divergence. In such situations, one expects the prediction from pQCD to be comparable to the experimental value *in the hadronic world*. Some exemples of CIS observables are: the inclusive production rate of jet in  $e^+e^-$  collisons, the thrus, or the C-parameter. The latter two are commonly called jet-shape observables<sup>2</sup>.

The main assumption in this approach is the notion of “local parton-hadron duality”; which relies on the following: Confinement is considered to be a “gentle process”, which does not reshuffle particle momenta when partons become hadrons. This is a picture where the momenta of final *partons* remain roughly identical after *hadronization*, to the momenta of detected hadrons.

The following procedure is used:

- Calculate some partonic cross section using pQCD and regularize collinear and/or infrared singularities if needed.
- Select a process such that the dependence of the regulator vanishes.
- Trust the “local parton-hadron duality”.
- Compare to data (and do it again if there is some unexpected behaviour).

---

<sup>2</sup> Particles momenta are noted  $\vec{p}_i$ . For a unit vector  $\vec{n}$ , the thrust is defined as  $T = \max_{\vec{n}} \left( \frac{\sum_i |\vec{p}_i \cdot \vec{n}|}{\sum_i |\vec{p}_i|} \right)$ . An angle between a particle  $i$  and a particle  $j$  is noted  $\theta_{ij}$ . The C-parameter is defined as  $C = \frac{3}{2} \frac{\sum_{i,j} |\vec{p}_i| |\vec{p}_j| \sin^2(\theta_{ij})}{(\sum_i |\vec{p}_i|)^2}$

This strategy involves several theoretical guesses and a comparison with data to be fruitful. At some points in this loop, there is a need for

1. formalisms (as model-independent as possible) to establish principles/law regarding a given physical mechanisms (that we are interested in) from the first principles of QCD;
2. and, phenomenological approaches to bring those theoretical principles and experimental observations on the same ground.

### 1.2.3 Factorization theorems

In general a cross section at high energy is a combination of long-distance and short-distance effects. The systematic approach of *factorization* is to separate the long-distance behaviour from the short-distance behaviour in the cross-section. Let us look at the intuitive picture behind the so-called factorization theorems [6].

The second strategy emphasizes on the *high energy* limit: “How does one compute high energy cross sections?”. As the energy of the collision increases, the target and probe in the center-of-mass frame behave as:

- Due to the Lorentz boost, the target and projectile (viewed in the center-of-mass frame) will be Lorentz contracted and the interaction time  $t_{int}$  between nucleons will be Lorentz dilated. The lifetime of virtual fluctuations is also Lorentz dilated.
- The interaction-time between probe and target  $t_{coll}$  decreases.

For large enough energies,  $t_{coll}$  becomes negligible compared to  $t_{int}$ . In this high energy limit, a hadron behaves as a single virtual state without any interaction between constituents. The hadron is “frozen” in a given Fock state, and since each parton does not interact with others, they can be thought of as carrying a fraction  $x$  of the hadron’s momentum.

Some additional considerations have to be made such as:

- Initial and final state interactions are expected to happen within time scales too long to interfere with the hard process time scale. As a result, we expect factorization and the universality of each [parton distribution function \(PDF\)](#).
- The nuclear density in the target is assumed to be not too high: there is only linear effects.
- For large momentum transfer, the probe will only interact once with the target.

A high energy scattering can be considered as classical and incoherent, and the hadronic cross section computed as a combination of probabilities rather than amplitudes. The partonic cross section can be calculated in pQCD in this kinematic region. Universal non-perturbative parts such as [PDFs](#) encode the ignorance of the confinement in hadrons. Thanks to this universality, one can extract [PDF](#) in a given process (e.g. [Deep Inelastic Scattering \(DIS\)](#)), and use them to predict other processes.

Factorization theorems are established (up to power corrections) for processes such as:

- [Deep Inelastic Scattering \(DIS\)](#):  $\text{lepton} + A \rightarrow \text{lepton}' + X$ .
- Inclusive annihilation:  $\gamma^* \rightarrow A + X$ .
- Drell-Yan processes:  $A + B \rightarrow \text{ElectroWeak} + X$ .
- Jet production:  $A + B \rightarrow \text{Jet} + X$ .
- Heavy quark production:  $A + B \rightarrow \text{heavy quark} + X$ .

Here  $A$  and  $B$  are incoming of tagged hadrons and  $X$  denotes all the remaining hadrons produced in the collision. It is interesting to note that all those processes have a “+ $X$ ” contribution. The observable needs to be inclusive enough to bypass our ignorance of the confinement. The main argument is: one does not observe parton states hence the probability for all remaining partons to become hadrons is unitary.

I will come back to a more formal formulation of the collinear factorization in Chapter 2 when addressing nuclear effects.

## 1.3 Medium-induced effects

### 1.3.1 Before hadron-hadron collisions

Probing the hadronic structure at small distance, can be done using three type of reactions involving QCD vacuum (i.e. [QED](#) currents) and/or hadrons:

1. vacuum  $\rightarrow$  hadrons. Those are  $e^+e^-$  annihilation into hadrons processes in collisions at the [Large Electron-Positron Collider \(LEP\)](#) or at the [Stanford Linear Accelerator Center \(SLAC\)](#).
2. vacuum + hadron  $\rightarrow$  hadrons. Those are [DIS](#) processes at the [Hadron-Electron Ring Accelerator \(HERA\)](#).
3. hadron + hadron  $\rightarrow$  hadrons (called hadron-hadron production) at the [Relativistic Heavy Ion Collider \(RHIC\)](#) or at the [Large Hadron Collider \(LHC\)](#)

Historically, reaction of type 1 and 2 served to visualize asymptotic freedom, verify the spin and color of quarks, verify the Bjorken scaling violations,... They provide a relatively clean environment to make precision tests of [QCD](#).

[HERA](#) and [DIS](#) studies served to probe the proton structure, the quark and gluon content over several orders of magnitude in the transfert momentum  $Q^2$ . Jet-shape analysis told us about the *soft* confinement. [pQCD](#) works from large scales down to  $Q \sim 2 \text{ GeV}$  where it is expected to work, it also works down to  $\sim 1 \text{ GeV}$  where it should not need to (as in the  $\tau$ -decay measurement, confinement effects are strongly suppressed), and finally it sometimes works down to  $0 \text{ GeV}$ : local parton-hadron duality [1].

In view of a better understanding of non perturbative one must look at more than just DIS and annihilation processes. Hadron-hadron collisions can bring a wealth of information.

### 1.3.2 My motivations to study medium-induced effects

Let us first define what are medium-induced effects, then look at some intriguing puzzle [7] to stress the theoretical interest of medium-induced effects.

#### Medium-induced effects

There is one important keyword for medium-induced effects, namely *difference*. Consider any partonic process in the presence of a medium characterized by the length  $L_0$  and an observable  $\mathcal{V}_0$  associated to this process. Denote by  $\mathcal{V}$  the same observable in the case of a different medium characterized by the length  $L$ , by definition the medium-induced effects  $\Delta\mathcal{V}$  is

$$\Delta\mathcal{V} = \mathcal{V} - \mathcal{V}_0 \tag{1.1}$$

How does one observe a non-vanishing medium-induced effect? If an observable  $\mathcal{V}$  scales with respect to the size of the medium  $\mathcal{V} \propto L^\delta$  with  $\delta \in \mathbb{R}$ , it yields a non vanishing medium-induced effect  $\Delta\mathcal{V} \neq 0$ , simply by this scaling property. For example, one can consider a quark passing through a nuclear medium. The final state average squared momentum  $\langle p^2 \rangle$  scales as the path length of the quark in the medium. This results in a medium-induced effect  $\langle \Delta p^2 \rangle$  to be proportional to the length difference of the two medium  $L - L_0$ . The physics is the same in both cases, namely elastic scattering, and one simply add incoherently elementary elastic scattering from  $L_0$  to  $L$ .

It is interesting to remark that due to the definition of medium-induced effects,  $\Delta\mathcal{V}$  can be finite even if  $\mathcal{V}$  and  $\mathcal{V}_0$  aren't. The same divergences, appearing in both cases, can compensate in order to give a finite result for the medium-induced effect.

#### Soft effects in a nucleus [7]

A legitimate question is: “Can one use perturbation theory PT to study *soft effects in a nucleus* ?”

Usually, a “soft” momenta region indicates an infra-red region which is not under PT jurisdiction. However, nuclear effects such as medium induced gluon radiation, or transverse momentum broadening often depend on the soft scale multiplied by the length  $L \propto A^{1/3}$  of the nuclear medium.

As one moves to larger nuclei, there are two effects:

- The complexity (from the many-body problem point of view) of the collision augments.
- Since the relevant “soft scale” in a nucleus  $Q_s^2 \propto A^{1/3}$  increases with  $A$ , one expects pQCD to be valid at large enough  $A$ .

Thus, hadronic collisions involving nuclei are a useful playground to improve our understanding of QCD.

### Collisions or participants: scaling puzzle.

*“It is in this harmlessly looking “simply rescaled” that the devil resides”*

Yu. L. Dokshitzer [7].

To characterize medium effects, one needs to consider the normalization between observables for the large nucleus  $\mathcal{V}_A$  and the proton reference  $\mathcal{V}_p$ . In other words, what is the “simple rescaling” expected when replacing  $\mathcal{V}_p$  by  $\mathcal{V}_A$  ?

Two possible answers are communly proposed:

- $N_{coll}$ -scaling, where  $N_{coll}$  is the number of binary nucleon-nucleon collisions.
- $N_{part}$ -scaling, with  $N_{part}$  the number of participants in the collision.

The usual argument for this choice is the commun belief that “hard interactions scale as  $N_{coll}$ ” and “soft interactions scale as  $N_{part}$ ”. But this commun belief has no firm basis, and can actually prove incorrect in some situation, as illustred by the following discussion [7].

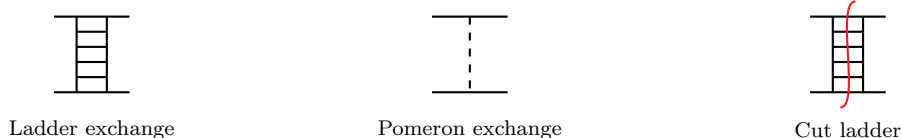
In QCD, the inclusive spectrum of medium-induced gluon radiation off an energetic parton introduces the number  $N_{coh}$  of scattering centers that act coherently during the formation time of the gluon. It scales as  $N_{coh} \sim k_{\perp}^2/\mu^2$  where  $k_{\perp}$  is the gluon transverse momentum of the gluon and  $\mu$  is the typical transverse momentum transfer in a scattering. This spectrum is represented in Fig. 1.3. This figure exhibits the three different regimes of induced radiation, namely, for increasing  $\omega$ : the fully incoherent Bethe-Heitler regime for  $\omega \lesssim \lambda\mu^2$ , the Landau-Pomeranchuk-Migdal (LPM) coherent regim for  $\mu^2\lambda < \omega < \omega_c$ , and the fully coherent regime for  $\omega > \omega_c$ .

Here is the puzzle: the high-energy hard part of the spectrum (where all centres in the target act coherently) scales as  $N_{part} = 1$ , whereas the low-energy (soft) part of the spectrum (the Bethe-Heitler regime of independent emissions from each scattering center) scales as  $N_{coll} = L/\lambda$ .

Thus for the present observable, “hard gluon radiation  $\rightarrow N_{part}$ ” and “soft gluon radiation  $\rightarrow N_{coll}$ ”, in contradiction with the commun belief. This is not the first time that a quantum theory result differs from the expected “common wisdom”.

### Multiple scattering: color radiator puzzle [7]

In order to illustrate this puzzle, let us recall that a pomeron [9, 10] can be viewed as a ladder-diagram describing small angle scattering of two hadrons.





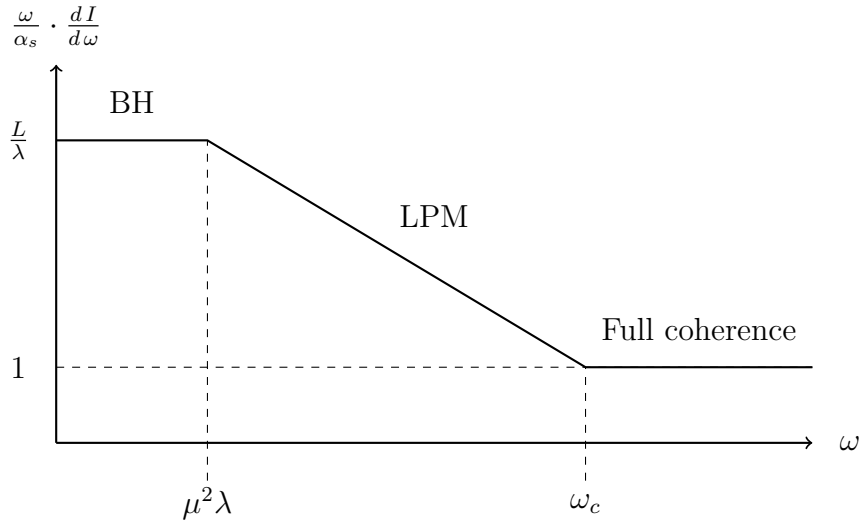


**Figure 1.3:** A sketch of the inclusive spectrum of medium-induced gluon radiation as a function of the radiated gluon energy  $\omega$ , with  $L$  the medium length,  $\lambda$  the projectile mean free path,  $\mu$  the typical transverse momentum transfer in a scattering, and  $\omega_c = \mu^2 L^2 / \lambda$  the critical value for full coherence. (See [8] and references therein).

A cut-Pomeron can be identified as a ladder diagrams cut along the ladder. Those cut diagrams produce off-shell partons that will later hadronize. The dominant part of the total hadron-hadron scattering cross section comes from a region of phase space with a strong ordering in  $x_i$  (the fraction of energy carried by the  $i^{\text{th}}$  particle)

$$x_1 \gg x_2 \gg \dots \gg x_n.$$

The cut-Pomeron produces a uniform distribution of hadrons: the so-called Feynman plateau from the Feynman gas approach to multiparticle production.

*A universal Pomeron and the QCD picture:*

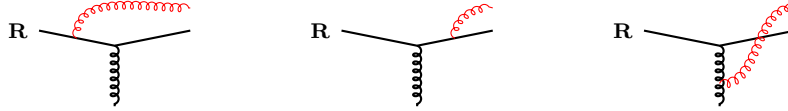
Consider either pion or proton inelastic scattering. Both scatterings will produce the same hadronic chain, with respectively a leading meson (quark chain) or a leading baryon (diquark chain).



This image is in accord with the local parton-hadron duality where secondary partons come from the restoration of the color field (gluon radiations). The gluon radiation intensity of the scattering of a parton on a scattering center is given by the color charge exchanged in the  $t$ -channel. In this sense the Pomeron picture is the one of an *universal object* that will produces hadrons after being cut.

Remember that for any non singlet parton of Irreducible representation (irrep)  $\mathbf{R}$  of  $SU(N_c)$ , the adjoint irrep  $\mathbf{8}$  is contained in  $\mathbf{R} \otimes \bar{\mathbf{R}}$  decomposition. The gluon radiation intensity of the scattering of a parton on a scattering center is given by the color charge

exchanged in the  $t$ -channel. The QCD picture (analogue to the universal pomeron) relies the following fact: the  $t$ -channel one-gluon single-scattering color structure *does not depend on the nature (irrep) of the projectile*. Radiations from either the initial parton-line, the final parton-line or the gluon-line are related by the structure constant of  $SU(N_c)$ :



The first two diagrams contain the same Lorentz structure up to a minus factor. Hence, one can use the structure constant definition to relate the first two color structure to the third diagrams color structures (independently of the irrep  $\mathbf{R}$ ).

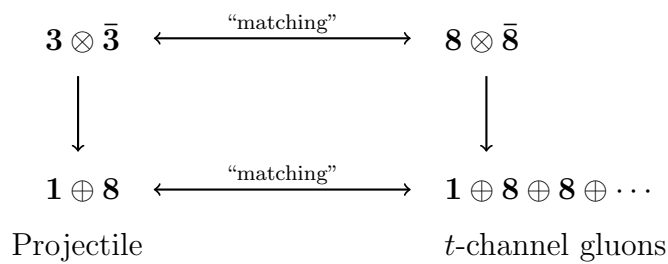
*The multiple scattering case:*

In the Pomeron picture, one can consider a contribution from two cut-Pomerons where the number of produced hadron double. In QCD, a two gluon exchange in the  $t$ -channel can be in multiple color state and the averaged color charge is given by

$$\sum_{\alpha} C_{\alpha} K_{\alpha} / K_A^2 = \frac{(0 \times 1 + 3 \times (8 + 8) + 6 \times (10 + 10) + 8 \times 27)}{64} = 6 = 2 \times 3$$

where  $\alpha$  run over the irrep of  $\mathbf{Adj} \otimes \mathbf{Adj}$  decomposition. This is twice the color factor obtained from the one gluon exchange in the  $t$ -channel, both results from QCD and cut-Pomeron, agree at first glance...

However, the nature of the projectile in the QCD picture was not taken into consideration! For an incoming parton in the fundamental representation of  $SU(N_c)$ , possible states in the  $t$ -channel are singlet and octet only. This cannot produce the doubling of the radiation intensity as the average color charge in the  $t$ -channel will always be less than 3. The following scheme must be realised in the  $t$ -channel:



Irreps in the left side decomposition (for the  $t$ -channel of the projectile) must “match” with available irreps in the right side decomposition (for the two mediating gluons). The average color charge of the left side is  $\sim 3$  as opposed to  $\sim 2 \times 3$  on the right side. This implies that a parton in the fundamental irrep cannot produce twice the number of hadron with two cut-Pomeron versus the one cut-Pomeron.

The situation becomes even more puzzling when one consider, instead of a single parton, systems such as “three-quark-baryon” (in a color singlet). This system can only be “repainted” in  $\mathbf{1} \oplus \mathbf{8} \oplus \mathbf{8} \oplus \mathbf{10}$  and the average color charge is  $\sim 1.5 \times 3$  with  $\sim 1.5$  the number of cut-Pomeron(s). What is one and a half gluon(s) in the  $t$ -channel?

An interesting lesson is: for  $n$  gluons to break the coherence of a given system (and having up to  $n$  times enhanced hadron density -  $n$  cut-Pomeron), the system should have enough “color-richness”. In the vocabulary of the previous puzzle for  $n$  going from  $N_{part}$  (coherent limit) to  $N_{coll}$  (incoherent limit), gluons must be able to probe the system at scales such that the color system has enough color capacity.

**Warning:** I will not find any solution to those puzzles in this manuscript. Those puzzles serve as a motivation for studying nuclear effects and color dynamics.

## 1.4 Plan of the manuscript

The following of the manuscript starts with the prelude [a](#), which is aimed to give a taste of the color aspects which will be relevant to the main part of my thesis.

The following chapter [2](#) is a short QCD history. I also sketch the idea of renormalization because of its importance in the theory. Then, I give a brief introduction to the two main approaches used in nuclear collisions to study nuclear effects at high energies: collinear factorization and the saturation approach. This chapter may be skipped by QCD practitioners.

The interlude [b](#) follows. This is an introduction to birdtracks: an amusing and efficient way to perform the algebra that one encounters in pQCD calculations. I will present some definitions and tricks. The interlude can serve to get used to birdtracks. I will heavily use birdtracks in the following chapters, hence the interlude can be useful before reading chapters [3](#), [4](#) and [5](#).

Chapter [3](#) is a study of a fast partonic-system passing through a cold nuclear medium. The main point of this chapter is the derivation of the final transverse momentum distribution of an “academic” asymptotic parton system. In particular, the impact of the medium on the distribution, and the associated color structure are emphasized.

The chapter [4](#) is the transposition of the situation considered in chapter [3](#) to realistic situations. An intuitive picture can be drawn in the compact pair limit. In this limit, the link between color states of the parton system and the evolution in the medium becomes transparent.

Finally, the chapter [5](#) gives an additional “colored note” on a key operator *the soft anomalous dimension matrix*  $\mathcal{Q}$ , used in Chapters [3](#) and [4](#). Usual QCD cases are considered, and  $\mathcal{Q}$  is derived in an economic way without having to use any change of basis. An unexpected symmetry relating inner dof (gauge group parameter) with external dof (kinematic factor) in  $\mathcal{Q}$  matrices is explored by introducing “*generalized parton*”.

## CHAPTER a

# PRELUDE: COLOR CONSIDERATIONS IN HADRON-HADRON COLLISIONS

There will be two *ludos* spread along the manuscript that are dedicated to color aspects of QCD. This *prelude* serves as a basis to argue that *irrep* can be used to decompose partonic cross sections and the utility of such decomposition for some observables. Then the *interlude* will introduce some of the color pictorial algebra tools called “birdtracks”. Finally the last chapter is a study of soft anomalous dimension matrices involving generalized partons using birdtracks.

## a.1 Unobserved degree of freedom

The QCD lagrangian relies on the gauge symmetry  $SU(N_c)$ . Confinement effects are ignored in the present discussion, we focus on time scales smaller than the hadronization scale. We thus live in the world of quarks and gluons and which are the “elementary” quantum states.

One can choose to rotate the quark and gluon fields arbitrarily at every point  $x^\mu$  without impacting the lagrangian and the equation of motion. One can easily be overwhelmed about the tedious book-keeping of color indices of each partons of a partonic wave function. Indeed, as in QED where the formal analogue would be the overall phase of the wave function, its actual value has no impact on a cross section, only phase differences matters (recall the Berry phase in quantum mechanics [11]).

This book-keeping is more subtle in QCD than in QED because the “rotation angle” becomes a matrix but the philosophy remains the same. One just needs a procedure to keep track of the only relevant piece of information: “a QCD phase subtraction”. The color index of a wave function is not observable. A quark may emit a very soft gluon and rotates its color index by growing its “color coat”. A finite<sup>1</sup>, observable quantity involves that the initial state and in the final state are dressed states.

Usually, the quantum numbers of the initial (final) particles which are not directly

---

<sup>1</sup>A true observable should not suffer from infra-red divergences present in the theory.

observed are averaged (summed over) at the cross section level. In QED and QCD, this is done for spin (more precisely, helicity) when non-polarized cross section are considered. In QCD, this is also done for color indices of initial and final partons, since the latter cannot be observed (a color index is not gauge invariant and thus not observable).

See Fig.a.1: focusing on final gluon indices  $j_1$  and  $j_2$ , summing over them seems required by the above argument. However, some information is lost by doing so. Indeed,  $j_1$  and  $j_2$  are gauge dependant, but the irrep of the final gluon pair is gauge invariant.

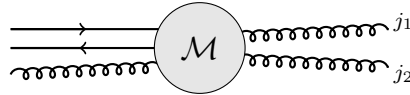


**Figure a.1:** A generic Feynman amplitude  $\mathcal{M}$  with final color indices  $j_1$  and  $j_2$ .

To make use of the color invariance of the theory in the example Fig.a.1, one has to introduce the decomposition into irreps of the final gluon pair:

$$\mathbf{8} \otimes \mathbf{8} = \mathbf{1} \oplus (\mathbf{8} \oplus \mathbf{8}) \oplus (\mathbf{10} \oplus \overline{\mathbf{10}}) \oplus \mathbf{27} \oplus \mathbf{0}$$

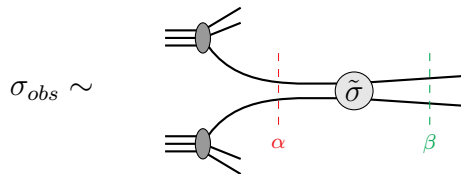
the decomposition is written for  $SU(N_c)$ , and the name of each representation is motivated by its dimension for  $N_c = 3$  (irrep  $\mathbf{0}$  appears for  $N_c \geq 4$ ). A projection of the gluon pair wave function into one of these irreps remains in the same irrep when the gauge field is arbitrarily rotated. Irreps are invariants of the gauge group  $SU(N_c)$ . In this regard, to characterize the color part of a partonic wave function, it is preferable to indicate the irrep of the system rather than book-keeping color indices.

A direct consequence of such a decomposition is that now one can use the orthogonality of irreps. Decompose  $\mathcal{M}$  in this basis, the cross section is an incoherent sum of cross sections for a given irrep in the final state. Additionally, all irreps are uniquely defined by a list of eigenvalues corresponding to the number of independent Casimir operators of the theory. For  $SU(N_c)$  there are  $N_c - 1$  independent Casimir operators (and thus only two for  $N_c = 3$ ).

This is not the only advantage of such a decomposition, and I will illustrate below that this decomposition is quite natural for some observables.

### Digression.

Consider a process with a factorized cross section  $\sigma_{obs}$ . This cross section will be given by a convolution between a partonic cross section  $\tilde{\sigma}$  and PDFs.



There is no doubt that using a decomposition into irrep for the partonic cross section  $\tilde{\sigma}$  only brings additional information on the partonic content as opposed to the usual color

averaged one. At this level, this is a legitimate approach because *irreps* separate  $\tilde{\sigma}$  into incoherent and gauge invariant pieces.

However, one can require that the final *partonic* system (before hadronization) is in an *irrep*  $\beta$  and being inclusive over the initial state  $\alpha$ . Does the factorization theorem for  $\sigma_{obs}$  hold after a projection into  $\beta$  color state?

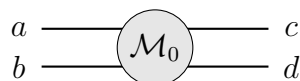
This situation can become even more blurry! Require the initial partonic state to be stated (in this sketch, by the red dashed line  $\alpha$ ) in addition to the final state. In order to say that a pair is a given *irrep*, one does not look at each individual constituents of the pair but instead at an overall system. This requirement to look at such initial pair as a system seems to contradict the fact that the two PDF involved here are independant and universal quantities.

I illustrated this argument using the factorization approach to high energy scattering, but it easily transpose to other models. As we still do not understand a part of the puzzle in QCD: confinement, any senario could happen in principle. From a group theoretical focused approach, the introduction of *irreps* brings us additional knowledge on the color structure associated to physical mechanisms. This digression does not apply to every observable, and one can always identify observable quantities free from such consideration.

## a.2 Radiation spectrum

My first example of how the non-abelian nature of QCD impacts the dynamics, is part of the calculation of the soft radiation intensity of energetic partons. I will be interested in the *radiation spectrum* and in particular on how it depends on *irreps* of the system involved. This will be the first example of how a physical process (the radiation of a soft gluon here) can rotate the color state of a system. This section serves as an introduction to the richer case presented in the following section (the two cases being closely related), where I will focus mainly on the origin of those color transitions.

At leading order in the radiated gluon energy, the radiation spectrum is of classical nature. The radiation is coming from color charged classical fields. To avoid falling into a color trivial case<sup>2</sup>, one can consider a process involving at least four partons. I choose the process  $ab \rightarrow cd$  for the rest of this section.



The *irrep* of parton  $i$  is denoted  $R_i$ , its momentum  $p_i$  and *color conservation* tells us that the initial  $ab$  state and final  $cd$  state are in the same *irreps*: labelled  $\alpha$ . Of course,  $\alpha$  verifies  $\alpha \subset R_a \otimes R_b$  and  $\alpha \subset R_c \otimes R_d$ . The inclusive (over all color states  $\alpha$ ) cross section

<sup>2</sup> It is always possible, with three partons (or less), to write down a product of two color generators as a sum of individual quadratic Casimir operators  $C_2[R]$ .

$$T_1^a + T_2^a + T_3^a = 0 \quad \longrightarrow \quad 2T_1^a T_2^a = T_3^2 - T_1^2 - T_2^2 \\ = C_2[3] - C_2[1] - C_2[2]$$

For a more detailed discussion on color triviality, see the appentix A.

is noted  $\sigma_0$  and it can be decomposed into the following sum

$$\sigma_0 = \sum_{\alpha} \sigma_0^{\alpha \rightarrow \alpha}.$$

The amplitude with an additional radiated soft gluon of momentum  $k$ , noted  $\mathcal{M}_1$ , is related to the elastic one  $\mathcal{M}_0$  as follow. In the soft gluon approximation, it is given by

$$\mathcal{M}_1 = \mathcal{M}_0 \cdot j + \text{“power suppressed terms”}$$

where “power suppressed terms” are suppressed as the energy of the radiated gluon over energy of the primary parton. This is a QCD realisation of the soft bremsstrahlung theorem of Low, Burnett and Kroll [12, 13]. The radiation current  $j$  is the sum over partons of the usual QED bremsstrahlung factor  $\mathcal{R}(p_i, k)$  times the associated color generator  $T_i^a$

$$j \equiv \sum_i \mathcal{R}(p_i, k) T_i^a.$$

Since the current  $j$  is factorized from the elastic amplitude, the square for all initial state irreps  $\alpha$  and final state irreps  $\beta \subset R_c \otimes R_d$  reads

$$\sigma_1^{\alpha \rightarrow \beta} = \begin{cases} \sigma_0^{\alpha \rightarrow \alpha} \times |j^2|^{\alpha \rightarrow \alpha}, & \beta = \alpha \\ \sigma_0^{\alpha \rightarrow \alpha} \times |j^2|^{\alpha \rightarrow \beta}, & \beta \neq \alpha \end{cases}$$

since the exclusive cross section  $\sigma_0^{\alpha \rightarrow \beta \neq \alpha}$  is zero by color conservation. There are two interesting features:

1. The squared current  $|j^2|^{\alpha \rightarrow \beta}$  involves color structures that cannot be reduced by any means into only quadratic Casimir operators applied to individual partons. In other words, the color charge (eigenvalue of the quadratic Casimir) of each parton is not sufficient to fully determine the color richness of a  $2 \rightarrow 2$  process.
2. For  $\beta \neq \alpha$ : the  $ab \rightarrow cd$  process did not allow the transition  $\alpha \rightarrow \beta$ , however an extra soft gluon can rotate the initial state  $\alpha$  into  $\beta$  with an appropriate cost the squared bremsstrahlung factor  $\mathcal{R}(p_i, k)^2$ .

## Cross channels

Let’s define the  $t$ -channel as the process  $a\bar{c} \rightarrow b\bar{d}$  and the  $u$ -channel as the process  $a\bar{d} \rightarrow b\bar{c}$ . In addition to each parton quadratic Casimir operators, one can choose to express the remaining color structure in terms of  $t$ -channel and  $u$ -channel quadratic Casimir operators. For exemple in the  $t$ -channel, one has

$$2(T_a \cdot T_c) = (T_a)^2 + (T_c)^2 - T_t^2.$$

In the r.h.s., the two operators  $(T_i)^2$  are both applied to individual partons so that in any channel basis, they are simply proportional to the identity. The remaining operator in the r.h.s.  $T_t^2$  is applied to the  $t$ -channel parton pair  $a\bar{c}$ . This operator is diagonal in the  $t$ -channel basis, with diagonal elements proportional to the quadratic Casimir eigenvalues of the  $t$ -channel irreps. The same discussion applies to the  $u$ -channel. *In fine*, the color structure can be fully described by the choice of quadratic Casimir operators: four individual Casimirs and two cross channel operators.

## Back to the $s$ -channel

Some non-trivial color algebra has to be performed to go from the cross channel basis to the  $s$ -channel basis. In order, to perform such calculations, the color pictorial method using birdtracks is particularly useful. This technique will be discussed in the interlude of this thesis.

Finally, one finds that the inclusive (over color state) cross section  $\sigma_1$  is given by a sum of elementary “colored” cross section

$$\sigma_1 = \sum_{\alpha} \sigma_0^{\alpha \rightarrow \alpha} \left( \sum_{\beta} |j^2|^{\alpha \rightarrow \beta} \right)$$

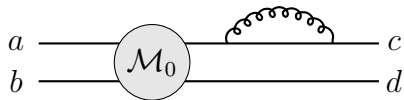
which captures all possible color transitions. The radiation intensity depends on both the initial and final color states of the pair (as seen from  $|j^2|$ ). This dependence involves non-trivial color factors coming from the cross channel Casimir eigenvalues.

It is interesting from a theoretical point of view to study the simple picture drawn by this decomposition, but also the technique to effectively derive them. For phenomenological applications, one can identify specific kinematical region (look at the dependance on the scattering angle of the process for example) in order to probe specific color contributions (in general the color charge grows as the dimension of the [irrep](#)). This will give additional information on how the color structure impacts the parton-dynamic.

## a.3 Soft anomalous dimension matrix

QCD is a field theory with a dimensionless coupling, thus a renormalizable theory [2]. As a consequence, after the renormalization procedure the first correction in  $\alpha_S$  to a Born cross section involves loops containing gluons that can produce large logarithms (collinear and/or soft). The treatment of those large logarithms also presents an interesting color structure to study.

Considering the previous process  $ab \rightarrow cd$ , given at Born level by the amplitude  $\mathcal{M}_0$ . A contribution at next order in  $\alpha_S$  would be



Logarithms can arise from two possibilities namely: the gluon can be collinear to parton  $c$ , and/or the gluon can be soft:

- A collinear **and** soft gluon: produces a double logarithmic (DL) contribution.
- A collinear **or** soft gluon: produces a single logarithmic (SL) contribution.

When the kinematics is such that that the logarithms are large and can compensate the smallness of  $\alpha_S$ , i.e.  $\alpha_S L^2 \sim \mathcal{O}(1)$ , the usual  $\alpha_S$  expansion becomes invalid. In those conditions, a resummation of all logarithmically enhanced contributions has to be performed to recover a well-defined expansion.



From the color perspective the above diagram is easy to grasp: the color tensor  $M_0$  associated to amplitude  $\mathcal{M}_0$  is composed with the quadratic Casimir operator applied to parton  $c$ :

$$M_0 \rightarrow (\mathbb{1}_a \otimes \mathbb{1}_b \otimes C_2[c] \otimes \mathbb{1}_d) \cdot M_0 = c_2[c] M_0$$

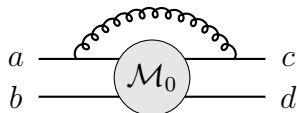
where  $\mathbb{1}$  is the identity,  $C_2[c]$  the quadratic Casimir operator applied to parton  $c$  with eigenvalue  $c_2[c]$ . This contribution is associated to an individual parton and contains DL (and also SL contributions) [14].

At the Leading Log (LL) accuracy, only DL are relevant and the series of diagrams with  $(\alpha_S^n L^{2n})$  constructs a Sudakov Factor for each partons involved in the process. Only individual quadratic Casimir operators are sufficient to describe every color structure involved in all LL-diagrams [15]. At this level of approximation, there is no interesting color feature to explore. In order to observe interesting color structure, one has to look beyond this leading approximation.

Beyond the LL approximation, or Next to the Leading Log (NLL), one have to carefully keep track of SL contributions. There are several source of SL, such as collinear hard splitting or large angle soft gluon radiation. Collinear hard splitting is taken into account by jet evolution, it is the large angle radiation that interests us here. In the case of soft and large angle radiation, individual quadratic Casimir operators are not sufficient to describe the color structure of all NLL-diagrams [16].

### Looking for NLL contributions.

In order to understand the previous statement, one needs to find a simple SL-contribution that does not involve only individual partons. At the same order in  $\alpha_S$  as the above diagram, we can draw



In the loop integral the gluon can be soft to yield an SL contribution. For the color structure, this diagram gives

$$M_0 \rightarrow (T_a^i \otimes \mathbb{1}_b \otimes T_c^i \otimes \mathbb{1}_d) \cdot M_0$$

where a sum over the color index  $i = 1 \dots N_c^2 - 1$  is implied. This contribution cannot be reduced to quadratic Casimir operators of individual partons by any use of color algebra. However, it is possible to use as in the previous section cross channel:

$$(T_a^i \cdot T_c^i)^2 = \frac{1}{2} (T_a^2 + T_c^2 - T_t^2)$$

The operator  $T_t^2$  cannot be further simplified into individual quadratic Casimir operators but it is diagonal in the  $t$ -channel basis with diagonal elements proportional to the quadratic Casimir eigenvalues of the system *irrep*.

Such SL contribution cannot be associated to any Sudakov form factor (the color structure cannot be that of an individual parton). However it must be resummed when

$\alpha_S L$  becomes of the order unity in some kinematic region. This resummation builds an additional cross channel form factor which is the exponential of a kernel  $\mathcal{Q}$  called the *soft anomalous dimension matrix* [16]. The prefix *soft* indicates that SL originate from a soft but collinear-safe kinematic region for the gluon in the loop integral.

### Soft anomalous dimension matrix and its color structure

It is visible from the previous paragraph that the action of the kernel  $\mathcal{Q}$  on the color structure  $M_0$  has a color matrix representation. It involves non diagonal operators in the  $s$ -channel basis because the operator  $T_t^2$  is diagonal in the  $t$ -channel only. Additionally, there is also  $u$ -channel operators such as  $T_u^2$ . Those operators have a simple expression in their respective basis but have to be expressed back to the  $s$ -channel. The situation is similar to the radiation spectrum in the previous section.

The resummation program demands to decompose  $\mathcal{M}_0$  into the *irreps* of various channels and express it in the  $s$ -channel. This is necessary to access NLL correction to an  $s$ -channel observable.



## CHAPTER 2

# B.A. BA OF QCD AND NUCLEAR EFFECTS AT HIGH ENERGIES

### 2.1 A bit of history

*“How did QCD become the theory of the strong interaction?”*

**In the early sixties** , most of the physicists did not believe that a QFT could describe the strong interaction. One could quote Landau [17]

*“It is well known that theoretical physics is at present almost helpless in dealing with the problem of strong interactions. We are driven to the conclusion that the Hamiltonian method for strong interactions is dead and must be buried, although of course with deserved honour.”*

or Goldberger [18]

*“My own feeling is that we have learned a great deal from field theory... that I am quite happy to discard it as an old, but rather friendly, mistress who I would be willing to recognize on the street if I should encounter her again.”*

to see that the nuclear community was moving away from QFT. The reasons for such attitude were mainly:

- Meson theories were based on local interactions (of the Yukawa kind) between hadron fields, and they did not work for years since the discovery of the nucleon in 1932 by Chadwick. Feynman in 1951 cautioned Fermi: *“Don't believe any calculation in meson theory which uses Feynman diagram!”*.
- Renormalizable theories existed already, e.g. QED or  $\phi^4$ -theory. However the methodology of renormalization was criticized as a mere tool to “sweep the infinities under the rug”.

Those years of QFT were not vain. Expected properties of the  $S$ -matrix were found such as analyticity, unitarity, crossing symmetry [19]. Those served as a corner stone for

the properties of the strong interaction. The two main approaches to address the strong interaction were:

- The nuclear democracy. Instead of a QFT, the idea was to use only quantities accessible in experiments, and use the properties of the  $S$ -matrix such as unitarity, analyticity, or crossing symmetry.
- The French cuisine: use QFT toy-models to study the observed symmetries, and extract algebraic properties that would later be used outside those toy-models. Quoting Gell-Mann [20]

*“We construct a mathematical theory of the strongly interacting particles, which may or may not have anything to do with reality, find suitable algebraic relations that hold in the model, postulate their validity, and then throw away the model. We may compare this process to a method sometimes employed in French cuisine: a piece of pheasant meat is cooked between two slices of veal, which are then discarded.”*

Nevertheless, part of the physicists community kept faith in QFT. A beacon of hope was brought in 1954 by the paper of Yang and Mills [21], about a new kind of QFT based on a local non-abelian symmetry. This theory was a direct generalization of QED.

This paper served as a basis for a new type of theories like Feynman’s quantum gravity [22], or Glashow  $SU(2) \times U(1)$  electroweak theory in 1961 [23]. The electroweak theory would be completed by Weinberg [24] and Salam [25, 26] including the Higgs mechanism to produce masses [27, 28]. However the theory still had problems, renormalization was poorly understood and the hadronic spectrum did not fit well. At the same time, Bogolyubov, Parasiuk, Hepp, Lehmann, Symanzik, and Zimmermann pursued the renormalization program for simpler theories than the Yang-Mills theory. Then came the  $\sigma$ -model of Gell-Mann and Levi [29] to describe protons, neutrons, and pions and chiral symmetry breaking. The  $\sigma$ -model structure was investigated by Symanzik [30], and Gervais and Lee [31].

The Yang-Mills theory was found to be renormalizable in the absence of massive particle. Slanov-Taylor identities (a kind of generalized Ward identities) guaranteed unitarity, causality, and renormalizability. Hence, it became natural to introduce the massive analogue of Yang-Mills theory through the Higgs mechanism [32]. At that time the Higgs mechanism was still thought of as an ugly idea as opposed to the clean Yang-Mills theory. The electroweak theory was an instant success using those concepts. With the rules in hand, the transition to hadrons and QCD came naturally.

In the sixties, DIS was studied at SLAC. The DIS cross section was thought to depend on two quantities, namely the energy  $\nu$  of the virtual photon defined as the difference between the final and initial electron energy, and the invariant mass  $q^2$  of the virtual photon. An unexpected result came from the data: the DIS cross section as a function of the invariant mass decreased much more slowly than the elastic one [33]. In 1968, Bjorken proposed to Kendall to plot  $\nu W_2^1$  as a function of  $\nu/q^2$ . The available data appeared to *scale*, i.e. data points followed a single curve  $F_2 = \nu W_2$  function only of the ratio  $\nu/q^2$  [33]. This scaling phenomenon suggested that the proton was, in fact, constituted of almost non-interacting constituents at high energies (the quarks). The proton probed at

---

<sup>1</sup>The proton structure functions  $W_1$  and  $W_2$  contain all the information about the proton accessible by unpolarized electron scattering.

low energy is a strongly bound object, but as we move to higher resolutions, it becomes a system of quasi-free constituents. This means that the coupling of the strong interaction not only runs (from the strongly bound system to the almost non-interacting one) but decreases at high energies.

The former was already known from QED, charge screening makes the coupling run. The latter was poorly understood at that time and corresponds to the negative sign of the  $\beta$ -function. In 1964, Vanyashin [34] had already obtained the sign of the  $\beta$ -function in the vector meson theory, but he attributed this to the non-renormalizability of the theory. In 1969, Khriplovich [35] calculated the charge renormalization in the ghost-free Coulomb gauge in Yang-Mills theories, but the relation to asymptotic freedom was not made. In 1971, 't Hooft already knew the sign of the  $\beta$ -function to be negative and that the coupling decreases at high energy. At the same time, Callan and Symanzik in 1970 pursued the study of the scaling behaviour and formulated the Callan-Symanzik equation. However, it was used in QED and  $\phi^4$ -theory but not in Yang-Mills theory and the result was a positive  $\beta$ -function. This positivity was thought to be some universal feature of QFT and could not explain Bjorken scaling. In 1973, Politzer, Gross, and Wilczek closed the discussion by calculating of the  $\beta$ -function in Yang-Mills theory, thus demonstrating the property of asymptotic freedom, and providing a first-principle explanation of Bjorken scaling.

In 1972, everything was already set in place to formulate QCD. The quark model of Gell-Mann led to a new internal dof named color. Nambu and Han in 1965 formulated the idea of quarks being confined due to the color gauge symmetry. Yang-Mills theory together with asymptotic freedom explained Bjorken scaling. All this led to the formulation of QCD as the theory of the strong interaction.

## 2.2 QCD

### 2.2.1 Lagrangian formulation

QCD is a quantum field theory based on a Lagrangian density. Before writing down the QCD Lagrangian  $\mathcal{L}_{QCD}$ , it is interesting to make a short detour to the QED Lagrangian. With the electron field denoted by  $\psi$  and the photon field by  $A$ , the QED Lagrangian reads

$$\mathcal{L}_{QED} = \bar{\psi} (i \gamma^\mu D_\mu - m) \psi - \frac{1}{4} F_{\mu\nu} F^{\mu\nu} \quad (2.1)$$

The symbol  $D_\mu$  denotes the covariant derivative, containing the photon field and the derivative operator,  $D_\mu = \partial_\mu + ieA_\mu$ , and  $F_{\mu\nu}$  is the Maxwell electromagnetic tensor, namely,  $F_{\mu\nu} = \partial_\mu A_\nu - \partial_\nu A_\mu$ .

As expected from QCD being a non-abelian generalization of QED, the resemblance between  $\mathcal{L}_{QED}$  and  $\mathcal{L}_{QCD}$  is striking:

$$\mathcal{L}_{QCD} = \sum_{i,j=1}^3 \bar{q}_i (i [\gamma^\mu D_\mu]_{ij} - m_q \delta_{ij}) q_j - \frac{1}{4} \sum_{a=1}^8 G_{\mu\nu}^a G_a^{\mu\nu} \quad (2.2)$$

Those two Lagrangians are almost identical in form. To obtain  $\mathcal{L}_{QCD}$  from  $\mathcal{L}_{QED}$ , one just replaces the field  $\psi$  by the field  $q_i$  that carries an additional color index  $i = 1, 2, 3$ .



## 2.2.2 A few words on renormalization

For QCD to be qualified as a quantum theory of the strong interaction, the renormalization played a major role. I will illustrate here the renormalization procedure in the spirit of Wilson, following the lines of the discussion which can be found in [36].

In QFTs, the number of dof is very large, actually there are fields taking values at each space-time point. To deal with such a large number of dof, one can use of the property of locality. The study of the whole system can be reduced to a small bulk of the initial system as long as this small bulk is at least larger than the correlation length. In a QFT this correlation length would be the Compton length of the lightest massive particle. Then the study on the whole space can be reduced to the study of a box of size given by this correlation length.

For a system interacting via some Hamiltonian  $\mathcal{H}_{int}$ , one expects that the behaviour of the system is dictated by the type of the interaction in  $\mathcal{H}_{int}$ . However, in some class of problem treated by the renormalization theory, the form of the interaction  $\mathcal{H}_{int}$  is placed in the background, and cooperative dofs are placed in the foreground. There are two purposes of the renormalization group approach:

1. Solve problems with a system involving many dofs.
2. Explain how features of cooperative behaviour arise.

The basic idea is, as in hydrodynamics, to use the notion of average over microscopic dofs to define macroscopic dofs. Hence, there will be less dofs than in the initial problem and the problem should be easier to solve. To reduce this number, the renormalization group approach consists in replacing step by step dofs by effective ones, and the Hamiltonian is replaced by an effective one,

$$\mathcal{H}_{int}^n \longrightarrow \mathcal{H}_{int}^{n+1} = \tau [\mathcal{H}_{int}^n] \longrightarrow \mathcal{H}_{int}^{n+2} = \tau [\tau [\mathcal{H}_{int}^n]] \quad (2.8)$$

At all steps, if the interactions within  $\mathcal{H}_{int}^n$  are local, each dof couples only to the dof of the close neighbourhood that are characterized by a distance  $\sim L_n$ . The hope is that the interaction range gradually increases when the density of dof decreases, up to the correlation length.

Under the previous iterations  $\tau$  on  $\mathcal{H}_{int}^0$ , there is the possibility that fixed points arise such that  $\tau [\mathcal{H}_{int}^*] = \mathcal{H}_{int}^*$ . Those fixed points appearing after a large number of iterations suggest that the final Hamiltonian depends more on the transformation  $\tau$  than on the actual form of  $\mathcal{H}_{int}^0$ .

Let's return to QCD, and start with a given bare Lagrangian  $\mathcal{L}_0$  defined at some high momentum scale  $\Lambda$  (in Euclidian momentum space). By gauge invariance the Lagrangian contains terms of the form 2.2.1 but also higher derivative terms (still gauge invariant) as long as the proper dimension is respected [mass<sup>4</sup>]. In the spirit of Wilson, one can define a "slice" of momentum  $k \in [b\Lambda, \Lambda]$  with  $b < 1$  and  $1 - b \ll 1$ . One integrates over this slice of momentum, constructs an effective Lagrangian  $\mathcal{L}_1$  from the initial one, and then rescales the new terms in the Lagrangian by the proper power of  $b$ . Let's call  $\tau$  the operator acting on the Lagrangian  $\mathcal{L}_0$  to produce the Lagrangian  $\mathcal{L}_1$  after this procedure. In the Lagrangian there are two kinds of terms: the relevant and the marginal terms. After



multiple iterations of the transformation  $\tau$  corresponding to multiple slices of momentum integrated out, relevant contributions will be preserved. Marginal contributions on the other hand (which may be non-renormalizable interactions) are kept in control and their impact on the physics at the lower scale will be negligible.

Following those iterations of  $\tau$  from the high momentum scale  $\Lambda$  to a scale comparable to actual experiments  $\mu$ , the sequence of all Lagrangians  $\mathcal{L}_0, \dots, \mathcal{L}_n$  is a curve in the space of all possible Lagrangians, see Fig. 2.1.

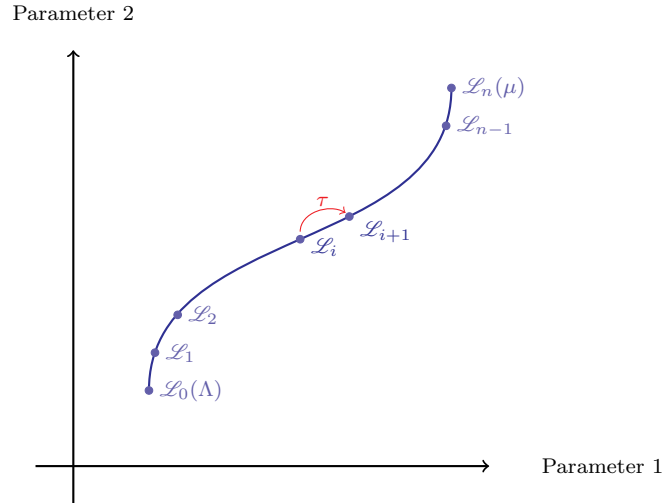


**Figure 2.1:** *A sketch of the projection of the space of all Lagrangians into a plane spanned by the value of two parameters. During the successive integrations of momentum slices, the initial Lagrangian defined at the scale  $\Lambda$  “moves” along the blue curve up to an effective Lagrangian at the scale  $\mu$ . The red arrow indicates an iteration of the operator  $\tau$  previously defined.*

Two important feature emerge:

- Considering the set of parameters from the original Lagrangian that are evolved to different scales, e.g.  $\mu_1 > \mu_2$ , the physics described by the Lagrangian at those two scales is equivalent.
- Taking a very large initial momentum  $\Lambda \gg \mu$  ensures that only relevant interactions, whose form is given by in the Lagrangian 2.2.1, “survive” this procedure. This “washing away” of marginal operators explains how the regularization procedure, which introduces operators with more derivatives, only regulates the UV behaviour and keeps the physics at our scale intact.

The procedure of renormalization in QCD leads to the property of asymptotic freedom of the strong coupling. Let me quote the one-loop result for the running coupling

$$g^2(\mu) = \left[ 1 + \frac{g_0^2}{16\pi^2} \underbrace{\left( \frac{11}{3}N_c - \frac{2}{3}N_f \right)}_{b_0} \log \frac{\Lambda_0^2}{\mu^2} + \mathcal{O}(g_0^4) \right] g_0^2 \quad (2.9)$$

with  $N_f$  the number of flavors. The bare coupling  $g_0$  is from the initial Lagrangian defined at the scale  $\Lambda_0$ . We see that the coupling constant  $g^2(\mu)$  increases as the renormalization scale  $\mu$  decreases. This behaviour is obtained from the analysis of Feynman graphs using perturbative approach, hence this result can be trusted as long as **PT** applies. At some point in the evolution of  $\mu$  to lower scales,  $g^2(\mu)$  becomes of order unity. In this domain, perturbative results become invalid, and the language of quarks and gluons itself becomes questionable. One enters the realm of confinement, which remains to be understood. It is not clear whether the true **QCD** coupling, at low energies needs to be large (of the order unity) to make confinement possible. A relatively small infra-red coupling could also lead to confinement [4, 37, 38].

This increase of the running coupling at low energies is called infra-red slavery [3]. It is the UV behaviour analysis that dictates this growth of the coupling. However, the infra-red slavery and large coupling value do not implies confinement (see 3.2 of [39]).

Following Wilson’s point of view, one can construct a differential equation for the strong coupling:

$$\mu \frac{d g^2(\mu^2)}{d \mu} = \beta[g^2(\mu^2)] \quad (2.10)$$

From the one-loop analysis, the beta function takes the form

$$\beta(g^2) = -\frac{b_0 g^4}{8\pi^2} \quad (2.11)$$

Solving the differential equation yields

$$\alpha_s(\mu^2) = \frac{g^2(\mu^2)}{4\pi} = \frac{2\pi}{b_0 \ln(\mu/\Lambda_{QCD})} \quad (2.12)$$

The two equations 2.9 and 2.12 coincide if one writes  $\Lambda_{QCD}$  as a function of  $\Lambda_0, g_0$ . The theory now depends on a dimensionful scale  $\Lambda_{QCD}$  and not on the two “unphysical” parameters  $\Lambda_0, g_0$ . This is called *dimensional transmutation*, and the set of  $\Lambda_{QCD}$  with quark masses now defines relevant dimensionful quantities in the theory. In particular, the process of confinement turns out to form hadrons of mass  $\sim \mathcal{O}(\Lambda_{QCD})$ .

I will now briefly present the two main approaches used to study nuclear effects at high energies. The first section 2.3 is dedicated to the collinear factorization approach and the use of nuclear parton distribution functions. The second section 2.4 presents the  $k_t$ -factorization approach and the saturation formalism.

## 2.3 Collinear factorization and nuclear parton distribution function

### 2.3.1 Collinear factorization in DIS

One problem in **QCD** is our inability to apply straightforwardly the theory for the computation of a given cross section. Because it is a field theory, one has to consider at the same time short distance, and long distance effects. Asymptotic freedom can help us with the former by using **PT**, but we are currently unable to treat the latter due to our lack of understanding of confinement (or our lack of mathematical knowledge beyond **PT**).

This motivates the collinear factorization approach. The main idea is to separate long distance and short distance effects in a way such that the cross section becomes the *product* of a calculable part and a measurable part. The hope is that with a proper separation, the measurable part will be universal, and one will be able to use PT for the calculable part.

In a renormalizable theory, the perturbative expansion of a physical observable is a function of three kinds of “masses”: the kinematic energy scale of the scattering usually noted  $Q$ , masses noted  $m$ , and the renormalization scale  $\mu$ . The latter only appears in ratios  $Q/\mu$  or  $\mu/m$ , and one is free to choose the value of  $\mu$  because an observable does not depend on such a scale. Problems emerge in loop calculations, where logarithmic contributions appear at all orders of the expansion. For instance, at the  $n$ -loop order, the factor  $\alpha_s$  may combine with logarithmic factors in the form:

$$\{\alpha_s(\mu) \log^{1,2}(\mu/m)\}^n \quad \text{or} \quad \{\alpha_s(\mu) \log^{1,2}(Q/\mu)\}^n \quad (2.13)$$

By setting  $\mu \sim Q$ , asymptotic freedom implies  $\alpha_s \ll 1$ , but a large factor  $\log(Q/m)$  appears, and the validity of the perturbative expansion is totally wasted. The other choice is to minimize the logarithmic contribution, but this means to keep a small value of  $\mu$  and being in the non-perturbative domain of QCD,  $\alpha_s \sim \mathcal{O}(1)$ . At least, one of the two ratios is large and the effective expansion parameter is not small.

In general, a cross section cannot be calculated from pQCD because of the combination of short and long distance effects.

Fortunately, there are exceptions! QCD collinear factorization theorems allow one to derive the production cross sections of some processes, provided some necessary conditions are satisfied:

1. Aside from masses, all scales are large and of the same order.
2. the considered process is inclusive meaning that all events containing the specific state are summed over.

Examples of such processes were given in the Introduction. The first requirement is rather strong, in particular, one cannot study the full  $p_t$ -dependence<sup>4</sup> because the  $p_t$  is either integrated out, or on the order of  $\sim Q$ .

## Deeply inelastic scattering and the parton model

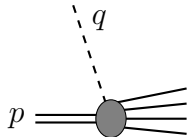
The prototype for collinear factorization theorems is DIS.

$$e + A \rightarrow e + X \quad (2.14)$$

with  $A$  the target hadron,  $X$  the remaining hadrons in the final state, and  $e$  an electron. There are several reasons for that: historically DIS was the process used to *see* point like partons inside hadrons, DIS is the cleanest QCD process (where the form of the factorization theorem is the simplest) allowing one to probe the PDFs of the target. (Most of the tabulated PDFs initially came from DIS.) The DIS amplitude looks like:

---

<sup>4</sup> $p_t$  being the transverse momentum of some final state tagged hadron.



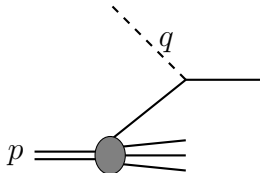
The momentum of the incoming hadron is  $p^\mu$ , and the virtual photon (dashed line) has momentum  $q^\mu$  with  $q^2 = -Q^2$ . The hadronic tensor associated to this process reads

$$W^{\mu\nu}(p, q) = \frac{1}{4\pi} \int d^4x e^{iq \cdot x} \sum_X \langle A | j^\mu(x) | X \rangle \langle X | j^\nu(0) | A \rangle \quad (2.15)$$

In the parton model, hadrons are assumed to be bound states of point like objects called partons. Those partons are identified to QCD quarks, antiquarks, and gluons. This means that hadrons can be described by a superposition of Fock states made of partons. Due to the non-perturbative nature of hadrons, we are not able to access to this information. However, PT enables us to calculate the scattering of a free parton off an electron.

At high energies and in the center of mass coordinate system, time dilatation and length contraction implies that the time for the projectile to pass through the target decreases. At the same time, both the projectile virtual fluctuation life time and the interaction time between partons in the target hadron are dilated. At high energies, the target hadron is thus a frozen single virtual state (that we want to understand) defined by a given set of partons. Each parton carries a momentum fraction of the target hadron. The projectile then interacts with a *free* parton rather than the whole hadron as a bound state. For large momentum transfer  $Q^2$  and not too high parton density, there will be only a single scattering.

Thus, at large  $Q^2$  with fixed  $x_B = Q^2/2q \cdot p$  (Bjorken limit), the picture becomes



The parton model leads to the formulation of QCD factorization theorem. For DIS the hadronic tensor becomes [6]:

$$W^{\mu\nu}(p, q) = \sum_a \int_{x_B}^1 \frac{d\xi}{\xi} f_{a/A}(\xi, \mu) H_a^{\mu\nu}(q, \xi p, \mu; \alpha_s(\mu)) + \dots \quad (2.16)$$

The expression 2.16 is called the *leading twist contribution* and the remainder (indicated by the dots and suppressed by at least a power of  $1/Q$ ) is called the *higher twist contribution*. The PDF  $f_{a/A}$  can be interpreted as the probability to find a parton  $a$  within the hadron  $A$  with momentum fraction contained between  $\xi$  and  $\xi + d\xi$  of the parent hadron momentum. The dependence on the factorization scale  $\mu$  (beyond the parton model) of the PDF  $f_{a/A}(\xi, \mu)$  comes from radiative correction to the previous picture. Those are taken into account by the mean of evolution equation such as DGLAP relating PDFs between two scales  $\mu$  and  $\mu'$ .

We stress that the long distance physics is contained in the factor  $f_{a/A}$ , and that the factor  $H_a^{\mu\nu}$  does not depend on  $A$  and is dominated by the ultraviolet region  $\sim \mathcal{O}(Q)$ .

Those two properties of  $H$  allow a pQCD calculation at the level of a simple parton  $a$  instead of  $A$  and a perturbative series with parameter  $\alpha_s(\mu) \ll 1$ .

One postulates that those long distance effects in the complete theory (not only its perturbative part) factorize in the same way (“*the Nature does respect its own rules of engagement*” [40]). With this postulate, PT is predictive and can be used to calculate  $H_a$ , and our ignorance is placed into the PDFs that can be measured. In the example of DIS, one can measure the Dirac form factor  $F_1$ , then extract  $f_{a/A}$ , and finally predict the Pauli form factor  $F_2$  using only PT. This is an example of the use of the universality of PDFs.

### 2.3.2 Nuclear parton distribution function

The study of nuclear effects in the framework of collinear factorization relies on the following observation: early DIS experiments suggested that nuclear PDFs can be formulated as a modification of the free nucleon PDF at some initial scale  $Q \sim 1$  or  $2 \text{ GeV}$ , then letting the  $Q^2$ -evolution of the PDF being taken care of by the DGLAP evolution equations.

One usually defines nuclear ratios  $R_i^A$  of parton densities as [41]

$$f_i^A(x, Q^2) = A f_i^{\text{nucleon}}(x, Q^2) R_i^a(x, Q^2) \quad (2.17)$$

This is an empiric approach, where all nuclear effects are placed into the  $R_i^A$  ratios. This data-driven method has to first parametrize the initial condition of DGLAP evolution, then evolve through DGLAP equation to larger values of  $Q^2$  to be compared to data points. Successive comparisons will iteratively adjust the parametrization. This procedure is called global analysis, and the more data are available as input (in particular from different processes such as DIS,  $e^+e^-$  annihilation, Drell-Yan production, ...), the more precise the adjustment shall be.

Nuclear effects are contained in the form of the parametrization, and does not need to be fully understood to still have a predictive power from this approach (see [41] for a list of different parametrizations of the initial condition for DGLAP evolution).

The quantitative description of nuclear effects from those analyses is contained in Fig.2.2. Four regions can be identified from the lower to higher values of  $x$ : shadowing, anti-shadowing, EMC effect, and Fermi motion. The former two regions are commonly attributed to multiple scattering where the shadowing is a region of destructive interferences and the anti-shadowing a region of constructive interferences, whereas the origin of the latter two is still unclear.

### 2.3.3 Collinear factorization in other processes

As we saw in the introduction, QCD factorization theorems hold for other processes than DIS. The prototype is the same as in DIS and relies on the fact that the long-distance effects do not interfere with the well localized hard partonic scattering. The expected cross section takes the form of a convolution between PDFs and partonic hard scattering cross section properly summed over flavors. For example, the inclusive jet cross section is

$$\sigma(A + B \rightarrow J + X) \equiv \sum_{a,b} f_{a/A} \otimes f_{b/B} \otimes \hat{\sigma}_{ab \rightarrow J+X} \quad (2.18)$$

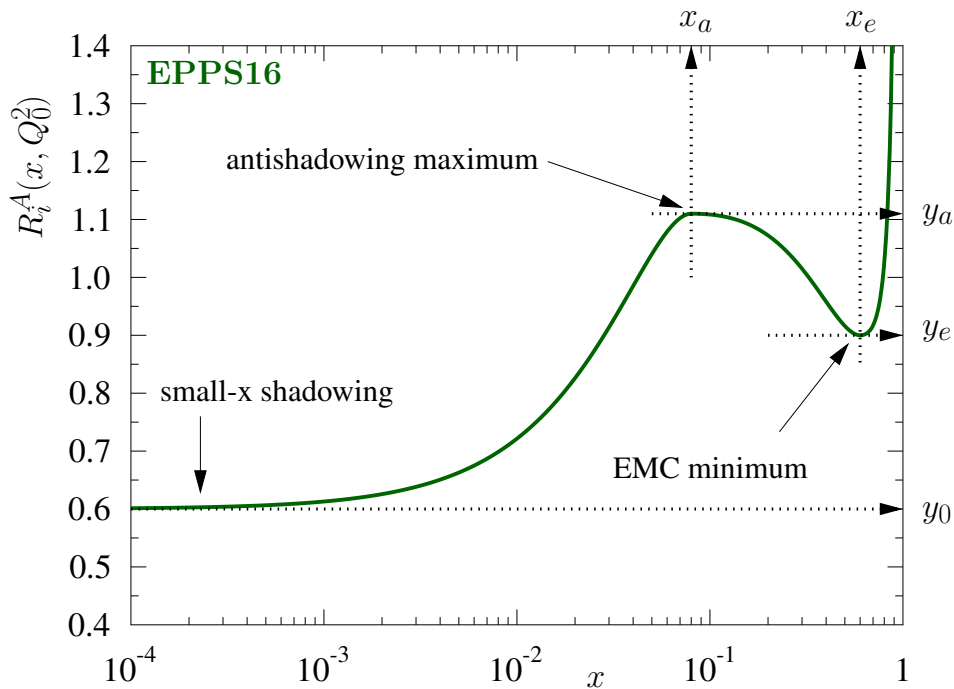


**Figure 2.2:** From [42]. Illustration of the EPPS16 fit function  $R_i^A(x, Q_0^2)$ .

with  $\otimes$  the convolution operator over relevant variables (in hadron productions, the proper fragmentation functions must be included). The two PDFs involved in this convolution are universal and can be extracted in DIS.

To study, nuclear effects in those collision, the same picture as in DIS can be applied, one can introduce the nuclear ratios  $R^A$  and  $R^B$  to express  $f_{a/A}$  and  $f_{b/B}$  from  $f_{a/p}$ . The nuclear effects presents in the previous section are also present: shadowing, antishadowing, EMC, Fermi motion. However, this factorization breaks down in the presence of medium-induced effects (subject of this thesis). Medium-induced effects modify the hard partonic cross section  $\hat{\sigma}$  by resumming some (possibly large) higher-twist contributions (within the dots of 2.16). The full treatment of those higher-twist contributions is a hard problem from the theoretical point of view. Fortunately in phenomenology, an empiric but theoretically motivated approach to include those higher-twist effects is to extract those medium-induced effects (from theoretical models) and add them by hand into the factorization theorem.

## 2.4 Saturation

Another approach to describe nuclear effects is the saturation approach used to study the phenomenon of gluon saturation in high-energy scattering.

### 2.4.1 Physical picture of saturation

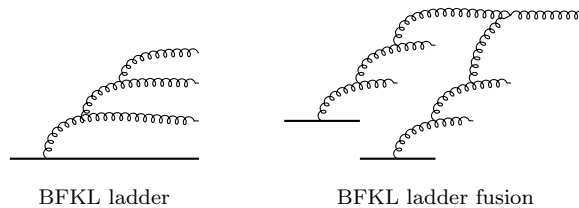
Since QCD has been established as the theory of the strong interaction, a major challenge is to understand the Fock wave function of hadrons in the high-energy limit. The possibility for a parton to radiate a gluon is given by the bremsstrahlung law. This probability diverges when  $x$  (the fraction of momentum of the gluon with respect to the parent parton) goes to zero. This divergence compensates the smallness of the coupling  $\alpha_s$  for small values of  $x$  and the (integrated) probability becomes of the order of one. This will favor an increase of the population of small- $x$  gluons in a given volume of phase-space, especially because the small- $x$  gluons can radiate themselves (a specific feature of non-abelian theory). However, the unitarity of the theory prevents this population from growing to arbitrary large densities. Non-linear effects come into play, and reduce the number of gluons at small values of  $x$  compared to what only linear evolution would produce. A new scale emerge from this picture called the saturation scale  $Q_s$ . It is this scale that defines the value of  $x$  at which the non-linear evolution becomes relevant.

#### Recombination

The number of gluons per unit volume of phase-space is counted by the Weizsäcker-Williams unintegrated gluon distribution  $\phi^{WW}(x, \vec{k})$ . Related to this distribution the integrated gluon distribution  $x G(x, Q^2)$  is defined as

$$x G(x, Q^2) = \int^{Q^2} d^2 \vec{k} \psi^{WW}(x, \vec{k}) \quad (2.19)$$

This unintegrated distribution is described using DGLAP or BFKL evolution equation. In those linear equations, the parton density is assumed to be dilute during the whole evolution. This hypothesis breaks down at large gluon density where non-linear evolution has to be considered. Such effects depend on the density, as illustrated bellow:



The process represented in the left corresponds to a linear contribution to the evolution, increasing only the number of gluons. The right contribution contribute to non-linear term in the evolution corresponding to the fusion of two gluon ladders. This is crucial to restore the unitarity of the theory.

#### Strong fields

Another aspect of saturation is the fact that a large gluon density is equivalent to the presence of strong gluon fields. This permits the use of classical techniques to study the small- $x$  dependence, in particular when large nuclei are involved.

In this picture, the McLerran-Venugopalan (MV) model [43] separates: on the one hand soft (small- $x$ ) gluons, on the other hand the high- $x$  static valence partons. A fast

parton either absorbs or emits soft gluons but it stays on its trajectory (eikonal approximation). Such energetic parton produces a classical color current, and the associated produced small- $x$  gluon field is found from the classical Yang-Mills equation of motion with such an external current. In the very high density limit, the solutions are described by a Gaussian distribution .

### 2.4.2 Color Glass Condensate

The color glass condensate (CGC) is the nick-name of an effective theory for the small- $x$  distribution in high energy scattering. This framework enables one to study the saturation phenomenon.

The starting point of the CGC theory is the MV-model: a picture of strong classical fields within the nucleus. However, quantum corrections to the classical MV-model can be large for small values of  $x$ . One of the main advantage of such an approach is that one can use first principles of QCD to hadron of nucleus.

Quantum corrections can be incorporated by a renormalization procedure in the spirit of Wilson renormalization. Those fluctuations are integrated out, and included in an effective distribution replacing the initial Gaussian one from the MV-model. The evolution between two scales  $x$  is then given by an evolution equation called the JIMWLK equation [44].

Another approach to include quantum corrections is to evolve the projectile instead of the target nucleus. This evolution can be done with the Balitsky hierarchy or the BK equation [44]. Consider a  $q\bar{q}$  dipole that scatters off a nucleus with some relative rapidity  $Y$  between them. The evolution of the cross section from  $Y$  to  $Y + dY$  can be viewed as increasing the momentum of the dipole. There is a small probability that the dipole radiates a gluon before crossing the nucleus. The Fock-state  $q\bar{q}g$  is populated from the  $q\bar{q}$  one.

The JIMWLK and BK evolution equations are related to the unitarity of the theory. This can be understood by since they both contain non-linear terms in their kernel.

Due to the presence of strong fields, usual PT does not apply. A resummation of large (logarithmic) contributions has to be performed, at all orders, to recover a predictive power in this framework. This is an additional feature of the CGC theory. This resummation includes contributions than would be labeled as higher-twist in the collinear factorization formalism.

### 2.4.3 Relation to my study

The saturation scale  $Q_s$  will appears as a parameter to study the medium broadening. The resummation of elastic scatterings in a medium for a system of parton will depend on this scale through the the dipole-nucleus cross section. From the geometry considered, the saturation scale grows as the path length  $L$ . In addition to this geometric growth, quantum corrections are expected. Those corrections promotes the saturation scale  $Q_s$  to be a function of  $x$ .

In this thesis the later are not considered, however the dependence on the color state



of the system is emphasized. A color stripped saturation scale  $\bar{Q}_s^2 = C_R^{-1} Q_s^2$  will be used instead. This gives the possibility to study how the associated color factor may evolve during the propagation of the medium in the MV-model, yielding some unusual color factors (distinct from  $N_C$  and  $C_F$ ) depending on the path length  $L$  of the system (with a given color state) within the medium.

## CHAPTER b

# INTERLUDE: BIRDTRACKS FOR BEGINNERS

This *interlude* is a basis for the color algebra technique that will be used in this manuscript. An efficient and fun way to perform algebra is to use pictorial notations called “*birdtracks*” [45].

## b.1 Feynman diagrams

### A bit of history

In the early 1930’s, theorists were battling against two problems:

- Even with a small coupling parameter  $\alpha \sim 1/137$ , pushing calculations beyond the simplest approximations produced unphysical infinities.
- The formalism used was cumbersome, and an algebraic nightmare with multiple terms to estimate. In the mid 1930s, Hans Euler performed a calculation at order  $\alpha^2$  : light by light scattering. This calculation contained hundreds of terms that needed to be summed over to quantify such a cross section.

The solution to the first problem was given by the procedure latter called *renormalization*. The solution to the second problem was introduced in spring 1948 by R. Feynman, during a talk at the Pocono Manor Inn in Pennsylvania. In his talk, he presented a book-keeping device for complicated calculations that would later be called “Feynman Diagrams”. It was thanks to the intervention of Dyson and his two papers in 1949 that the situation became clear. The first paper [46] demonstrates the equivalence of Feynman’s diagrammatic approach with Tomonaga-Schwinger theory and the second [47] indicates the computation rules for the S-matrix elements using Feynman diagrams and the rules associated with each diagram. Then it was through Oppenheimer’s “*intellectual hotel*” for two-year postdoctoral stays<sup>1</sup> that those diagrams did spread.

The introduction of Feynman diagrams changed how physicists approached scattering problems. Feynman diagrams were first used as a mnemotechnic tool to write down

<sup>1</sup>At the Institute for Advanced Study, Princeton

integrals in QED, and now they are used to organize calculational problems over a large scope of topics. In a way, the representation of quantum mechanisms using diagrams gives us an intuition of quantum effects.

Any Feynman diagram contributing to a QCD scattering amplitude is a tensor in color space. This feature arises in QCD simply because any field at a given position is valued in a vector space (color index). Those color tensors are built at all orders by contracting a bunch of rank 2 tensors (propagators) and rank 3 tensors (interaction vertices)<sup>2</sup>.

History has already proven how efficient diagrammatic methods are, we just need an extra step in QCD from the usual color algebra to birdtracks.

## b.2 Getting started with birdtracks

For the rest of this interlude, I will introduce elementary rules of the birdtracks techniques. In the context of QCD, birdtrack calculus is an algebraic tool to compute, simplify and manipulate color tensors associated to Feynman diagrams. Instead of color tensors and the associated algebraic calculus, I will use the terminology “color structure”.

It is also noteworthy that in QCD, the color structure is not the only application of birdtracks. The study of “spin-traces” by means of the Clifford algebra can also be treated nicely with birdtracks (See chapter 11 of [45]).

*Let us now introduce the basics of the birdtrack technique step by step. This technique is described in length in [45]*

### b.2.1 Quarks and the fundamental representation

Let the space  $V$  be the defining  $N_c$ -dimensional complex vector representation space and  $\bar{V}$  its dual. A vector  $q \in V$ , also noted  $q_i$  with  $i = 1, \dots, N_c$ , denotes one of all possible color states of a quark in the defining representation. Similarly, a vector  $\bar{q}^j$  with  $j = 1, \dots, N_c$  denotes one of all possible color states of an antiquark in the dual representation  $\bar{V}$ . In view of constructing invariant quantities under the  $SU(N_c)$  gauge group of color “rotations”, it is useful to start by building a scalar as

$$\langle q, \bar{q} \rangle = q \cdot \bar{q} = q_i \bar{q}^i = q_i \delta^i_j \bar{q}^j \quad (\text{b.1})$$

The Kronecker delta is an primitive invariant (a tensor that preserve the norm of a complex vector) of  $SU(N_c)$  which is represented in birdtrack notation simply by a line with an arrow. The arrow will flow by convention from the upper index to the lower index:

$$\delta^i_j = i \longrightarrow j$$

In birdtrack notation the above scalar reads:

---

<sup>2</sup>There is a four gluon vertex in QCD, however its color structure reduces to contractions of rank 2 and rank 3 tensors.

$$\begin{array}{c} \textcircled{q} \longrightarrow \textcircled{\bar{q}} \end{array} = q \cdot \bar{q}$$

where all unnecessary indices from the sum convention can be removed.

In general, a QCD amplitude involves tensors with a lot of color indices. As an example, a tensor  $x \in V^{\otimes a} \otimes \bar{V}^{\otimes b}$  would be in birdtrack notation

$$x^{i_1, i_2, \dots, i_a}{}_{j_1, j_2, \dots, j_b} = \begin{array}{c} \begin{array}{c} \xrightarrow{i_1} \\ \xrightarrow{i_2} \\ \vdots \\ \xrightarrow{i_a} \end{array} \textcircled{x} \begin{array}{c} \xrightarrow{j_1} \\ \xrightarrow{j_2} \\ \vdots \\ \xrightarrow{j_b} \end{array} \end{array}$$

## b.2.2 Irreducible representation and Fierz identity

An important case is the tensor product  $V \otimes \bar{V}$ . With the invariant  $\delta_j^i$ , we can already construct two operators that map  $V \otimes \bar{V} \rightarrow V \otimes \bar{V}$ :

$$\begin{array}{l} \text{Identity : } I = \begin{array}{c} \xrightarrow{\quad} \\ \xleftarrow{\quad} \end{array} \\ \text{Trace : } T = \begin{array}{c} \xrightarrow{\quad} \\ \downarrow \quad \uparrow \end{array} \end{array}$$

To compute  $T^2$  using birdtracks, we place the two tensors side by side and we connect lines,

$$T^2 = \begin{array}{c} \downarrow \quad \uparrow \quad \downarrow \quad \uparrow \\ \downarrow \quad \uparrow \end{array} = \begin{array}{c} \downarrow \quad \square \quad \uparrow \\ \downarrow \quad \uparrow \end{array} = N_c \begin{array}{c} \downarrow \quad \uparrow \\ \downarrow \quad \uparrow \end{array} = N_c T \quad (\text{b.2})$$

where we used  $\square = \delta_i^i = N_c$ .

In the tensor space of all linear maps  $V \otimes \bar{V} \rightarrow V \otimes \bar{V}$  spanned by  $\{I, T\}$ , the action of  $T$  is given by the matrix

$$M_T = \begin{pmatrix} 0 & 1 \\ 0 & N \end{pmatrix} \quad \text{with eigenvalues } \{\lambda_1, \lambda_2\} = \{0, N\}. \quad (\text{b.3})$$

The projection operator on the eigenspace associated to  $\lambda_1$  projects on the color singlet [irrep](#) subspace

$$\mathcal{P}_\bullet = \frac{1}{N_c} \begin{array}{c} \downarrow \quad \uparrow \\ \downarrow \quad \uparrow \end{array} \quad (\text{b.4})$$

and the projection operator associated to  $\lambda_2 = N_c$  projects on the adjoint [irrep](#) subspace

$$\mathcal{P}_{Adj} = \begin{array}{c} \xrightarrow{\quad} \\ \xleftarrow{\quad} \end{array} - \frac{1}{N_c} \begin{array}{c} \downarrow \quad \uparrow \\ \downarrow \quad \uparrow \end{array} = a^{-1} \begin{array}{c} \downarrow \quad \uparrow \\ \downarrow \quad \uparrow \end{array} \quad (\text{b.5})$$

The meaning of the last birdtrack of [b.5](#) is just a short handed notation for the moment. It is related to the color generator of the next section where  $a$  is usually defined by  $\text{tr}(t^a t^b) = a \delta^{ab} = \frac{1}{2} \delta^{ab}$ .

The two projectors span an orthonormal basis so that

$$\mathcal{P}_\bullet \cdot \mathcal{P}_{Adj} = 0, \quad (\mathcal{P}_\bullet)^2 = \mathcal{P}_\bullet, \quad (\mathcal{P}_{Adj})^2 = \mathcal{P}_{Adj} \quad (\text{b.6})$$

In the case where  $N_c = 3$ , the singlet and adjoint irreps have dimensions 1 and 8; the decomposition is thus often noted

$$\mathbf{3} \otimes \bar{\mathbf{3}} = \mathbf{1} \oplus \mathbf{8} \quad (\text{b.7})$$



An alternative would be to use the Yusti notation [49]. As color generator are defined right-handed, the l.h.s. inner part is an antiquark generator, and the r.h.s. inner part is a quark generator. Hence from this convention, the exchange of two legs in a generator contributes to a minus sign. This statement alone is wrong, it should be understood as the result of the action of flipping lines in a birdtracks and the convention for particle and anti-particle. In b.14, it is only the inner structure that is changed, the tensor initially defined anti-clockwise by the indices  $q\bar{q}g$ , remains the same.

The Lie bracket (commutator) of two color generators is related to the structure constant by<sup>3</sup>

$$[t^a, t^b]^j_k = (t^a)^j_\ell (t^b)^\ell_k - (t^b)^j_\ell (t^a)^\ell_k = i f_{abc} (t^c)^j_k \quad (\text{b.15})$$

or using birdtracks

$$\begin{array}{c} j \quad k \\ \hline \begin{array}{c} \text{wavy} \\ a \end{array} \quad \begin{array}{c} \text{wavy} \\ b \end{array} \end{array} - \begin{array}{c} j \quad k \\ \hline \begin{array}{c} \text{wavy} \\ a \end{array} \quad \begin{array}{c} \text{wavy} \\ b \end{array} \end{array} = \begin{array}{c} j \quad k \\ \hline \begin{array}{c} \text{wavy} \\ a \end{array} \quad \begin{array}{c} \text{wavy} \\ b \end{array} \end{array} \quad (\text{b.16})$$

with the three-gluons vertex  $\mathcal{V}_{ggg}$  defined by

$$\begin{array}{c} c \\ \text{wavy} \\ \begin{array}{c} a \quad b \end{array} \end{array} = i f_{abc} \quad (\text{b.17})$$

## b.3 Simple computations using birdtracks

### b.3.1 Color conservation

Structure constants of  $SU(N_c)$  verify the Jacobi identity, which similar to b.16 up to the replacement of the quark line by a gluon line:

$$\begin{array}{c} \text{wavy} \\ \text{wavy} \end{array} + \begin{array}{c} \text{wavy} \\ \text{wavy} \end{array} + \begin{array}{c} \text{wavy} \\ \text{wavy} \end{array} = 0 \quad (\text{b.18})$$

The Jacobi identity is one among many relations based on color conservation. Color conservation in birdtrack for an arbitrary number of legs (of arbitrary irreps) is given by

$$\begin{array}{c} \text{blob} \\ \vdots \end{array} + \dots + \begin{array}{c} \text{blob} \\ \vdots \end{array} = 0 \quad (\text{b.19})$$

The sum is over all possible gluon attachments to the external legs and holds independently of the form of the inner “blob”. The right side of the blob is in a singlet state as

<sup>3</sup>We don’t need a distinction between upper and lower indices for gluons since the adjoint representation  $A$  is over the field of real numbers. By opposition,  $V$  and its dual  $\bar{V}$  are over the field of complex numbers and require a distinction between upper and lower indices.

there is no color flux on the left side of the blob. Hence the sum the color generators of all legs of the singlet system must vanish.

We already saw color conservation at work in previous identities: the structure constant can be viewed as b.19 applied to a singlet  $q\bar{q}g$  system, the Jacobi identity b.18 arises when applying b.19 to a singlet  $ggg$ -system, and the sign convention between a quark and an antiquark color generator b.14.

### b.3.2 Casimir operators

An important operator for practical applications is the quadratic Casimir operator. When there is no ambiguity, I will call the quadratic Casimir operator “the Casimir operator” and its eigenvalue “the Casimir”. Let us start with an arbitrary generalized parton in some irrep  $\mathbf{R}$  of  $SU(N_c)$  built from a tensor product of defining representations for instance.

#### Building blocks

The first tensor to think of in this case is the trivial Kronecker delta  $\delta_j^i$ , where  $i$  and  $j$  are indices that takes values  $1, \dots, K_R$  where  $K_R$  is the dimension of the irrep. Following the quark convention in the previous section, I will introduce an oriented dashed line for such a tensor.

$$\delta_j^i \equiv i \text{ -----} j$$

In the decomposition of the tensor product  $\mathbf{R} \otimes \bar{\mathbf{R}}$ , there is always at least one adjoint irrep denoted “ $\mathbf{A}$ ”. This means that in birdtrack notation there exists a vertex of the following form:

$$\forall R : \text{---} \text{---} \text{---} \longrightarrow \begin{array}{c} \text{---} \text{---} \text{---} \\ \text{---} \\ \text{---} \end{array}$$

where the curly line obviously carries the adjoint irrep. This diagram can be interpreted as a color generator often noted as  $(T_R^a)_j^i$ , a linear map:  $\mathbf{R} \otimes \bar{\mathbf{R}} \rightarrow \mathbf{A}$ , or a non-zero Clebsch-Gordan coefficient. As for in quark generator, this generator is related to the generator of irrep  $\bar{\mathbf{R}}$  by  $(T_R^a) = -(T_{\bar{R}}^a)$

#### Quadratic Casimir operator

The quadratic Casimir operator is defined in birdtracks as:

$$\text{---} \text{---} \text{---} \text{---} \text{---} = C_R \text{---} \text{---} \text{---} \text{---} \text{---} \tag{b.20}$$

It is the usual  $T_R^a T_R^a$  operator that maps  $\mathbf{R} \rightarrow \mathbf{R}$  with eigenvalue  $C_R$ . As the color generator is anti-symmetric under the crossing of two legs, the Casimir for an irrep or its

conjugate irrep is identical:

The diagram shows a dashed line with a wavy loop on top, followed by an equals sign, then a dashed line with a wavy loop on the bottom, followed by another equals sign, and finally the symbol  $C_R$  followed by a dashed line with an arrow pointing left.

### Casimir operator and systems

We consider a projection operator from two irreps  $\mathbf{R}_1$  and  $\mathbf{R}_2$  into an irrep noted  $\alpha$ . The linear map associated is  $\mathbf{R}_1 \otimes \mathbf{R}_2 \rightarrow \alpha \rightarrow \mathbf{R}_1 \otimes \mathbf{R}_2$  and following this logic I will denote a projector  $\mathcal{P}_\alpha$  as

The diagram shows a circle labeled  $\alpha$  with four external legs. The top two legs are labeled  $R_1$  and the bottom two are labeled  $R_2$ . This is followed by an equals sign, then a diagram of two lines merging into a dashed line labeled  $\alpha$ , which then splits back into two lines. This is followed by another equals sign and the label  $C_R$ .

The l.h.s. will often be used in calculation and the inner blob typically contain a sum over different contractions between external legs and simple tensors. The r.h.s. can be used for simple cases (as in the Fierz identity for  $q\bar{q} \rightarrow q\bar{q}$  where the dashed line would be identified as a gluon line up to factors) but can be hard to obtain as it requires to know the associated Clebsch-Gordan coefficient. However, it proves to be very useful in formal calculations.

The color generator of a system is simply given by a sum over individual color generators (this is simply color conservation, see b.19). Using the notation of the r.h.s. of b.21, it is

The diagram shows a sum of two diagrams. The first has a red wavy line entering from the bottom left and connecting to the top left of the merging lines. The second has a red wavy line entering from the bottom left and connecting to the bottom left of the merging lines. This is followed by an equals sign and a diagram with a red wavy line entering from the bottom left and connecting to the top right of the merging lines.

After squaring this color generator, one finds

The diagram shows a sum of three terms. The first is a diagram with a red wavy line connecting the top left and top right of the merging lines. The second is a diagram with a red wavy line connecting the bottom left and bottom right of the merging lines. The third is a diagram with a red wavy line connecting the top left and bottom right of the merging lines. This is followed by an equals sign and a diagram with a red wavy line connecting the top left and top right of the merging lines.

If the red gluon connects to the same line twice, it can be identified as a Casimir operator. The latter expression thus reduces to

The diagram shows a diagram with a red wavy line connecting the top left and bottom left of the merging lines, followed by an equals sign, then the fraction  $\frac{C_{R_1} + C_{R_2} - C_\alpha}{2}$ , followed by another equals sign and a diagram with a red wavy line connecting the top left and top right of the merging lines.

This expression is valid for any  $\alpha \subset \mathbf{R}_1 \otimes \mathbf{R}_2$  and will be very useful in practice.

### b.3.3 Simplification tips

From the set of simple rules shown in the previous section, one can obtain a handful number of simplification tricks to address the color structure in QCD. I will derive a few in the rest of this section, to get more familiar with birdtrack calculations.



### Using color conservation

Consider a "parton" of irrep  $R$ : it can be the fundamental, the adjoint or any irrep built from a tensor product of two  $SU(N_c)$  irreps. There is always the adjoint irrep, within the decomposition of the tensor product  $R \otimes \bar{R}$ . Analogously to b.18, one can apply color conservation to the color generator:

$$\begin{array}{c} \color{red}{\text{wavy}} \\ \color{red}{\text{wavy}} \\ \color{red}{\text{wavy}} \end{array} + \begin{array}{c} \color{red}{\text{wavy}} \\ \color{red}{\text{wavy}} \\ \color{red}{\text{wavy}} \end{array} + \begin{array}{c} \color{red}{\text{wavy}} \\ \color{red}{\text{wavy}} \\ \color{red}{\text{wavy}} \end{array} = 0 \tag{b.24}$$

One can then connect the red gluon in different ways.

i) one can connect the red gluon to the remaining gluon leg of the initial vertex as follows:

$$\begin{array}{c} \color{red}{\text{wavy}} \\ \color{red}{\text{wavy}} \\ \color{red}{\text{wavy}} \end{array} + \begin{array}{c} \color{red}{\text{wavy}} \\ \color{red}{\text{wavy}} \\ \color{red}{\text{wavy}} \end{array} + \begin{array}{c} \color{red}{\text{wavy}} \\ \color{red}{\text{wavy}} \\ \color{red}{\text{wavy}} \end{array} = 0$$

The first and third diagrams are the same: if one flips the two vertices involving the red gluon in the third diagram, it introduces a factor  $(-1)^2$ . The second diagram reduces using the following steps: 1/ flip one of the two  $ggg$  vertices, 2/ recognize the Casimir operator applied to the gluon line and 3/ replace the Casimir operator by its eigenvalue  $C_A = N_c$ . This leads to the relation (valid for any irrep  $R$ ):

$$\begin{array}{c} \color{red}{\text{wavy}} \\ \color{red}{\text{wavy}} \\ \color{red}{\text{wavy}} \end{array} = \frac{C_A}{2} \begin{array}{c} \color{red}{\text{wavy}} \\ \color{red}{\text{wavy}} \\ \color{red}{\text{wavy}} \end{array}$$

ii) in b.24, one can connect the red gluon to one dashed line, say the top line:

$$\begin{array}{c} \color{red}{\text{wavy}} \\ \color{red}{\text{wavy}} \\ \color{red}{\text{wavy}} \end{array} + \begin{array}{c} \color{red}{\text{wavy}} \\ \color{red}{\text{wavy}} \\ \color{red}{\text{wavy}} \end{array} + \begin{array}{c} \color{red}{\text{wavy}} \\ \color{red}{\text{wavy}} \\ \color{red}{\text{wavy}} \end{array} = 0$$

The first diagram contributes as the bare color generator times the Casimir of the irrep  $\mathbf{R}$ . The second diagram is the opposite of the previous result, that is the bare generator times  $-C_A/2$ . This leads to the relation (valid for any irrep  $\mathbf{R}$ ):

$$\begin{array}{c} \color{red}{\text{wavy}} \\ \color{red}{\text{wavy}} \\ \color{red}{\text{wavy}} \end{array} = \frac{2C_R - C_A}{2} \begin{array}{c} \color{red}{\text{wavy}} \\ \color{red}{\text{wavy}} \\ \color{red}{\text{wavy}} \end{array}$$

### Trace representation of $ggg$ -vertices

From the structure constant definition (see b.16) one can choose to contract the quark and antiquark lines with the quark color generator:

$$a^{-1} \left[ \begin{array}{c} \text{---} \\ \text{---} \\ \text{---} \end{array} \right] + \begin{array}{c} \text{---} \\ \text{---} \\ \text{---} \end{array} \right] = \begin{array}{c} \text{---} \\ \text{---} \\ \text{---} \end{array} \quad (\text{b.25})$$

where  $a$  was defined in b.5. It is also useful to introduce the other linear combination:

$$a^{-1} \left[ \begin{array}{c} \text{---} \\ \text{---} \\ \text{---} \end{array} \right] - \begin{array}{c} \text{---} \\ \text{---} \\ \text{---} \end{array} \right] = \begin{array}{c} \text{---} \\ \text{---} \\ \text{---} \end{array} \quad (\text{b.26})$$

The l.h.s. of b.25 (resp b.26) is a trace representation of the three-gluon anti-symmetric  $f_{abc}$  (resp symmetric  $d_{abc}$ ) vertex. Those two relations with the Fierz identity are the basic blocks used to decompose any color structure in a Feynman diagram in the “trace basis”, using the following simple algorithm. For each Feynman diagram:, 1/ express each  $ggg$  vertex in the previous trace representation, 2/ use the Fierz identity to remove all gluon lines, 3/ replace each closed quark loop by a factor  $N_c$ .

**Summary of birdtracks identities involving fundamental and/or adjoint irrep of  $SU(N_c)$  .**

Dimensions

$$\bigcirc = K_F = N_c \tag{b.27}$$

$$\odot = K_A = N_c^2 - 1 \tag{b.28}$$

”Self-energy graph”

$$\begin{array}{c} \text{---} \text{---} \text{---} \\ \text{---} \text{---} \text{---} \end{array} = \frac{N_c^2 - 1}{2N_c} \text{---} \tag{b.29}$$

$$\begin{array}{c} \text{---} \text{---} \text{---} \\ \text{---} \text{---} \text{---} \end{array} = N_c \text{---} \tag{b.30}$$

$$\begin{array}{c} \text{---} \text{---} \text{---} \\ \text{---} \text{---} \text{---} \end{array} = a \text{---}, \quad a = 1/2 \tag{b.31}$$

$$\begin{array}{c} \text{---} \text{---} \text{---} \\ \text{---} \text{---} \text{---} \end{array} = \frac{N_c^2 - 4}{N_c} \text{---} \tag{b.32}$$

$$\begin{array}{c} \text{---} \text{---} \text{---} \\ \text{---} \text{---} \text{---} \end{array} = 0 \tag{b.33}$$

One loop correction to  $q\bar{q}g$ -vertex

$$\begin{array}{c} \text{---} \text{---} \text{---} \\ \text{---} \text{---} \text{---} \end{array} = \frac{-1}{2N_c} \begin{array}{c} \text{---} \text{---} \text{---} \\ \text{---} \text{---} \text{---} \end{array} \tag{b.34}$$

$$\begin{array}{c} \text{---} \text{---} \text{---} \\ \text{---} \text{---} \text{---} \end{array} = \frac{N_c}{2} \begin{array}{c} \text{---} \text{---} \text{---} \\ \text{---} \text{---} \text{---} \end{array} \tag{b.35}$$

$$\begin{array}{c} \text{---} \text{---} \text{---} \\ \text{---} \text{---} \text{---} \end{array} = -\frac{N_c^2 - 4}{2N_c} \begin{array}{c} \text{---} \text{---} \text{---} \\ \text{---} \text{---} \text{---} \end{array} \tag{b.36}$$

$$\begin{array}{c} \text{---} \text{---} \text{---} \\ \text{---} \text{---} \text{---} \end{array} = +\frac{N_c^2 - 4}{2N_c} \begin{array}{c} \text{---} \text{---} \text{---} \\ \text{---} \text{---} \text{---} \end{array} \tag{b.37}$$

One loop correction to  $ggg$ -vertex

$$\begin{array}{c} \text{---} \text{---} \text{---} \\ \text{---} \text{---} \text{---} \end{array} = \frac{N_c}{2} \begin{array}{c} \text{---} \text{---} \text{---} \\ \text{---} \text{---} \text{---} \end{array} \tag{b.38}$$

$$\begin{array}{c} \text{---} \text{---} \text{---} \\ \text{---} \text{---} \text{---} \end{array} = \frac{N_c}{2} \begin{array}{c} \text{---} \text{---} \text{---} \\ \text{---} \text{---} \text{---} \end{array} \tag{b.39}$$

$$\begin{array}{c} \text{---} \text{---} \text{---} \\ \text{---} \text{---} \text{---} \end{array} = \frac{N_c^2 - 4}{2N_c} \begin{array}{c} \text{---} \text{---} \text{---} \\ \text{---} \text{---} \text{---} \end{array} \tag{b.40}$$

$$\begin{array}{c} \text{---} \text{---} \text{---} \\ \text{---} \text{---} \text{---} \end{array} = \frac{N_c^2 - 12}{2N_c} \begin{array}{c} \text{---} \text{---} \text{---} \\ \text{---} \text{---} \text{---} \end{array} \tag{b.41}$$

An other useful relation

$$\begin{array}{c} \text{---} \text{---} \text{---} \\ \text{---} \text{---} \text{---} \end{array} = \frac{1}{2N_c} \text{---} + \frac{1}{2} \begin{array}{c} \text{---} \text{---} \text{---} \\ \text{---} \text{---} \text{---} \end{array} + \frac{1}{2} \begin{array}{c} \text{---} \text{---} \text{---} \\ \text{---} \text{---} \text{---} \end{array} \tag{b.42}$$

This chapter studies the transverse momentum broadening of a fast parton system crossing a nuclear medium. It is based on the publication [50]. I will consider the case of an academic pair (or system) of asymptotic partons crossing a QCD medium. This case is not a realist one, but those results will be used in the next chapter where I will consider production cross section. The emphasize is done on the color structure associated to this process. The aim is to give an answer to a question that one may often ask in phenomenology: "what is the associated color factor associated to this process?".

### 3.1 Color structure of the $p_t$ -broadening process

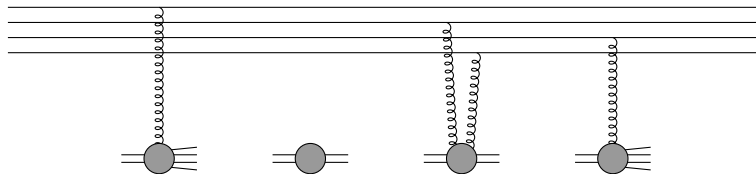
#### 3.1.1 Scattering process and multipole picture

Let us consider a system of  $n$  asymptotic partons in some given irreps denoted by  $\mathbf{R}_i$  with  $i = 1, \dots, n$ . This system is prepared in the far past (when  $t \rightarrow -\infty$ ) and will be observed in the far future (when  $t \rightarrow +\infty$ ). Along its way, the system will cross a nuclear medium (a nucleus  $A$ ) between  $t = 0$  and  $t = L$ . This is the ideal situation to compute  $S$ -matrix elements.

In the rest frame of the target nucleus, the process looks like

$$\{\text{system}\} + A \rightarrow \{\text{system}\} + X \quad (3.1)$$

where  $X$  denotes remnants produced after the collision and arising from inelastic parton-nucleon collisions. For  $n = 4$ , this situation is represented by Feynman amplitudes such as:

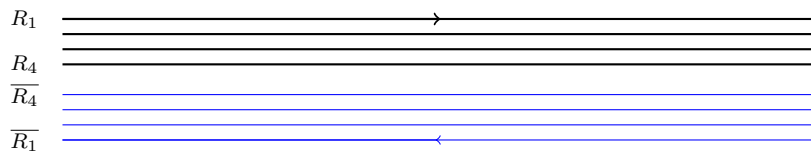


The four upper lines indicate the fast parton system crossing the medium. Interactions with the medium are represented by gluon exchanges over the target nucleons:

- A single gluon exchange with a nucleon indicates that the latter will break up. The conjugate amplitude also contains a single gluon exchange (off the same nucleon). This correspond to inelastic parton-nucleon scattering.
- A two gluon exchange correspond to a virtual correction to the cross section. In this case the nucleon remains intact and the conjugate amplitude contains no gluon exchange on that nucleon. This nucleon is said to undergo an elastic scattering.

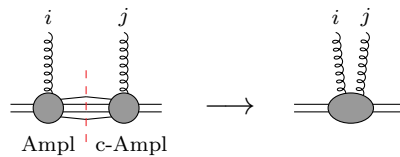
Along the lines of the dipole picture [51, 52], one can choose to directly draw diagrams contributing to the cross section rather than just the amplitude.

First, the am lines of the parton system in the amplitude and its conjugate are placed on top of each other as follows:

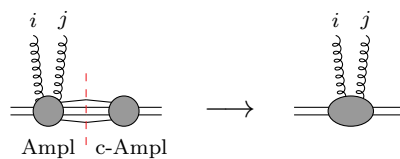


Note that due to complex conjugation, the direction of arrows is reversed in the conjugate amplitude.

An inelastic interaction in the amplitude, together with its counterpart in the conjugate amplitude, is represented as:



A virtual correction is represented similarly as:



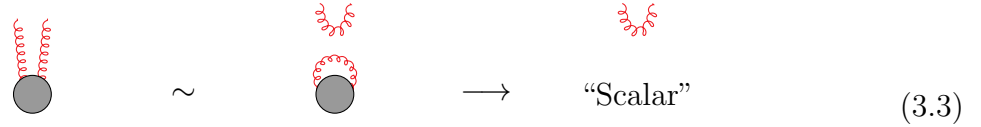
A generic contribution to the cross section will thus be of the form:

**Remarks:**

1. Virtual corrections have a relative minus sign, and a symmetry factor 1/2 when the two gluons are attached to the same line. It will be properly taken into account later. For the moment, I want to focus on the color space associated to such contributions to the cross section.
2. From the point of view of 3.2, the blob attached to each two-gluon interaction does not break up. As the observable considered is inclusive over the remnants produced in the nucleus breakup, there is an implicit summation over produced remnant. This is equivalent to consider a forward scattering amplitude for the  $2n$ -parton system which is elastic with respect to target nucleons.

### 3.1.2 Color space at the cross section level

At the level cross section, each interaction represented in 3.2 is a two-gluon exchange, which must be a color singlet since each number remains singlet in the forward "multipole" scattering amplitude. This means that using birdtracks the associated color structure (tensor) looks like the following

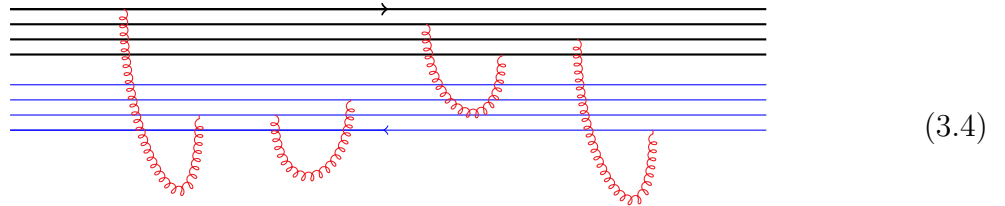


$$\text{blob with 2 red gluons} \sim \text{blob with 2 red gluons top, 2 red gluons bottom} \longrightarrow \text{"Scalar"} \quad (3.3)$$

where the two red gluons connect to the projectile (the  $2n$ -parton system).

This greatly simplifies the color structure for the evolution of the  $2n$ -parton system in the nuclear medium. Each interaction of the parton system with a nucleon of the target is simply a color tensor proportional to  $\delta^{ab}$ , contracted with two color generators  $T_i^a$  and  $T_j^b$  where  $i$  and  $j$  label the line where the two gluons connect.

Each interaction with the nucleus is a map  $\otimes_{i=1}^n (\mathbf{R}_i \otimes \overline{\mathbf{R}}_i) \longrightarrow \otimes_{i=1}^n (\mathbf{R}_i \otimes \overline{\mathbf{R}}_i)$ . In order to compute the color structure, one can take the Feynman diagram 3.2 and remove every nucleon from the gluon line connecting the parton lines to obtain the associated color tensor:



$$\text{Diagram with black and blue lines and red gluon loops} \quad (3.4)$$

The first interaction with the medium as the color structure  $(T_{R_1}^a T_{R_2}^b) \delta_{ab}$ . A kinematic factor  $\omega_{1\bar{2}}$  that I will discuss soon. From 3.4, we already see the iteration of an operator of the form

$$\hat{O} \equiv \omega_{ij} \times [T_i^a T_j^a] \quad (3.5)$$

acting on the vector space  $V = (\mathbf{R}_1 \otimes \cdots \otimes \mathbf{R}_n) \otimes (\overline{\mathbf{R}}_1 \otimes \cdots \otimes \overline{\mathbf{R}}_n)$ .

In the sum over all Feynman diagram, there will be a sum over  $i, j = \{1, 2, 3, 4; \bar{4}, \bar{3}, \bar{2}, \bar{1}\}$ .

### 3.1.3 Vector space and basis choice.

*A basis to span them all.*

Almost Tolkien's story.

To identify the relevant part of the vector space  $V$  to be considered, one should move back from the  $2n$ -parton system (at the cross section level) to the  $n$ -parton system (at the amplitude level). The most straightforward case to consider is to require that the initial (resp. final) state of the  $n$ -parton system is in a given **irrep** for both amplitude and its conjugate. This requirement reduces the full vector space  $V$  to singlet subspaces. In general, there are several singlet subspaces, and a basis to span all possible singlet subspaces may prove to be useful!

**“How many singlets?”** There are many tools available to decompose a tensor product such as  $V$ , however one can use the following tips. The amplitude and its conjugate have the same number and same type of partons involved. The decomposition of the amplitude color space reads

$$V_{ampl} = \otimes_{i=1}^n \mathbf{R}_i = \oplus_{\mathbf{i}} \alpha_{\mathbf{i}} \quad (3.6)$$

with  $\alpha_i$  all possible **irreps** that decompose  $V_{ampl}$ . Obviously,  $V_{am\bar{pl}} = \oplus_i \bar{\alpha}_i$ . Now, each singlet of  $V = V_{ampl} \otimes V_{am\bar{pl}}$  can only be obtained when  $\alpha_i$  and  $\bar{\alpha}_j$  are conjugate to each other. If an **irrep** appears only once in the decomposition of  $V_{ampl}$ , there is only one singlet associated in  $V$ . If an **irrep** appears several times in the decomposition of  $V_{ampl}$  with multiplicity  $m$ , there will be  $m^2$  associated singlet in  $V$ .

#### Basis choice

I will denote a color singlet of  $V$  as  $|w^{(2n)}\rangle$ , the upperscript indicating the number of elementary partons involved. Following the previous tips, if  $u_i$  is an **irrep** of  $V_{ampl}$  and  $v_j$  is an **irrep** of  $V_{am\bar{pl}}$ , a singlet of  $V$  arise when  $u_i$  and  $v_j$  are conjugate to each other,

$$|w^{(2n)}\rangle \longrightarrow |u_i, v_j = \bar{u}_i\rangle \equiv \text{Singlet of } V \quad (3.7)$$

To get used to this, consider a digluon pair. The decomposition of  $V_{ampl}$  is given by:

$$\mathbf{8} \otimes \mathbf{8} = \mathbf{1} \oplus \mathbf{8}_a \oplus \mathbf{8}_s \oplus \mathbf{10} \oplus \bar{\mathbf{10}} \oplus \mathbf{27} \oplus \mathbf{0} \quad (3.8)$$

the two subscripts  $a$  and  $s$  label the two different octets of the decomposition. The list of color singlets of  $V = \mathbf{8} \otimes \mathbf{8} \otimes \mathbf{8} \otimes \mathbf{8}$  contains

$$|1, 1\rangle, \quad |10, \bar{10}\rangle, \quad |\bar{10}, 10\rangle, \quad |27, 27\rangle, \quad |0, 0\rangle$$

when an **irrep** appears once in the amplitude or its conjugate. It also contains

$$|\mathbf{8}_a, \mathbf{8}_a\rangle, \quad |\mathbf{8}_s, \mathbf{8}_s\rangle, \quad |\mathbf{8}_a, \mathbf{8}_s\rangle, \quad |\mathbf{8}_s, \mathbf{8}_a\rangle$$

when an **irrep** (the octet in the present case) appears twice.

## Gauge invariance

It is now easy to build a scalar under gauge rotation for the considered process. Pick an arbitrary contribution at the cross section level such as 3.2. The associated color structure is given by 3.4. Contracting this tensor with  $\langle u_a, v_b |$  (on the left) and with  $|u_c, v_d\rangle$  (on the right) it gives

$$\langle u_a, v_b | \prod_t \left\{ \sum_{ij} \omega_{ij}^t \times [T_i T_j] \right\} | u_c, v_d \rangle \equiv \sigma_{b \rightarrow d}^{a \rightarrow c} \quad (3.9)$$

where  $a$  and  $c$  label irreps of  $V_{ampl}$ ,  $b$  and  $d$  irreps of  $V_{\bar{ampl}}$ , and  $\omega_{ij}^t$  is a kinematic factor associated to the gluon exchange between  $i$  and  $j$  in the medium at the time  $t$ .

The scalar 3.9 is written in such a way to emphasize the irrep of the parton system in the initial state ( $u_a$  in the amplitude and  $v_b$  in the conjugate amplitude) and in the final state ( $u_c$  and  $v_d$ ).

## Projector basis

From the digluon example, one can see that when an irrep appears more than once in a decomposition, one has to be careful.

Consider a vector space in an amplitude  $V_1$  and in a complex amplitude  $V_2$ . For an irrep  $\alpha \subset V_1$  and an other irrep  $\beta \subset V_2$ .

- If the two irreps have the same Young Diagram (the shape of a Young Tableau) then I will denote  $\alpha \equiv \beta$ .
- If the two irreps have the same Young Tableau (same shape and same number in each box) then I will denote  $\alpha = \beta$ .

The previous basis of all singlets of  $V$  is currently called the *vector basis* (name inspired by table 2 of [48]). As we saw in the digluon case, the vector basis may contain elements such as  $|u_i, v_j\rangle = |8_a, 8_s\rangle$  where  $8_a \equiv 8_s$  but  $8_a \neq 8_s$ !

One defines the *projector basis* as the set of all elements of the *vector basis* that verifies  $u_i = \bar{v}_j$ . Let us look at the digluon pair again. The projector basis contains

$$|1, 1\rangle, \quad |10, \bar{10}\rangle, \quad |\bar{10}, 10\rangle, \quad |27, 27\rangle, \quad |0, 0\rangle, \quad |8_s, 8_s\rangle, \quad |8_a, 8_a\rangle$$

but not

$$|8_s, 8_a\rangle, \quad |8_a, 8_s\rangle$$

## Utility of the projector basis ?

Due to the form of the medium interaction described at the beginning of this chapter, it turns out that for a *parton pair* we do not need to consider the vector space but only the projector space.

Let's see why in the case of the digluon pair. Take the bra  $\langle 8_a, 8_s |$  (an element of the vector basis but not in the projector basis) and the ket  $|8_a, 8_a\rangle$  (an element of the

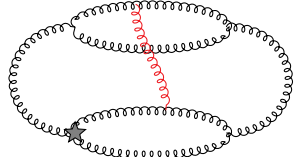


projector basis). A possible mixing between those states might arise through the following birdtrack:



$$(3.10)$$

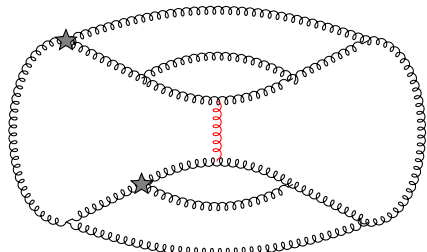
As the system (from left to right) is an overall singlet at any time of the evolution, color conservation leads to



$$3.10 = (-) (3.11)$$

The birdtrack in 3.11 is equal to the birdtrack in 3.10 since exchanging the two gluon lines in the amplitude introduces a symmetry factor  $(-1)^2$ . Due to the minus sign of 3.11 the birdtrack must vanish. In conclusion, there is no mixing between  $|\mathfrak{8}_a, \mathfrak{8}_s\rangle$  and  $|\mathfrak{8}_a, \mathfrak{8}_a\rangle$ . Assuming (as we will do) the pair color state at a given time (for instance the initial time) to be the same in the amplitude and its conjugate, i.e. assuming that we start from a state in the *projector basis*, we will remain in the projector basis at any time.

**A remark.** This reduction from the vector basis to the projector basis for the broadening seems hard to achieve for  $n$ -parton systems with  $n \geq 3$ . It can easily be checked for three gluons the contribution



$$(3.12)$$

does not vanish. This birdtrack corresponds to  $\langle \mathfrak{8}_s^{(a)}, \mathfrak{8}_a^{(s)} | T_3 T_{\bar{3}} | \mathfrak{8}_a^{(a)}, \mathfrak{8}_a^{(a)} \rangle$  where the notation is inspired by the historical construction method for projectors [48]. In  $\mathfrak{8}_a^{(s)}$  the superscript indicates that two gluons are first projected into the symmetric octet, and the subscript indicates that the remaining gluon together with the digluon is projected into an anti-symmetric octet. Let us note that there are eight octets built from three gluons that are labelled in this convention by:

$$\mathfrak{8}^{(1)}, \quad \mathfrak{8}_s^{(s)}, \quad \mathfrak{8}_a^{(s)}, \quad \mathfrak{8}_s^{(a)}, \quad \mathfrak{8}_a^{(a)}, \quad \mathfrak{8}^{(10)}, \quad \mathfrak{8}^{(\bar{10})}, \quad \mathfrak{8}^{(27)}$$

### Completeness relation and color kernel

The  $2n$ -parton system to be considered here is projected into a singlet state. This is done by either choosing the projector basis (for a pair,  $n = 2$ ) or the vector basis (for  $n \geq 3$ ). At any time in the medium, the  $2n$ -partons are in a color singlet, hence one can write a completeness relation

$$\mathbb{1} = \sum_i |w_i^{(2n)}\rangle \langle w_i^{(2n)}| \quad (3.13)$$

where  $\mathbb{1}$  is the identity map  $V_{singlet} \rightarrow V_{singlet}$  and  $w_i^{(2n)}$  is an element of the singlet basis chosen to span  $V_{singlet}$ . Inserting this identity between each interaction in 3.9, we are basically looking at

$$\langle w_\ell^{(2n)} | \hat{\mathcal{O}} | w_r^{(2n)} \rangle \quad (3.14)$$

where  $\hat{\mathcal{O}}$  was defined 3.5 as  $\hat{\mathcal{O}} \equiv \omega_{ij} \times [T_i^a T_j^a]$ .

## 3.2 Kinetic equation and evolution kernel

This section is dedicated to the derivation of the transverse momentum distribution of asymptotic parton systems. Notations will be introduced in the case of a single fast parton. Then the generalization to an asymptotic pair in the same formalism is presented. Finally, some general properties are discussed for systems involving an arbitrary number of partons.

### 3.2.1 Scattering potential and single parton case

This subsection is dedicated to the simplest case of the  $p_t$ -broadening, namely the single parton case. The main purpose here is to fix some notations that will be used to study parton systems, and to recall the derivation of  $p_t$ -broadening using a kinetic equation.

The first step is to introduce the "scattering potential" of the parton off a nucleon, a key ingredient of the problem. The second step is to use a probabilistic approach to describe the evolution of the fast parton along the medium. It will be argued later (see section 3.2.2) when such approach is valid. The final step is to obtain the transverse momentum distribution by going to the transverse position space.

#### Scattering potential

Let us choose the fast single parton to be in an **irrep**  $\mathbf{R}$ . The parton-nucleon cross section is proportional to the *scattering potential*  $\mathcal{V}$  defined as a function of the transverse momentum  $\vec{q}$  exchanged between the parton and the nucleon ,

$$\mathcal{V}(\vec{q}) = \frac{\mu^2}{\pi(\vec{q}^2 + \mu^2)^2} \quad \int d^2 \vec{q} \mathcal{V}(\vec{q}) = 1 \quad (3.15)$$

Here, all vectors are two dimensional vectors and they live in the plane transverse to the direction of the initial parton. The quantity  $\mathcal{V}$  is a screened Coulomb potential with screening length  $1/\mu$ . This screening is expected in QCD because of color neutrality at large distances. The scale  $\mu$  should be understood as commensurate to the QCD parameter,  $\mu \sim \mathcal{O}(\Lambda_{QCD})$ .

Associated to this potential, an interaction comes with a color structure. This color structure is simple since the parton stays in **irrep**  $\mathbf{R}$  (it only rotates its color index after gluon exchanges). At the cross section level, as shown in the previous section, this interaction is a map  $\mathbf{R} \otimes \bar{\mathbf{R}}|_{singlet} \rightarrow \mathbf{R} \otimes \bar{\mathbf{R}}|_{singlet}$ . There is obviously only one singlet  $w^{(2)}$  here, so the color structure always reduces to:

$$\langle w^{(2)} | T_i T_j = C_R \langle w^{(2)} | \quad \forall \{i, j\} = 1, 2 \quad (3.16)$$

with the Casimir  $C_R$  which will factor out at each interaction.

We give the Fourier transform of the scattering potential

$$\tilde{\mathcal{V}}(\vec{b}) = \int d^2\vec{q} e^{i\vec{q}\cdot\vec{b}} \mathcal{V}(\vec{q}) = \mu|\vec{b}| K_1(\mu|\vec{b}|), \quad (3.17)$$

since as we will see, it is natural to solve such a problem in transverse coordinate space

### Evolution in the medium

Let's consider that the distribution in transverse momentum of the parton is known at a given "time"  $t_0$  and is denoted as  $f(\vec{p}, t)$ . One can segment the path of the parton along its eikonal trajectory (a straight line in the medium with length  $L \sim A^{1/3}$  for a target nucleus) into small paths  $\delta t$  corresponding to the average distance between nucleons (typically  $\delta t \sim 1 fm \sim \Lambda_{QCD}^{-1}$ ). The probability that the parton interacts with a nucleon along a small path  $\delta t$  in the nuclear medium is related to the parton mean free path  $\lambda_R$ . The latter is related to the color charge of the parton as expected from 3.16, to the nuclear density and also to the parton-nucleon cross section. Anticipating the next section, it is useful to define a "color-stripped" mean free path as  $\lambda_0 = \lambda_R C_R$ .

In the limit  $\delta t/\lambda_R \ll 1$ , we can keep only the linear term in the probability for the parton to interact with a nucleon:

$$P^{(int)}(\delta t \ll \lambda_R) = \frac{\delta t}{\lambda_R} + \mathcal{O}\left(\left(\frac{\delta t}{\lambda_R}\right)^2\right) \ll 1 \quad (3.18)$$

If an interaction happens along this path  $\delta t$ , the potential  $\mathcal{V}(\vec{q})$  gives the probability to exchange the momentum  $\vec{q}$  between the parton and the nucleon.

Let us represent what one expects for the distribution  $f(\vec{p}, t + \delta t)$  as follows:

$$f(\vec{p}, t) \left[ \begin{array}{l} \xrightarrow{1 - \frac{\delta t}{\lambda_R}} f(\vec{p}, t) \\ + \\ \xrightarrow{\frac{\delta t}{\lambda_R}} \int d^2\vec{q} \mathcal{V}(\vec{q}) f(\vec{p} - \vec{q}, t) \end{array} \right] \Rightarrow f(\vec{p}, t + \delta t)$$

The initial distribution at time  $t$  may be affected in two ways: Two possibilities:

- During  $\Delta t$ , there is no interaction with a nucleon. This occurs with an associated probability  $1 - \frac{\delta t}{\lambda_R}$ . This possibility thus contributes to  $f(\vec{p}, t + \delta t)$  as  $\left(1 - \frac{\delta t}{\lambda_R}\right) \times f(\vec{p}, t)$ .
- During  $\Delta t$ , there is an interaction with a nucleon, with an associated probability  $\frac{\delta t}{\lambda_R}$ . In this case, one has to sum over all possible exchanged momenta distributed according to the scattering potential  $\mathcal{V}$ .

This possibility contributes to  $f(\vec{p}, t + \delta t)$  as  $\left(\frac{\delta t}{\lambda_R}\right) \times \int_{\vec{q}} \mathcal{V}(\vec{q}) f(\vec{p} - \vec{q}, t)$ .

The sum gives an equation relating  $f(\vec{p}, t + \delta t)$  to  $f(\vec{p}, t)$

$$f(\vec{p}, t + \delta t) = \left(1 - \frac{\delta t}{\lambda_R}\right) \times f(\vec{p}, t) + \frac{\delta t}{\lambda_R} \int_{\vec{q}} \mathcal{V}(\vec{q}) f(\vec{p} - \vec{q}, t). \quad (3.19)$$

### Solution in the transverse coordinate space

Equation 3.19 can be rewritten as

$$f_{t+\delta t}(\vec{p}) = [(1 - a) f_t + a \mathcal{V} \otimes f_t](\vec{p}) \quad (3.20)$$

with  $\otimes$  the convolution operator,  $a = \delta t / \lambda_R$ . In auxiliary  $\vec{b}$ -space it becomes

$$\begin{aligned} f_{t+\delta t}(\vec{b}) &= [(1 - a) f_t + a \mathcal{V} \cdot f_t](\vec{b}) \\ &= [1 - a(1 - \mathcal{V})] f_t(\vec{b}) \end{aligned}$$

With  $n = L/\delta t$ , the previous equation becomes

$$f_{t+\delta t}(\vec{b}) = \left[1 - \frac{A}{n}\right] f_t(\vec{b})$$

with  $A = \frac{L}{\lambda_R} [1 - \mathcal{V}]$ . One can easily iterate this expression along the path in the medium from  $t = 0$  to  $t = L$ . The distribution is then given by

$$f_L(\vec{b}) = f_0(\vec{b}) \left[1 - \frac{A}{n}\right]^n \quad (3.21)$$

and in the limit where  $n = L/\delta t \gg 1$ , it becomes

$$f_L(\vec{b}) = f_0(\vec{b}) e^{-A} = f_0(\vec{b}) e^{-\frac{L C_R}{\lambda_0} [1 - \mathcal{V}(\vec{b})]} \quad (3.22)$$

Going back to momentum space by Fourier transform, one obtains

$$f_L(\vec{p}) = \int \frac{d^2 \vec{b}}{(2\pi)^2} e^{i \vec{p} \cdot \vec{b}} f_0(\vec{b}) e^{-\frac{L C_R}{\lambda_0} [1 - \mathcal{V}(\vec{b})]} \quad (3.23)$$

for the transverse momentum distribution of the parton after crossing the medium.

Alternatively, the above result can be obtained by taking the limit  $\delta t \rightarrow 0$  directly in 3.19. This give the integro-differential equation

$$\frac{\partial}{\partial t} f(\vec{p}, t) = \frac{1}{\lambda_R} \int d^2 \vec{q} \mathcal{V}(\vec{q}) [f(\vec{p} - \vec{q}, t) - f(\vec{p}, t)] \quad (3.24)$$

which in transverse coordinate space reads

$$\frac{\partial}{\partial t} f(\vec{b}, t) = -\frac{1}{\lambda_R} [1 - \mathcal{V}(\vec{b})] f(\vec{b}, t) \quad (3.25)$$

Requiring that  $\mathcal{V}(\vec{b})$  is independent of  $t$ , the solution at  $t = L$  with initial condition at  $t = 0$  reproduces 3.22, and 3.23 follows

### Interpretation

The expression 3.23 is well-known. Aside from the kinetic approach used in [53], it can be obtained by evaluating the correlator of two Wilson lines in the MV-model [43, 54].

In the auxiliary  $\vec{b}$ -space, the exponential factor is related to the scattering amplitude of a color dipole  $\mathbf{R}\bar{\mathbf{R}}$  with transverse separation  $\vec{b}$  off a nucleus. This scattering amplitude depends on  $C_R \cdot L/\lambda_0$ .

Equation 3.24 is the Boltzmann transport equation for the fast parton momentum distribution with only the collision term (collision with nucleons along the path of the parton).

### 3.2.2 Validity and limitations

Some assumptions are required in order to consider a kinetic approach to study the nuclear broadening. Those assumptions should be kept in mind when using the kinetic equation derived in the previous section.

#### Incoherent scattering

Each scattering between the fast parton and a nucleon is assumed to be independent of previous scatterings. This holds when the scattering range of the potential given by a the scale  $1/\mu$  is negligible compared to the parton mean free path  $\lambda_0$ . The quantum coherence from a scattering is destroyed when the next scattering occurs. When  $1/\mu \ll \lambda_0$ , successive scatterings occurs incoherently.

#### Static and homogeneous medium

Over the path of the fast parton in the medium (from  $t = 0$  to  $t = L$ ) the medium has been assumed to be static and homogeneous. As a consequence the parameters of the model ( $\mu$  and  $\lambda_0$ ) can be treated as independent of the time and space coordinates.

#### Length scales

In the form of 3.24 the kinetic equation relies on the demonstration assuming the step  $\delta t$  to be small compared to the mean free path  $\lambda_0$ :  $\frac{\delta t}{\lambda_0} \ll 1$ . This assumption could be relaxed, but in the derivation one should consider the probability of interaction  $P^{(int)}(\delta t) = 1 - e^{-\delta t/\lambda_0}$  instead of  $\delta t/\lambda_0$  (see [53]). The medium size  $L$  has to be large compared to the elementary step  $\delta t$ :  $L\mu \gg 1$ .

This follows from the fact that 3.24 is a Boltzmann transport equation, hence the infinitesimal element ( $\delta t$ ) needs to be small compared to the scale of the problem ( $L$ ) (see [55]).

Before moving to the parton pair let us look at the pictures associated with this approach for the medium.

**A bag of marbles.** The first picture which comes to mind is the nucleus being a big bag of marbles. Each marble represents a nucleon with effective radius  $\sim 1/\mu$  associated with a probability that the parton interacts  $\delta t/\lambda_0$  and a scattering potential  $\mathcal{V}$ . In this case one should consider the limit where  $\delta t \rightarrow 1/\mu$  and the other two scales verify  $\frac{1}{\mu} \ll \lambda_0 \ll L$ . The limit  $L \rightarrow \infty$  stands for  $L \gg \lambda_0$  and leads to the simple solution 3.23. Even if this limit seems to be drastic, it is in fact a good approximation to the finite (but large)  $L$  limit.

**A bag of water.** Another picture is to consider another bag filled with water. This corresponds to the limit  $\frac{\delta t}{\lambda_0} \rightarrow 0$ . At the same time, it means that  $n = L/\delta t \rightarrow \infty$ . Compared to the previous picture, one has to deal with pointlike objects with a very small interaction probability  $\delta t/\lambda_0 \rightarrow 0$ . Even if it is formally possible in 3.24 to imagine such limit, this is not a realistic picture for cold nuclear matter with finite size nucleons.

### 3.2.3 Asymptotic parton pair

We now consider the first minimal example where the non-abelian structure of QCD makes the problem of  $p_t$ -broadening non-trivial, namely the  $p_t$ -broadening of a parton pair.

To derive the transverse momentum distribution of the pair, I will start by defining the initial state of an asymptotic pair and recall the color basis used .. Then, I will use the kinetic theory approach to derive the pair distribution in the final state (i.e. after crossing the medium).

#### Initial state

Let us consider an initial asymptotic parton pair, and label the first (second) parton by 1 (resp. 2) in the amplitude and by 4 (resp. 3) in the conjugate amplitude. This labeling follows that of section 3.1 and the parton irreps verify

$$\mathbf{R}_1 = \bar{\mathbf{R}}_4 \quad , \quad \mathbf{R}_2 = \bar{\mathbf{R}}_3$$

In transverse momentum space, the pair is described by a wave function  $\psi$  that depends on transverse momenta  $\vec{p}_1$  and  $\vec{p}_2$ . Guided by the single parton case, it is natural to consider the Fourier transform of this wave function. In  $\vec{b}$ -space, the wave function depends only on transverse position  $\vec{x}_1$  and  $\vec{x}_2$ . The wave function is assumed to be invariant under transverse translations, and thus can depend only on  $\vec{x}_{12} = \vec{x}_1 - \vec{x}_2$ . Interactions between constituents of the system are turned off during and after the medium. This is motivated by phenomenological application of this model where we expect those interactions to be negligible when the relative momentum of the pair is large. Additionally, those interaction does not change the irrep of the system, the point emphasize by this study If the pair is made of two identical partons, the *full* wave function is obviously required to respect Bose or Fermi statistics. This latter point will be discussed soon.

The quantity of interest here is the transverse momentum distribution  $f$  of the pair after crossing the medium. It is noteworthy that for  $L = 0$ , the distribution  $f$  will be simply given by the inverse Fourier transform of  $\psi(\vec{x}_{12})\psi^*(\vec{x}_{43})$ .

#### Color basis

As opposed to the single parton case, for a pair one has to define some color basis. For simplicity, let us use the projector basis defined in section 3.1.3 with  $\alpha$ 's defined by

$$\mathbf{R}_1 \otimes \mathbf{R}_2 = \oplus_i \alpha_i \tag{3.26}$$

where  $i$  labels all possible distinct irreps. An element of the projector basis will be denoted by the shorthand notation (for a bra)  $\langle \alpha_i |$  instead of  $\langle \alpha_i, \bar{\alpha}_i |$ :

$$\langle \alpha_i | = \frac{1}{\sqrt{K_{\alpha_i}}} \alpha_i \begin{array}{c} \text{---} R_1 \\ \text{---} R_2 \\ \text{---} R_3 \\ \text{---} R_4 \end{array} \tag{3.27}$$

Here the dimension of the irrep  $\alpha_i$  is noted  $K_{\alpha_i}$  and the birdtrack indicates a projector as defined in b.21. One should not be confused by the two vertices used here. Let's illustrate

this with the digluon antisymmetric octet:

$$8_a \text{ (birdtrack)} = \frac{1}{C_A} \text{ (birdtrack)}$$

The l.h.s. is understood as a birdtrack for a projector, and the r.h.s. birdtrack involves usual tensors such as  $f_{abc}$  and  $\delta_{ab}$ . The  $1/C_A$  factor is a normalization factor for the projector to verify  $\mathcal{P}_{8_a}^2 = \mathcal{P}_{8_a}$  (see the interlude). The square root in 3.27 is required for the orthonormality of the basis vectors  $\langle \alpha_i | \alpha_j \rangle = \delta_{ij}$ .

From now I will omit the labelling  $R_1$  to  $R_4$  on every birdtrack because parton lines will always be drawn in the same order, from top to bottom.

The transverse momentum distribution  $f$  should be seen as a map from the (restricted) color singlet space (spanned by the projector basis) to itself. The projection of  $f$  into selected initial (and final) color states  $\alpha$  (and  $\beta$ ),

$$\langle \alpha | f | \beta \rangle = f_{\alpha \rightarrow \beta} \tag{3.28}$$

is the distribution of interest. An immediate consequence is that for  $L = 0$  the distribution reads in transverse coordinate space

$$f_{\alpha \rightarrow \beta} (\{\vec{x}_{12}, \vec{x}_{23}, \vec{x}_{34}\}; L = 0) = \underbrace{\langle \alpha | \beta \rangle}_{=\delta_{\alpha\beta}} \psi(\vec{x}_{12}) \psi^*(\vec{x}_{43}) \tag{3.29}$$

### Initial state wave function and indistinguishable particles

When the two partons of the pair are identical ( $qq$ ,  $\bar{q}\bar{q}$ , or  $gg$ ), the initial wave function  $\psi(\vec{x}_1, \vec{x}_2)$  should be such that the proper Bose or Fermi statistic is satisfied for the full wave function

Let's illustrate this in the case of a gluon pair.

We introduce the generalized coordinates  $r_i = \{\vec{x}_i, s_i, c_i\}$  (with  $i = 1, 2$ ) for position, spin, and color. Since the two gluons are indistinguishable particles, the full initial wave function  $\Psi$  verifies Bose statistics,

$$\Psi(r_1, r_2) = \sigma_B \Psi(r_2, r_1) \tag{3.30}$$

where  $\sigma_B = +1$ . One can factorize the full wave function (with obvious notations) as

$$\Psi(r_1, r_2) = \psi_c(c_1, c_2) \psi_s(s_1, s_2) \psi_x(\vec{x}_{12}) \tag{3.31}$$

The overall *signum* under  $1 \leftrightarrow 2$  permutation of all factors in this equation is  $\sigma_B$ , hence

$$\sigma_s \sigma_c \sigma_x = \sigma_B \tag{3.32}$$

As an illustration, let's choose the spin state of the gluon pair to be symmetric:  $\psi_s(s_1, s_2) = \psi_s(s_2, s_1)$ . Then if the digluon is a color (anti)symmetric state, the function  $\psi_x(\vec{x}_{12})$  must be even (odd).

A final remark about Bose or Fermi symmetry, I will introduce in the next paragraph an evolution operator  $e^{\mathcal{B}}$  building the momentum distribution of after crossing a medium

of length  $L$ . The symmetry property of the initial wave function given by  $\sigma_B = +1$  or  $\sigma_F = -1$  can be shown to hold after the medium (as expected). The demonstration relies on some birdtrack tricks and is similar to the property 3.49. The permutation (of two generalized coordinates) operator  $P$  commutes with  $\mathcal{B}$ , and so does the operator  $(\mathbb{1} \pm P)/2$  that projects the wave function  $\Psi$  into its symmetric (resp. antisymmetric) part. A consequence of this property is that for indistinguishable particles, Feynman diagrams involving the exchange of particles with respect to the (Bose or Fermi) statistics are encoded in the symmetry of the initial wave function.

### Evolution in the medium

As in section 3.2.1 the medium is characterized by its length  $L$ , density  $\rho$ , and is supposed to be invariant under translation in the transverse plane.

At the cross section level, for a single fast parton the dipole could exchange two gluons with each nucleon either from "real" exchange (one gluon connects to line 1 in the amplitude and the other to line 2 in the conjugate amplitude) or "virtual" exchange (both gluons connect to line 1 or line 2). For a fast parton pair, one has to consider each two-gluon exchange connected in all possible ways to the partons of the quadrupole. The scattering potential 3.15 in  $\vec{b}$ -space depends on the relative transverse separation  $\vec{x}$  of the two involved partons, and due to the form of the scattering potential, only on  $|\vec{x}|$ . Additionally, each interaction is associated with a color structure that is a mapping in color space

$$(\mathbf{R}_1 \otimes \mathbf{R}_2) \otimes \overline{(\mathbf{R}_1 \otimes \mathbf{R}_2)} \longrightarrow (\mathbf{R}_1 \otimes \mathbf{R}_2) \otimes \overline{(\mathbf{R}_1 \otimes \mathbf{R}_2)}$$

as explained in section 3.1.1. As an illustration color structure of the exchange connecting line 1 and line 3 reads

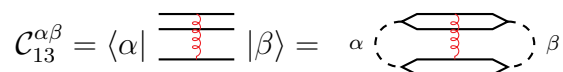


$$(3.33)$$

where the r.h.s. is obtained following 3.1.2. As we have already chosen the projector basis to span all relevant color singlet states, the completeness relation

$$\mathbf{1} = \sum_i |\alpha_i\rangle\langle\alpha_i| \quad (3.34)$$

can be inserted between two successive interactions. The relevant quantity to consider in the previous example is



$$\mathcal{C}_{13}^{\alpha\beta} = \langle\alpha| \text{ [diagram] } |\beta\rangle = \alpha \text{ [diagram] } \beta \quad (3.35)$$

In  $\mathcal{C}_{ij}^{\alpha\beta}$ , the indices  $ij$  indicate to which lines the red gluon attaches to, and the two superscript  $\alpha\beta$  denote the color states used to project the color structure. Let's call  $\mathcal{C}_{ij}$  the color structure before latter projection. Notice that  $\mathcal{C}_{ij}$  is unchanged when  $i$  and  $j$  are exchanged (one gets a factor  $(-1)$  for each color generator) but also when  $\alpha$  and  $\beta$  are exchanged (this is easily understood from the birdtrack representation in the r.h.s of 3.35).



At any time of the evolution, the quadrupole is in a singlet state, and color conservation gives

$$\begin{array}{c} \color{red}{\curvearrowright} \\ \text{---} \\ \text{---} \\ \text{---} \end{array} + \begin{array}{c} \color{red}{\curvearrowright} \\ \text{---} \\ \text{---} \\ \text{---} \end{array} + \begin{array}{c} \color{red}{\curvearrowright} \\ \text{---} \\ \text{---} \\ \text{---} \end{array} + \begin{array}{c} \color{red}{\curvearrowright} \\ \text{---} \\ \text{---} \\ \text{---} \end{array} = \sum_{i=1}^4 T_i = 0 \quad (3.36)$$

Using this relation, one can easily relate  $\mathcal{C}_{ij}$  when  $i = j$  to  $\mathcal{C}_{ij}$  when  $i \neq j$ .

$$\mathcal{C}_{ii} = \sum_{j \neq i} -\mathcal{C}_{ij} \quad (3.37)$$

The sum over all gluon connections is given by one half<sup>1</sup> of

$$\begin{aligned}
 \sum_{i,j=1}^4 \mathcal{C}_{ij} \times \tilde{V}(\vec{x}_{ij}) &= \sum_{i=1}^4 \mathcal{C}_{ii} \times 1 + \sum_{i,j=1; i \neq j}^4 \mathcal{C}_{ij} \times \tilde{V}(\vec{x}_{ij}) \\
 &= \sum_{i=1}^4 \sum_{j=1, j \neq i}^4 (-1) \mathcal{C}_{ij} \times 1 + \sum_{i,j=1; i \neq j}^4 \mathcal{C}_{ij} \times \tilde{V}(\vec{x}_{ij}) \\
 &= \sum_{i < j=1}^4 \mathcal{C}_{ij} \times 2(\tilde{V}(\vec{x}_{ij}) - 1)
 \end{aligned}$$

Defining  $\omega(\vec{x}_{ij}) = \omega_{ij} = 1 - \tilde{V}(\vec{x}_{ij})$ , one finds the operator  $\mathcal{K}$  defined as:

$$\mathcal{K} = - \sum_{i < j=1}^4 \mathcal{C}_{ij} \omega_{ij} \quad (3.38)$$

This operator takes a similar form for any number  $n$  of partons in the "multipole". In particular, for  $n = 2$  the projection on the only possible singlet gives:

$$\langle w^{(2)} | \mathcal{K} | w^{(2)} \rangle = -C_R \left[ 1 - \tilde{V}(\vec{x}_{12}) \right] \quad (3.39)$$

Using a dimensionless evolution time  $\tau = t/\lambda_0$ , one immediately recognizes the kernel used in 3.25.

Now that all color subtleties have been taken care of, the transverse momentum distribution of the pair is still solution of a kinetic equation. In  $\vec{b}$ -space<sup>2</sup>, the kinetic equation reads (projected between initial and final color states  $\alpha$  and  $\beta$ )

$$\langle \alpha | \frac{\partial}{\partial \tau} f(\{\vec{x}\}; \tau) | \beta \rangle = \sum_{\gamma} \langle \alpha | f(\{\vec{x}\}; \tau) | \gamma \rangle \langle \gamma | \mathcal{K} | \beta \rangle \quad (3.40)$$

where  $\{\vec{x}\}$  is the set of transverse separations  $\{\vec{x}\} = \{\vec{x}_{12}, \vec{x}_{23}, \vec{x}_{34}\}$ . The solution at  $\tau = L/\lambda_0$  is

$$\langle \alpha | f(\{\vec{x}\}; L/\lambda_0) | \beta \rangle = \sum_{\gamma} \langle \alpha | f(\{\vec{x}\}; 0) | \gamma \rangle \langle \gamma | e^{\frac{L}{\lambda_0} \mathcal{K}} | \beta \rangle \quad (3.41)$$

<sup>1</sup>In Feynman rules, one divide by a symmetry factor equivalent connected diagrams. In this case, the symmetry factor 2 is the permutation of the two gluons exchanged by the target nucleon.

<sup>2</sup>As it was shown in the single parton case, the auxiliary space gives a fast way to the solution.

Let's define the momentum distribution  $f$  with  $\mathcal{B} = \frac{L}{\lambda_0} \mathcal{K}$  and also  $\hat{\Gamma}_{ij} = \frac{L}{\lambda_0} \omega_{ij}$ , and go to momentum space,

$$\begin{aligned} \langle \alpha | f(\vec{p}_1, \vec{p}_2; L/\lambda_0) | \beta \rangle &= \int \frac{d^2 \vec{x}_{12} d^2 \vec{x}_{23} d^2 \vec{x}_{34}}{(2\pi)^6} e^{i \vec{p}_1 \cdot (\vec{x}_{12} + \vec{x}_{34}) + i (\vec{p}_1 + \vec{p}_2) \cdot \vec{x}_{23}} \\ &\times \sum_{\gamma} \langle \alpha | f(\{\vec{x}\}; 0) | \gamma \rangle \langle \gamma | e^{\mathcal{B}} | \beta \rangle \end{aligned} \quad (3.42)$$

with

$$\mathcal{B} = - \sum_{i < j} \mathcal{C}_{ij} \times \hat{\Gamma}_{ij} \quad (3.43)$$

Some remarks have to be done regarding the Fourier phase in 3.42. There are only three independent transverse separations because of the assumed invariance under transverse translations. One of the  $\vec{x}$ -integral produces a trivial  $\delta^{(2)}(\sum \vec{p})$  factor that can be removed by a trivial redefinition of the transverse momentum distribution. Initially the Fourier phase is simply  $\varphi = \sum_i \vec{p}_i \cdot \vec{x}_i$ . The phase in 3.42 follows from the identification  $\vec{p}_1 = -\vec{p}_4$  and  $\vec{p}_2 = -\vec{p}_3$  in the final state.

Plugging into 3.42 the initial wave function, the distribution becomes

$$f_{\alpha \rightarrow \beta} \left( \vec{p}_1, \vec{p}_2; \frac{L}{\lambda_0} \right) = \int_{\vec{x}_{12}, \vec{x}_{23}, \vec{x}_{34}} e^{i \vec{p}_1 \cdot (\vec{x}_{12} + \vec{x}_{34}) + i (\vec{p}_1 + \vec{p}_2) \cdot \vec{x}_{23}} \psi(\vec{x}_{12}) \psi^*(\vec{x}_{43}) \langle \alpha | e^{\mathcal{B}} | \beta \rangle \quad (3.44)$$

The equation 3.44 will be used to describe the broadening of a two-parton final state. This equation is somewhat academic (it holds for an asymptotic pair) but it contains all information regarding the color rotation arising from the propagation of the pair in the medium.

### 3.2.4 Asymptotic parton system

This section generalizes the results 3.43 and 3.44 for an asymptotic pair to arbitrary  $m$ -parton systems. A limiting aspect in this derivation, is the rapid growth of the dimension of the color vector space associated to the of considered process.

There are some useful limits that can be used to compensate this growth. First, I will look at the operator  $\mathcal{B}$  when two arguments are set to the same value. This will naturally lead to the pointlike limit where a pair in the amplitude (and the conjugate pair in the conjugate amplitude) is set to have a vanishing transverse separation. Within this pointlike limit of  $\mathcal{B}$ , one is able to find how the distribution  $f$  simplifies into simpler distributions involving less partons. Another approach is to consider a system with a large number of partons but an observable that requires to observe only a few of them. In such a situation, the complicated evolution of the  $2m$ -parton system in the medium relates to the simpler  $2n$ -parton system evolution (with  $n < m$ ). This evolution is described by a thus a convolution in momentum space of an *initial* distribution  $h$  with a *broadening* distribution  $f_n$  encoding the evolution in the medium.

#### Direct generalization

The discussion in the previous section leads us to the transverse momentum distribution  $f$  of a pair given by 3.44. The generalization to larger a system with  $m > 2$  partons follows the same steps.

Labeling the transverse positions in the amplitude (and its conjugate) by  $\vec{x}_i$  (and  $\vec{x}'_i$ ) where  $i = 1, \dots, m$ , the phase becomes

$$\varphi_m = \sum_{i=1}^{m-1} \vec{p}_i \cdot (\vec{x}_{im} - \vec{x}'_{im}) + \sum_{i=1}^m \vec{p}_i \cdot \underbrace{(\vec{x}_m - \vec{x}'_m)}_{\Delta_m} \quad (3.45)$$

where  $\vec{x}_{im} = \vec{x}_i - \vec{x}_m$  and  $\vec{x}'_{im} = \vec{x}'_i - \vec{x}'_m$ . The operator  $\mathcal{B}$  is defined as in the two-parton case 3.43 but with a summation of indices  $i < j$  over all the labels of  $\vec{x}$  and  $\vec{x}'$ . The wave function  $\psi$  in the amplitude depends on  $m - 1$  transverse separations grouped into the set  $\{\vec{x}\}_m$  (and similarly  $\{\vec{x}'\}_m$  for its conjugate). Let's choose a color singlet basis spanned by  $|\alpha^{(2m)}\rangle$ 's.

$$\langle \alpha^{(2m)} | f(\vec{p}_1, \dots, \vec{p}_m; L) | \beta^{(2m)} \rangle = \int \left[ \prod_{i=1}^{m-1} \frac{d^2 \vec{x}_{im}}{(2\pi)^2} \frac{d^2 \vec{x}'_{im}}{(2\pi)^2} \right] \frac{d^2 \Delta_m}{(2\pi)^2} e^{i\varphi_m} \psi(\{\vec{x}\}_m) \psi^*(\{\vec{x}'\}_m) \langle \alpha^{(2m)} | e^{\mathcal{B}} | \beta^{(2m)} \rangle \quad (3.46)$$

One of the main difficulties with such a case is to find an effective way to deal with the basis elements  $|\alpha^{(2m)}\rangle$ . In the case of a pair, the projector basis was sufficient, however it is not for  $m > 2$ . The vector basis  $|\alpha^{(m)}, \beta^{(m)}\rangle$  as defined in 3.1.3 is required but the number of elements of such a basis grows rapidly with the number of partons.

For  $N_c = 3$ , the number of projectors goes from 6 to 29 when one passes from two gluons to three gluons. At the same time the number of vectors goes from 8 to 145... Of course, the situation does not get better with more gluons!

As we will see in the following paragraphs, in some simplifying limits the problem can still be handled.

### Limits of $\mathcal{B}$

Consider a system of  $m$  asymptotic partons, and the associated operator  $\mathcal{B}_{(m,m)}$ . The subscript indicates the number of parton lines considered in the amplitude and its conjugate. I will choose that the partons at positions  $\vec{x}_1$  and  $\vec{x}_2$  to form a pointlike pair (i.e.  $\vec{x}_{12} = 0$ ) with an associated charge given by their **irrep**  $\beta$

$$\mathcal{B}_{(m,m)}(\vec{x}_1, \vec{x}_2, \vec{x}_3, \dots, \vec{x}_m; \vec{x}'_m, \dots, \vec{x}'_1) \longrightarrow \mathcal{B}_{(m,m)}(\vec{u}, \vec{u}, \vec{x}_3, \dots, \vec{x}_m; \vec{x}'_m, \dots, \vec{x}'_1)$$

To indicate that the parton pair (1, 2) is in an **irrep**  $\beta$ , we introduce in birdtrack notation the following operator:

$$\begin{array}{c} \text{---} \text{---} \text{---} \\ \text{---} \text{---} \text{---} \\ \text{---} \text{---} \text{---} \\ \text{---} \text{---} \text{---} \\ \text{---} \text{---} \text{---} \\ \text{---} \text{---} \text{---} \\ \text{---} \text{---} \text{---} \end{array} \begin{array}{c} \text{---} \text{---} \text{---} \\ \text{---} \text{---} \text{---} \\ \text{---} \text{---} \text{---} \\ \text{---} \text{---} \text{---} \\ \text{---} \text{---} \text{---} \\ \text{---} \text{---} \text{---} \\ \text{---} \text{---} \text{---} \end{array} = \mathcal{R}_{(1,2) \rightarrow \beta} \quad (3.47)$$

The parton lines are ordered as in the previous section from top to bottom by  $1, 2, 3, \dots, m, m', (m-1)', \dots, 1'$ . The upper vertex (with the two plain lines and the dashed line) should be

understood as a “half-projector”<sup>3</sup>. Indeed, contracting this vertex with its vertical mirror image (where arrow should be flipped) builds the projector  $\mathbf{R}_1 \otimes \mathbf{R}_2 \rightarrow \beta$  defined in b.21.

From the definition of  $\mathcal{B}$  in 3.43, one can always group together terms with a gluon connecting to a line  $j \neq 1, 2$  with line 1 and 2 leaving the rest unchanged, and use color conservation:

$$\hat{\Gamma}_{1j} + \hat{\Gamma}_{2j} = \hat{\Gamma}_{uj} \quad (3.48)$$

following from  $\vec{x}_{12} = \vec{0}$ . The contribution where the gluon connects to both lines 1 and 2 vanishes since  $\hat{\Gamma}(\vec{0}) = 0$ . Up to the tensor  $\mathcal{R}_{(1,2) \rightarrow \beta}$  factorizing on the left, one can recognize the expression of  $\mathcal{B}_{(m-1,m)}$  with the first parton in irrep  $\beta$ . It follows that

$$\mathcal{B}_{(m,m)} \mathcal{R}_{(1,2) \rightarrow \beta} = \mathcal{R}_{(1,2) \rightarrow \beta} \mathcal{B}_{(m-1,m)} \quad (3.49)$$

where  $\mathcal{B}_{(m-1,m)}$  depends on  $\vec{u}, \vec{x}_3, \dots, \vec{x}_m, \vec{x}'_m, \dots, \vec{x}'_1$ . Of course, 3.49 also implies

$$e^{\mathcal{B}_{(m,m)}} \mathcal{R}_{(1,2) \rightarrow \beta} = \mathcal{R}_{(1,2) \rightarrow \beta} e^{\mathcal{B}_{(m-1,m)}} \quad (3.50)$$

which will be used in the next paragraph.

This procedure naturally iterates: starting with  $\mathcal{B}_{(m,m)}$ , this little game relates  $\mathcal{B}_{(a \leq m, b \leq m)}$  to limits of  $\mathcal{B}_{(m,m)}$  where some arguments  $\vec{x}_{ij}$  are set to  $\vec{0}$ .

### Broadening distribution and pointlike limit

In order to fix the parton pair (1, 2) to be pointlike, the initial wave function’s  $\vec{x}$ -dependence is written as

$$\psi_m(\{\vec{x}\}_m) = \delta^{(2)}(\vec{x}_1 - \vec{x}_2) \psi_{m-1}(\{\vec{x}\}_{m-1}) \quad (3.51)$$

The previous paragraph already gave us the tools to treat the color structure. Take partons (1, 2) in irrep  $\beta$  and partons (1', 2') in irrep  $\bar{\beta}$  to obtain

$$e^{\mathcal{B}_{(m,m)}} \mathcal{R}_{(1,2) \rightarrow \beta} \mathcal{R}_{(1',2') \rightarrow \bar{\beta}} = \mathcal{R}_{(1',2') \rightarrow \bar{\beta}} \mathcal{R}_{(1,2) \rightarrow \beta} e^{\mathcal{B}_{(m-1,m-1)}} \quad (3.52)$$

where  $\mathcal{B}_{(m-1,m-1)}$  depends on  $\vec{u}, \dots, \vec{x}_m, \vec{x}'_m, \dots, \vec{u}'$ . The two operators  $\mathcal{R}$  now act on the left as

$$\begin{array}{c} \text{---} \beta \\ \text{---} \\ \dots \\ \text{---} \\ \dots \\ \text{---} \\ \text{---} \bar{\beta} \end{array} \quad (3.53)$$

to project elements of the basis  $\langle v_i^{(m)}, \bar{v}_j^{(m)} |$  into  $\langle w_i^{(m-1)}, \bar{w}_j^{(m-1)} |$  for the color part of the squared wave function.

<sup>3</sup>More precisely, this half-projector denotes a Clebsch-Gordan for  $\mathbf{R}_1 \otimes \mathbf{R}_2 \rightarrow \beta$ . See Chapter 4.2 of [45] for a matrix representation of Clebsch-Gordan coefficients. The associated normalization is such that the simplification in 3.55 occurs.

As an illustration to this procedure, let's consider the  $m = 2$  distribution given by 3.44, introduce the wave functions

$$\psi(\vec{x}_1, \vec{x}_2)\psi^*(\vec{x}_4, \vec{x}_3) = \delta^{(2)}(\vec{x}_{12})\delta^{(2)}(\vec{x}_{43}), \quad (3.54)$$

and require that the (observed) pair is in irrep  $\beta$ . Two out of three integrals ( $\vec{x}_{12}$  and  $\vec{x}_{34}$ ) become trivial. The pair distribution reads

$$f_{\alpha \rightarrow \beta}(\vec{p}_1, \vec{q}; L/\lambda_0) = |\psi(\vec{p}_1)|^2 \int \frac{d^2 \vec{x}}{(2\pi)^2} e^{i\vec{q} \cdot \vec{x}} e^{-C_\beta \hat{\Gamma}(\vec{x})} \underbrace{\langle \alpha | \mathcal{R}_\beta \mathcal{R}'_\beta | \beta \rangle}_{\delta_{\alpha\beta}} \quad (3.55)$$

where  $\vec{q} = \vec{p}_1 + \vec{p}_2$ . The  $\vec{p}_1$ -dependence of  $f$  factorizes into  $|\psi(\vec{p}_1)|^2$ . Under the remaining integral, there is only some  $\vec{q}$ -dependence affected by the medium. Setting  $L = 0$  in  $\hat{\Gamma}$  leads to a  $\delta^{(2)}(\vec{q})$  distribution, and for  $L \neq 0$  the factor  $e^{-C_\beta \hat{\Gamma}(\vec{x})}$  leads to medium-induced broadening of the  $\vec{q}$ -distribution. This broadening is associated with color charge  $C_\beta$ .

In the pointlike limit, the medium does not probe each parton individually but only the global charge of the pair, and it is only the global charge  $C_\beta$  of the pair that contributes to the broadening. This statement generalizes to arbitrary pointlike systems. If  $m$ -partons are in a pointlike configuration (i.e.  $\vec{x}_1 = \vec{x}_2 = \dots = \vec{u}$  and  $\vec{x}'_1 = \vec{x}'_2 = \dots = \vec{u}'$ ), the same procedure can be used and only the global charge of the system appears in  $e^{-C_\beta \hat{\Gamma}(\vec{x})}$ .

### Broadening distribution with unobserved partons

In the previous paragraph, the pointlike limit allows to simplify the complexity of the problem presented at the beginning of this section, however it restrict the initial wave function. Instead of fixing the initial wave function, one can also choose to integrate out some dof in the distribution 3.23 or 3.46, for instance by deciding to tag only  $n$  out of  $m$  partons (with  $n < m$ ). This situation is relevant when the observable of interest only requires to observe a subset of the propagating system.

Starting from 3.46, I will consider that partons  $n+1, \dots, m$  will not be observed. It means that one has to integrate over  $d^2 \vec{p}_{n+1} \dots d^2 \vec{p}_m$ , and also to introduce the reduction operator

$$\mathbb{1}^{m \rightarrow n} = \begin{array}{c} R_1 \text{ ---} \\ \dots \\ R_n \text{ ---} \\ R_{n+1} \text{ ---} \\ \dots \\ R_m \text{ ---} \end{array} \quad (3.56)$$

since a summation over unobserved color dofs is required. The procedure is similar to the previous paragraph: moving the reduction operator  $\mathbb{1}^{m \rightarrow n}$  to the left of the operator  $\mathcal{B}_{(m,m)}$  will give the operator  $\mathcal{B}_{(n,n)}$  on the right of  $\mathbb{1}^{m \rightarrow n}$ , as we show below.

The momentum integrals set each  $\vec{x}_j - \vec{x}'_j = \vec{0}$  for all  $j > n$ , as it can be seen from the phase 3.45. When one end of the gluon attaches to a line  $i \leq n$  (either in the amplitude or its conjugate) and the other end attaches to  $j > n$  (in the amplitude or its conjugate),



The second factor in the convolution is given by:

$$f_n(\vec{p}_1 \cdots \vec{p}_n; \vec{p}_1 \cdots \vec{p}_n; \vec{P}_n) = \int \left[ \prod_{k=1}^{n-1} \frac{d^2 \vec{x}_{jn}}{(2\pi)^2} \frac{d^2 \vec{x}'_{jn}}{(2\pi)^2} \right] \cdot \frac{d^2 \Delta_n^-}{(2\pi)^2} e^{i\varphi_n} \langle \alpha | e^{\mathcal{B}(n,n)} | \beta \rangle \quad (3.62)$$

where  $\langle u_a^{(m)}, \bar{u}_b^{(m)} | \mathbb{1}^{m \rightarrow n} = \langle \alpha |$  and  $| v_c^{(n)}, \bar{v}_d^{(n)} \rangle = | \beta \rangle$ . The expression 3.60 can be written as:

$$\begin{aligned} \int_{\vec{p}_{n+1} \cdots \vec{p}_m} \langle u_a^{(m)}, \bar{u}_b^{(m)} | f(\vec{p}_1 \cdots \vec{p}_m; L/\lambda_0) \mathbb{1}^{m \rightarrow n} | v_c^{(n)}, \bar{v}_d^{(n)} \rangle \\ = [h \otimes f_n](\vec{p}_1 \cdots \vec{p}_n; \vec{p}_1 \cdots \vec{p}_n; \vec{P}_n) \end{aligned} \quad (3.63)$$

The distribution  $h$  is interpreted as the initial distribution of the parton momenta before the medium. This distribution is in general a skewed momentum distribution because the momenta in the amplitude and its conjugate do not match. However, in the special case  $n = 1$ , all momenta in the amplitude and in the conjugate amplitude do match (there is a  $\delta^{(2)}(\vec{R}_n - \vec{R}'_n)$  distribution fixing  $\vec{r}_1 = \vec{r}'_1$  in addition to all  $\vec{r}_i = \vec{r}'_i$  for  $i > 1$  by definition of  $h$ ) and this distribution becomes a probability density  $|\psi(\vec{r}_1 \cdots \vec{r}_{m-1})|^2$ .

**Medium induced broadening:** The operator  $e^{\mathcal{B}(n,n)}$  is the evolution operator of an  $n$ -parton system in the medium (an overall color singlet of  $2n$  pointlike charges). The above result shows that the broadening of the  $n$  tagged partons is as if the partons  $n+1$  to  $m$  were absent. This nice feature provide a simple solution to the problem posed whenever one only cares on the medium-induce broadening of a subsystem of tagged partons.

For example, a four-gluon system would involve a 3 598 -dimensional vector basis ( $N_c = 3$ ) to study the color evolution in the medium. Tagging only two of the four gluons reduces the basis to a mere 6-dimensional projector basis!

### 3.3 A random walk in color space

In this section, I will detail another limit of 3.23 and 3.46, namely the compact pair limit. In this limit, the color structure simplifies and an intuitive picture can be formulated for the momentum distribution in the final state.

I will start by defining the compact pair limit. Then I will consider the case of the pair with a color transition occurring in the medium and illustrate it with a gluon pair. And finally, I will compare to the case where the pair initial and final color states are identical.

#### 3.3.1 Compact pair limit

The pointlike limit allows to simplify the expression 3.46 when all transverse separations are set to zero. The broadening of the system is then given by the simple contribution  $e^{-C_\beta \hat{\Gamma}}$ . Let us relax a bit this very strong assumption  $\vec{x}_i = \vec{u}$  and  $\vec{x}'_i = \vec{u}'$  for all  $i \leq m$  by considering instead that all  $\vec{x}_i$  are *close* to  $\vec{u}$ . By *close*, I mean that the separation  $|\vec{x}_i - \vec{u}|$  is negligible compared to the spatial transverse resolution of the medium  $\sim 1/\bar{Q}_s$ ,

with  $\bar{Q}_s$  the color-stripped saturation scale defined by (to recover the saturation scale of parton with irrep  $\mathbf{R}$ , simply take  $C_R \bar{Q}_s^2$ ):

$$\frac{L}{\lambda_0} = \frac{\bar{Q}_s^2}{2\mu^2} \quad (3.64)$$

Let's define the momentum imbalance of the system by

$$\vec{q} = \vec{P}_n = \sum_{i=1}^m \vec{p}_i \quad (3.65)$$

and focus on the region of the  $|\vec{q}|$ -distribution where the imbalance satisfies  $|\vec{q}| \lesssim \bar{Q}_s$ . The phase 3.45 of 3.46 indicates that  $|\vec{q}|$  is related to  $\sim 1/|\Delta_m^-|$ , and in the compact pair limit  $\Delta_m^- \simeq \vec{u} - \vec{u}'$ . This limit will enable us to expand  $|\vec{x}_i - \vec{x}_j|$  and  $|\vec{x}'_i - \vec{x}'_j|$  for all  $i, j \leq m$  around zero at fixed  $|\Delta_m^-|$ .

### 3.3.2 Compact pair limit - color transitions

Returning to the notations of section 3.2.3 for the parton pair, we have:

$$\begin{aligned} \Delta_m^- &\rightarrow \vec{x}_{23} \\ \{\vec{x}\}_m &\rightarrow \vec{x}_{12} \\ \{\vec{x}'\}_m &\rightarrow \vec{x}_{43} \end{aligned}$$

The momentum distribution is

$$f_{\alpha \rightarrow \beta} \left( \vec{p}_1, \vec{p}_2; \frac{L}{\lambda_0} \right) = \int_{\vec{x}_{12}, \vec{x}_{23}, \vec{x}_{34}} e^{i \vec{p}_1 \cdot (\vec{x}_{12} + \vec{x}_{34}) + i (\vec{p}_1 + \vec{p}_2) \cdot \vec{x}_{23}} \psi(\vec{x}_{12}) \psi^*(\vec{x}_{43}) \langle \alpha | e^{\mathcal{B}} | \beta \rangle$$

Up to now, I did not explicitly detail the value of  $\langle \alpha | \mathcal{B} | \beta \rangle$  in the projector basis. Chapter 5 is dedicated to such a calculation, thus I will only use some results in this section without demonstration.

#### Properties of $\mathcal{B}$ in the compact pair limit

In the compact pair limit, the leading contribution on the diagonal of  $\mathcal{B}$  is given by the pointlike limit. That is  $\langle \alpha | \mathcal{B} | \beta \rangle$  diagonal elements are given by (up to linear corrections in  $|\vec{x}_i - \vec{u}|$  and  $|\vec{x}'_i - \vec{u}'|$ )

$$\langle \alpha | \mathcal{B}(\vec{u}, \vec{u}; \vec{u}', \vec{u}') | \beta \rangle = \delta_{\alpha\beta} C_\alpha \hat{\Gamma}(\vec{u} - \vec{u}') \quad (3.66)$$

with  $\vec{u} = \vec{x}_1 = \vec{x}_2$  and  $\vec{u}' = \vec{x}_3 = \vec{x}_4$ .

The non-diagonal contribution to  $\langle \alpha | \mathcal{B} | \beta \rangle$  reads

$$\langle \alpha | \mathcal{B} | \beta \neq \alpha \rangle = \frac{1}{4} \left\{ \underbrace{(\hat{\Gamma}_{14} + \hat{\Gamma}_{12})}_{\omega^{(t)}} - \underbrace{(\hat{\Gamma}_{13} + \hat{\Gamma}_{24})}_{\omega^{(u)}} \right\} \underbrace{\langle \alpha | [T_t^2 - T_u^2] | \beta \neq \alpha \rangle}_{\mathcal{F}_{\alpha\beta}} \quad (3.67)$$

with  $T_t^2 - T_u^2$  being a color tensor (its matrix representation is given in 5). The kinematic term  $\omega^{(t)} - \omega^{(u)}$  vanishes in the pointlike limit, and will be expanded in the compact pair limit, i.e.  $x_{12}, x_{34} \ll x_{23}$ .



First, we split the operator  $\mathcal{B}$  into its diagonal part  $\mathcal{D}$  and non-diagonal part  $\mathcal{F}$  as follows

$$\mathcal{B} = \mathcal{D} + X\mathcal{F}, \quad X = \omega^{(t)} - \omega^{(u)}, \quad (3.68)$$

We then use the identity:

$$e^{\mathcal{D}+X\mathcal{F}} = e^{\mathcal{D}} + \int [d\delta]_2 e^{\delta_1 \mathcal{D}} X\mathcal{F} e^{\delta_2 \mathcal{D}} + \int [d\delta]_3 e^{\delta_1 \mathcal{D}} X\mathcal{F} e^{\delta_2 \mathcal{D}} X\mathcal{F} e^{\delta_3 \mathcal{D}} + \dots \quad (3.69)$$

with

$$\int [d\delta]_n = \left[ \prod_{i=1}^n \int_0^1 d\delta_i \right] \delta \left( \sum_{j=1}^n \delta_j - 1 \right) \quad (3.70)$$

Finally, we take the compact pair limit  $x_{12}, x_{34} \ll x_{23}$ .

When  $\vec{x}_{12}, \vec{x}_{34} \rightarrow \vec{0}$  the diagonal part is finite. One can safely substitute

$$\mathcal{D}(\vec{x}_{12}, \vec{x}_{34}, \vec{x}_{23}) \rightarrow \mathcal{D}(\vec{0}, \vec{0}, \vec{x}_{23}) = -\delta_{\alpha\beta} C_\alpha \hat{\Gamma}_{23} \quad (3.71)$$

When the final and initial color states are distinct, the first contribution in the r.h.s of 3.69 is zero because  $e^{\mathcal{D}}$  is diagonal. The first non-zero contribution comes from the linear term in “ $X$ ”:

$$\begin{aligned} \langle \alpha | e^{\mathcal{B}} | \beta \neq \alpha \rangle &= X \int_0^1 d\delta \langle \alpha | e^{\delta \mathcal{D}} \cdot \mathcal{F} \cdot e^{(1-\delta)\mathcal{D}} | \beta \rangle + \mathcal{O}(X^2) \\ &= X \int_0^1 d\delta \langle \alpha | e^{\delta \mathcal{D}} | \alpha \rangle \langle \alpha | \mathcal{F} | \beta \rangle \langle \beta | e^{(1-\delta)\mathcal{D}} | \beta \rangle + \mathcal{O}(X^2) \\ &= \mathcal{F}_{\alpha\beta} X \int_0^1 d\delta e^{-\delta C_\alpha \hat{\Gamma}_{23}} e^{-(1-\delta) C_\beta \hat{\Gamma}_{23}} + \mathcal{O}(X^2) \\ &= \mathcal{F}_{\alpha\beta} X \int_0^1 d\delta e^{-[\delta C_\alpha + (1-\delta) C_\beta] \hat{\Gamma}_{23}} + \mathcal{O}(X^2) \end{aligned} \quad (3.72)$$

To change the color state of the pair, one should have a transition from  $\alpha$  to  $\beta$  at some point, that is, select an off-diagonal element of  $e^{\mathcal{B}}$ . One see that for a compact pair, it will come with two factors:  $\mathcal{F}_{\alpha\beta}$  is a group-theoretic factor, and  $X(\vec{x}_{12}, \vec{x}_{34}; \vec{x}_{23})$  depends on the kinematics (it is small in the compact pair limit). The latter factor reads

$$X = \hat{\Gamma}_{23} + \hat{\Gamma}_{14} - \hat{\Gamma}_{13} - \hat{\Gamma}_{24} \rightarrow \left( 1 + e^{(\vec{x}_{12} + \vec{x}_{34}) \cdot \vec{\nabla}} - e^{\vec{x}_{12} \cdot \vec{\nabla}} - e^{\vec{x}_{34} \cdot \vec{\nabla}} \right) \hat{\Gamma}_{23} \quad (3.73)$$

and in the compact pair limit the first non-vanishing contribution is

$$(\vec{x}_{12} \cdot \vec{\nabla})(\vec{x}_{34} \cdot \vec{\nabla}) \hat{\Gamma}_{23} \quad (3.74)$$

The parton pair propagates in the medium as a pointlike object of color charge  $C_\alpha$  up to the  $z$ -position  $\delta L$ . At the position  $z = \delta L$ , a color transition occurs and the pair color state  $|\alpha\rangle$  becomes  $|\beta\rangle$ . Finally, the parton pair propagates in the remaining slice of medium  $(1 - \delta)L$  as a pointlike object of color charge  $C_\beta$ . This simple picture suggests what kind of broadening one expects in such a case. After the  $\delta$ -integral, the pair effective charge  $\delta C_\alpha + (1 - \delta)C_\beta$  can be approximated by the average of the initial and final charges of the pair  $\frac{1}{2}(C_\alpha + C_\beta)$ .

### Illustration

Let's illustrate this with an initial gluon pair in an irrep  $\mathbf{8}_a$ <sup>4</sup> and a final gluon pair in an irrep  $\mathbf{27}$ . After the  $\vec{p}_1$ -integral of 3.42, the momentum imbalance distribution reads

$$\langle 8_a | f(\vec{q}; L/\lambda_0) | 27 \rangle = \int \frac{d^2 \vec{x}_{23}}{(2\pi)^2} \frac{d^2 \vec{x}}{(2\pi)^2} e^{i\vec{q} \cdot \vec{x}_{23}} |\psi(\vec{x}_{12})|^2 \langle 8_a | e^{\mathcal{B}(\vec{x}, -\vec{x}; \vec{x}_{23})} | 27 \rangle \quad (3.75)$$

where I used the factor  $\delta^{(2)}(\vec{x}_{12} + \vec{x}_{34})$  arising from the  $\vec{p}_1$ -integral. At leading order in the compact pair limit  $X$  becomes

$$X = (\vec{x}_{12} \cdot \vec{\nabla})(-\vec{x}_{12} \cdot \vec{\nabla}) \hat{\Gamma} \Big|_{23} + \mathcal{O}(\vec{x}_{12}^4) \quad (3.76)$$

$$= - \left[ \frac{\vec{x}_{12}^2}{x_{23}} \Gamma'(z) - \frac{(\vec{x}_{12} \cdot \vec{x}_{23})^2}{x_{23}^3} \Gamma'(z) + \frac{(\vec{x}_{12} \cdot \vec{x}_{23})^2}{x_{23}^2} \Gamma''(z) \right]_{z=x_{23}} + \mathcal{O}(\vec{x}_{12}^4) \quad (3.77)$$

where in the last line I used the fact that the scattering potential is a radial function  $\hat{\Gamma}(\vec{x}) = \Gamma(|\vec{x}|)$  since the only dependence on the angle  $\varphi$  between  $\vec{x}_{12}$  and  $\vec{x}_{23}$  is from the scalar product  $\vec{x}_{12} \cdot \vec{x}_{23}$ , the angular integration gives

$$\begin{aligned} (\vec{x}_{12} \cdot \vec{x}_{23})^2 &\longrightarrow \frac{1}{2} x_{12}^2 x_{23}^2 \\ \vec{x}_{12}^2 &\longrightarrow x_{12}^2 \end{aligned}$$

and  $X$  becomes

$$\langle X \rangle_{\varphi_{12}} \simeq x_{12}^2 \left\{ \frac{\Gamma'}{z} + \Gamma'' \right\} \Big|_{z=x_{23}} \quad (3.78)$$

The curly bracket is just half of the Laplacian of  $\Gamma$  taken at the value  $x_{23}$  denoted by  $[\frac{1}{2}\Delta\hat{\Gamma}]_{23}$  in the following. The remaining  $x_{12}^2$  factor combines with the squared wave function into

$$\langle x_{12}^2 \rangle = \int \frac{dx_{12}^2}{4\pi} x_{12}^2 |\psi(\vec{x}_{12})|^2 \quad (3.79)$$

namely a moment of the  $|\psi(\vec{x}_{12})|^2$  probability distribution. The momentum imbalance distribution is then

$$f_{8_a \rightarrow 27}(\vec{q}; L/\lambda_0) = \langle x_{12}^2 \rangle \mathcal{F}_{(8_a, 27)} \int_{\vec{x}_{23}} e^{i\vec{q} \cdot \vec{x}_{23}} \int_0^1 d\delta e^{-C(\delta)} \hat{\Gamma}(\vec{x}_{23}) \left[ \frac{1}{2} \Delta \hat{\Gamma} \right]_{23} \quad (3.80)$$

where  $C(\delta)$  is defined as  $\delta C_\alpha + (1 - \delta) C_\beta$ .

### Interpretation

Recall that in 3.42 the  $\vec{p}_1$ -integrated distribution for  $L = 0$  yields the distribution

$$f_{\alpha \rightarrow \beta}(\vec{q}; L/\lambda_0 = 0) = \delta_{\alpha\beta} \delta^{(2)}(\vec{q}) \quad (3.81)$$

with  $\int_{\vec{p}} |\psi(\vec{p})|^2$  normalized to unity. There is obviously no color transition when there is no medium.

<sup>4</sup>One can think of the realistic situation where  $g \rightarrow gg$  splitting occurring before the medium.

In the compact pair limit, the momentum imbalance distribution 3.80 obtained in the case of a color transition is given by a factor

$$\langle x_{12}^2 \rangle \mathcal{F}_{\alpha\beta} \times L/\lambda_0 \quad (3.82)$$

corresponding to the cost to have a color transition times a linear superposition of distributions for pointlike color charge  $C(\delta)$ <sup>5</sup>.

$$\int_0^1 d\delta \int_{\vec{x}_{23}} e^{i\vec{q}\cdot\vec{x}_{23}} e^{-C(\delta) \hat{\Gamma}(\vec{x}_{23})} \left[ \frac{1}{2} \Delta(1 - \tilde{\mathcal{V}}) \right]_{23} \quad (3.83)$$

The probability for a color transition scales as the length  $L$  of the medium. This scaling is expected within the eikonal approximation where trajectories are straight lines.

### 3.3.3 Compact pair limit - Same initial and final color states

For the pair to stay in the same color state, one has to project the evolution operator  $e^{\mathcal{B}}$  into  $\langle \alpha |$  and  $|\beta = \alpha \rangle$ . We already know from the pointlike pair limit that  $e^{\mathcal{B}}$  does not vanish on its diagonal. The first term is

$$\lim_{\substack{\vec{x}_{12} \rightarrow \vec{0} \\ \vec{x}_{34} \rightarrow \vec{0}}} \langle \alpha | e^{\mathcal{B}} | \alpha \rangle = e^{\mathcal{D}} \quad (3.84)$$

However, in order to work at the same accuracy level as 3.80, one needs to extract corrections to this result.

There are two kinds of corrections: one can consider staying in the same color state  $|\alpha\rangle \rightarrow |\alpha\rangle$ , or one can consider a rotation in a given **irrep** followed by an other rotation back to the initial **irrep**. The latter kind of correction will be leading when calculating the broadening of a color singlet in the medium. It is however suppressed by a factor  $X^2$  in the compact pair limit. Let's focus on the former kind of correction in the following paragraph.

#### Non-singlet case, and diagonal contribution

Consider the expression 5.14 for  $\mathcal{B}$  with identical partons

$$\mathbf{R}_1 = \mathbf{R}_2 = \bar{\mathbf{R}}_3 = \bar{\mathbf{R}}_4 \quad (3.85)$$

One can write  $\mathcal{B}$  as

$$\mathcal{B} = -C_R \left( \hat{\Gamma}_{12} + \hat{\Gamma}_{34} \right) + \frac{C_\alpha}{4} (X_t + X_u) - \frac{T_t^2 - T_u^2}{4} (X_t - X_u) \quad (3.86)$$

Due to the symmetry of  $s$ -channel projectors under permutation of partons, the contribution  $\langle \alpha | T_t^2 - T_u^2 | \beta \rangle$  vanishes for  $\alpha = \beta$ . The diagonal of the matrix  $\langle \alpha | \mathcal{B} | \beta \rangle$  is

$$\mathcal{D}_{\alpha\beta} = -C_R \left( \hat{\Gamma}_{12} + \hat{\Gamma}_{34} \right) + \frac{C_\alpha}{4} \left( 2\hat{\Gamma}_{12} + 2\hat{\Gamma}_{34} - \hat{\Gamma}_{14} - \hat{\Gamma}_{23} - \hat{\Gamma}_{13} - \hat{\Gamma}_{24} \right) \delta_{\alpha\beta} \quad (3.87)$$

<sup>5</sup>Recall that  $\hat{\Gamma}$  is defined as  $\hat{\Gamma}(\vec{x}) = \frac{L}{\lambda_0} (1 - \tilde{\mathcal{V}}(\vec{x}))$  with  $\tilde{\mathcal{V}}$  being the Fourier transform of the scattering potential 3.15.

In the pointlike limit  $\vec{x}_{12} = \vec{x}_{34} = \vec{0}$ , one recovers  $-C_\alpha \hat{\Gamma}_{23}$ . Let's expand  $\mathcal{D}$  in the compact pair limit ( $x_{12}, x_{34} \ll x_{23}$ ):

$$\begin{aligned} \mathcal{D} = & -C_\alpha \hat{\Gamma}_{23} - C_\alpha \left( \vec{x}_{12} \cdot \vec{\nabla} + \vec{x}_{34} \cdot \vec{\nabla} \right) \hat{\Gamma}_{23} - \frac{2C_R - C_\alpha}{2} \left( \vec{x}_{12} \cdot \vec{\nabla} \hat{\Gamma}_{12} + \vec{x}_{34} \cdot \vec{\nabla} \hat{\Gamma}_{34} \right) \\ & - \frac{C_\alpha}{2} \left( (\vec{x}_{12} \cdot \vec{\nabla})^2 + (\vec{x}_{34} \cdot \vec{\nabla})^2 + (\vec{x}_{12} \cdot \vec{\nabla})(\vec{x}_{34} \cdot \vec{\nabla}) \right) \hat{\Gamma}_{23} + \dots \end{aligned}$$

Linear contributions in  $\vec{x}_{12}$  and  $\vec{x}_{34}$  vanish after angular integration. Following the steps of section 3.3.1,  $d^2 \vec{p}_1$  and  $d^2 \vec{x}_{34}$  integrals set  $\vec{x}_{34} = -\vec{x}_{12}$ , and the previous expression becomes

$$\mathcal{D} = -C_\alpha \hat{\Gamma}_{23} - \frac{C_\alpha}{2} (\vec{x}_{12} \cdot \vec{\nabla})^2 \hat{\Gamma}_{23} + \dots \quad (3.88)$$

To compare with 3.80, let's consider the initial pair to be a digluon pair in an **irrep**  $\mathbf{8}_a$ . Recall that the pointlike limit gives the leading contribution

$$\langle 1 \rangle \int \frac{d^2 \vec{x}}{(2\pi)^2} e^{i\vec{q} \cdot \vec{x}} e^{-C_A \hat{\Gamma}(\vec{x})} \quad (3.89)$$

where  $\langle 1 \rangle$  is the wave function  $\psi$  normalization. Then the correction up to the same level of accuracy as in 3.80, reads

$$- \langle x_{12}^2 \rangle \frac{L}{\lambda_0} C_A \int \frac{d^2 \vec{x}}{(2\pi)^2} e^{i\vec{q} \cdot \vec{x}} e^{-C_A \hat{\Gamma}(\vec{x})} \left[ \frac{1}{2} \Delta(1 - \tilde{\mathcal{V}}) \right]_{23} \quad (3.90)$$

## Discussion

For an initial wave function and a medium that justify the use of the compact pair limit, one can look at the impact of the length of the medium on the final state distribution. In order to do so, let's consider at first the limit of a zero-sized medium, then we will slowly increase the size of the medium.

Both contributions 3.80 and 3.90 are proportional to  $L/\lambda_0$ , and in the limit  $L \rightarrow 0$ , one recovers the initial  $\delta^{(2)}(\vec{q})$  distribution from 3.89. This checks that the  $L \rightarrow 0$  limit of the compact pair limit indeed coincides with the result expected from 3.44 with  $L = 0$ .

Now let's consider a small medium where the prefactors in both 3.80 and 3.90 are small compared to the initial wave function normalization:

$$\frac{\langle x_{12}^2 \rangle}{\langle 1 \rangle} \frac{L}{\lambda_0} \rightarrow 0 \quad (3.91)$$

Neglecting the possibility that a color rotation occurs in such a medium, the distribution is given by the pointlike limit. Let's simplify a bit the discussion by expanding the dipole cross section at small  $x = |\vec{x}|$

$$\hat{\Gamma}(\vec{x}) = \frac{\bar{Q}_s^2}{2\mu^2} [1 - x\mu K_1(x\mu)] \underset{x\mu \ll 1}{\simeq} \frac{\bar{Q}_s^2}{4} x^2 \log(1/x\mu) \quad (3.92)$$

and considering the log as a constant  $\sim \mathcal{O}(1)$ . The broadening of the distribution which depends on  $e^{-C \hat{\Gamma}_{23}}$  (with color factor  $C$ ) then becomes a Gaussian distribution. Its Fourier

transform is also a Gaussian distribution of width  $\sigma^2 = C \bar{Q}_s^2$ . The initial sharp distribution  $\delta^2(\vec{q})$  will be broadened only through this Gaussian whose width is proportional to the initial state color factor  $C_{in}$  (using the previous illustration with a two-gluon pair in an initial octet state, one finds  $C_{in} = C_A$ ).

Increasing the length of the medium further (still in the small- $x$  region), one has to consider the possibility for a color rotation to occur. This means that in addition to the previous rise in the broadening width  $\sigma^2 \propto L$ , the parton pair has access to “new” color states compared to the pointlike result. Those new color states have distinct color factor  $C = (C_{in} + C_\beta)/2$  where  $\beta$  labels the final state *irrep* of the pair.

At leading order in the compact pair limit, the impact of the length of the medium is twofold: the first effect is the augmentation of the width  $\sigma^2$  of the broadening distribution ( $\sigma^2 \propto L$ ), the second effect is the possibility to change color state and thus give additional color charges (eventually larger than naively expected, e.g.  $(C_A + C_{27})/2 = (3+8)/2 = 5.5$ , approximately twice the gluon color charge) also impacting the width  $\sigma^2 \propto C$ .

**A small note:** as we increase the length of the medium further, multiple color rotations will become relevant and one should reach a region similar to the color randomization process recently underlined by [56]. This regime is also interesting to study in itself as one would expect to eventually see how the *shape* of the available color space<sup>6</sup> impacts the final state distribution.

---

<sup>6</sup>For a two-gluon pair there is a limited number of possible color transitions encoded in the operator  $\mathcal{B}$ . For example, the singlet to decuplet transition is not allowed because the associated color factor vanishes. The *shape* indicates the space of allowed color transitions for the considered process.

## 4.1 Broadening distribution in realistic cases

The previous chapter was devoted to the study of asymptotic systems and in particular asymptotic parton pairs. In the real world, a parton pair cannot be asymptotic, hence one has to abandon the probability density distribution  $f$  used in chapter 4, in favour of a production cross section  $\sigma$ .

In the rest frame of the target nucleus  $A$ , the cross section for the scattering of parton  $a_0$  from the projectile off the nucleus  $A$  to produce partons  $a_1$  and  $a_2$  denoted by

$$\left( \frac{d\sigma(a_0 + A \rightarrow a_1 a_2 + X)}{S_\perp dz d^2\vec{p}_1 d^2\vec{p}_2} \right)_{\alpha \rightarrow \beta} \quad (4.1)$$

and we are inclusive over all hadronic remnants  $X$ . The longitudinal momentum fraction of parton  $a_1$  in the final state is denoted  $z$ , and the transverse momenta of partons  $a_1$  and  $a_2$  are  $\vec{p}_1$  and  $\vec{p}_2$ . For simplicity, let's denote this differential cross section  $\sigma_{\alpha \rightarrow \beta}$ .

The production of a forward dijet (in the target rest frame) at high energies typically arise from the splitting of a parton in the projectile into two partons that will later hadronize into two jets. Being inclusive over the hadronic remnants suggests that one can use a factorized form to study the dijet production cross section, where the partonic part is given by 4.1. The fluctuation time of the pair  $a_1 a_2$  in the incoming parton  $a_0$  is large at high energies, hence the splitting

$$a_0 \rightarrow a_1 a_2$$

typically occurs either long before or long after the medium. Such a splitting contains a longitudinal momentum dependence given by the Altarelli-Parisi splitting function  $\Phi(z)$

$$\begin{array}{c}
 \begin{array}{ccc}
 & a_1, z & \\
 & / & \\
 a_0, 1 \text{ ---} & \bullet & \\
 & \backslash & \\
 & a_2, 1-z &
 \end{array}
 & = & \Phi_{a_0 \rightarrow a_1 a_2}(z)
 \end{array} \quad (4.2)$$

The precise form of  $\Phi(z)$  depends on the partons involved, and is dictated by the QCD Lagrangian [57, 15]. In addition to the longitudinal dependence, the splitting of a parton

in two partons yields a factor (at the amplitude level)

$$\vec{x}_{12}/\vec{x}_{12}^2 \quad (4.3)$$

which is simply the Fourier transform of the usual bremsstrahlung factor  $\sim \vec{x}/\vec{x}^2$  in momentum space. The cross section  $\sigma_{\alpha \rightarrow \beta}$  is the sum of four contributions:

- If both amplitude and conjugate amplitude splittings occur before the medium, the evolution in the medium is described by the four-point correlator  $e^{\mathcal{B}(\vec{x}_{12}, \vec{x}_{34}, \vec{x}_{23})}$  where the dependence of  $\mathcal{B}$  in  $L/\lambda_0$  is implicit.
- If both amplitude and conjugate amplitude splittings occur after the medium, the two-point correlator  $e^{\mathcal{B}(\vec{u}-\vec{u}')}$  describes the evolution in the medium. The two-point correlator depends on  $\vec{u} - \vec{u}'$  where  $\vec{u} = \vec{x}_1 z + \vec{x}_2(1-z)$  and  $\vec{u}' = \vec{x}_4 z + \vec{x}_3(1-z)$ .
- In addition, there are two interference terms depending on  $\vec{x}_1, \vec{x}_2, \vec{u}'$  or  $\vec{u}, \vec{x}_3, \vec{x}_4$ , involving three-point correlators.

As we saw in the previous chapter, one can relate the pointlike limit of an  $m$ -point correlator to an  $n$ -point correlator with  $n < m$ . This yields the cross section

$$\sigma_{\alpha \rightarrow \beta} = \alpha_s \Phi(z) \int_{\vec{x}_{12}, \vec{x}_{23}, \vec{x}_{34}} e^{i \vec{p}_1 \cdot (\vec{x}_{12} + \vec{x}_{34}) + (\vec{p}_1 + \vec{p}_2) \cdot \vec{x}_{23}} \frac{\vec{x}_{12} \vec{x}_{43}}{\vec{x}_{12}^2 \vec{x}_{43}^2} \sqrt{K_\beta / K_\alpha} \langle \alpha | \Sigma | \beta \rangle \quad (4.4)$$

with

$$\Sigma = e^{\mathcal{B}(\vec{x}_1, \vec{x}_2; \vec{x}_3, \vec{x}_4)} + e^{\mathcal{B}(\vec{u}, \vec{u}; \vec{u}', \vec{u}')} - e^{\mathcal{B}(\vec{x}_1, \vec{x}_2; \vec{u}', \vec{u}')} - e^{\mathcal{B}(\vec{u}, \vec{u}; \vec{x}_3, \vec{x}_4)} \quad (4.5)$$

We recover an expression previously derived in [58, 59, 60]. With the normalization  $\sqrt{K_\beta}$ , one can sum over  $\beta$  and recover usual *color-summed* correlators calculated in the literature [61, 62, 63]. The other normalization factor  $\sqrt{1/K_\alpha}$  accounts for the average over initial color indices. We immediately see the analogy between 4.4 and the probability density  $f_{\alpha \rightarrow \beta}$  used in chapter 3: the initial wave function is replaced by the bremsstrahlung factor

$$\psi(\vec{x}) \longrightarrow \frac{\vec{x}}{\vec{x}^2} \quad (4.6)$$

In the following two section I will distinguish two cases, namely the possibility for the initial and final states to have distinct or identical color states.

### 4.1.1 Requiring a color transition between initial and final color states

One can first focus on the case where the initial color state  $\alpha$  is distinct from the final color state  $\beta$ . In this case only the four-point correlator contributes in 4.5 to 4.4. The other correlators cannot rotate the color state of the system because of color triviality (see A.2 for a discussion about color triviality). When the splitting occurs after the medium in the amplitude, it is the parton  $a_0$  that propagate in the medium. This implies that the color state in the conjugate amplitude is fixed by

$$\bar{\mathbf{R}}_{a_0} \equiv \mathbf{R}_3 \otimes \mathbf{R}_4 \quad (4.7)$$

Recall that the  $\equiv$  symbol means that the **Young Diagram (YD)** is the same (in shape). As a matter of fact, the splitting comes with an associated color structure  $\mathcal{R}_\beta$ . This color tensor will be used to reduce  $\mathcal{B}_{(2,2)}$  to  $\mathcal{B}_{(1,2)}$ , and at the same time will remove any ambiguity in the choice of the **Young Tableau (YT)**.

Any color transition between the initial and final states is realized by the four-point correlator. It is possible to use our knowledge in the situation of an asymptotic pair to study how the medium impacts the cross section  $\sigma_{\alpha \rightarrow \beta \neq \alpha}$ . Let's consider the following kinematics:

$$p \sim |\vec{p}_1| \sim |\vec{p}_2| \gg \bar{Q}_s \quad q = |\vec{p}_1 + \vec{p}_2| \ll p \quad (4.8)$$

In this region the integral 4.4 is dominated by  $|\vec{x}_{12}|, |\vec{x}_{34}| \ll |\vec{x}_{23}|$  and the compact pair limit becomes a good approximation to compute  $\langle \alpha | e^{\mathcal{B}} | \beta \rangle$ . Trading  $\vec{p}_2$  in favor of  $\vec{q}$ , the cross section reads

$$\sigma_{\alpha \rightarrow \beta} = \alpha_s \Phi(z) \int_{\vec{x}_{12} \vec{x}_{23} \vec{x}_{34}} e^{i \vec{p}_1 (\vec{x}_{12} + \vec{x}_{34}) + i \vec{q} \vec{x}_{23}} \frac{\vec{x}_{12} \cdot \vec{x}_{43}}{\vec{x}_{12}^2 \vec{x}_{43}^2} \langle \alpha | e^{\mathcal{B}(\vec{x}_1, \vec{x}_2; \vec{x}_3, \vec{x}_4)} | \beta \rangle \sqrt{\frac{K_\beta}{K_\alpha}}$$

A color transition is associated with the term in  $\mathcal{B}$ :

$$+ \frac{1}{4} \langle \alpha | T_t^2 - T_u^2 | \beta \rangle \underbrace{\left( \hat{\Gamma}_{23} + \hat{\Gamma}_{14} - \hat{\Gamma}_{13} - \hat{\Gamma}_{24} \right)}_X \quad (4.9)$$

Let's expand the factor  $X$  at fixed  $\vec{x}_{23}$ , up to the second order in the small quantities  $x_{12}$  and  $x_{34}$ . It will involve the Hessian matrix<sup>1</sup> of the function  $\hat{\Gamma}$  valued at  $\vec{x}_{23}$  that I note  $H_{23} = H(\hat{\Gamma}) \Big|_{23}$ .

$$\begin{aligned} 2X &= [(\vec{x}_{12} + \vec{x}_{34}) \cdot H_{23} \cdot (\vec{x}_{12} + \vec{x}_{34})] - [\vec{x}_{12} \cdot H_{23} \cdot \vec{x}_{12}] - [\vec{x}_{34} \cdot H_{23} \cdot \vec{x}_{34}] + \dots \\ &= \vec{x}_{12} \cdot H_{23} \cdot \vec{x}_{34} + \vec{x}_{34} \cdot H_{23} \cdot \vec{x}_{12} + \dots \end{aligned}$$

As the function  $\hat{\Gamma}$  is a radial function, the matrix  $H_{23}$  is symmetric and we can write

$$X = \vec{x}_{12} \cdot H_{23} \cdot \vec{x}_{34} + \dots$$

Using [50] or B.2, the factor  $X$  reads:

$$X \simeq \vec{x}_{12} \cdot \vec{x}_{34} \frac{\bar{Q}_s^2}{4} \log \left( \frac{1}{\mu^2 x_{23}^2} \right) \quad (4.10)$$

Inserting this into the relation 3.72 yields the cross section

$$\begin{aligned} \sigma_{\alpha \rightarrow \beta} &= \alpha_s \Phi(z) \frac{\mathcal{F}_{\alpha\beta} \sqrt{K_\beta}}{\sqrt{K_\alpha}} \int_{\vec{x}_{12} \vec{x}_{34}} e^{i \vec{p}_1 (\vec{x}_{12} + \vec{x}_{34})} \frac{(\vec{x}_{12} \cdot \vec{x}_{43})^2}{\vec{x}_{12}^2 \vec{x}_{43}^2} \\ &\quad \int_{\vec{x}_{23}} e^{i \vec{q} \vec{x}_{23}} \int_0^1 d\delta e^{-[\delta C_\alpha + (1-\delta) C_\beta] \hat{\Gamma}_{23}} \frac{\bar{Q}_s^2}{4} \log \left( \frac{1}{\mu^2 x_{23}^2} \right) \quad (4.11) \end{aligned}$$

<sup>1</sup>A square matrix of second-order partial derivatives of a scalar valued function.



The integral in the first line can be performed using

$$\int_{\vec{x}_{12} \vec{x}_{34}} e^{i\vec{p}_1(\vec{x}_{12}+\vec{x}_{34})} \frac{(\vec{x}_{12} \cdot \vec{x}_{43})^2}{\vec{x}_{12}^2 \vec{x}_{43}^2} = \frac{1}{2\pi^2|\vec{p}|^4} \quad (4.12)$$

It is instructive to compare 4.11 with the expression 3.80 obtained in chapter 3. After the  $d^2\vec{p}_1$  integral, the first factor of 4.11 compares with the factor  $\langle \vec{x}_{12}^2 \rangle$  of 3.80. It gives information on the effective size of the pair in the medium, set by the wave function in the case of an asymptotic pair, and by the bremsstrahlung factor in the realistic case of pair production. The  $d^2\vec{p}$  integral is only valid at large  $|\vec{p}|$  since the expansion is done for small values of  $x_{12}$  and  $x_{34}$ . However one can still integrate over large momenta, i.e.  $|\vec{p}| \geq P$ , then the effective size of the pair for those events is given by  $\langle x_{12}^2 \rangle \sim (2\pi P^2)^{-1}$ .

In both cases, the final distribution is a product of a suppression factor (the cost for the transition to occur), and a linear superposition of broadening distributions for pointlike color charges (given by the remaining integral over  $d^2\vec{x}_{23}$ ). In particular the dependence on the momentum imbalance is the same in both cases. In particular, the broadening of the imbalance distribution scales as the average  $\frac{C_\alpha+C_\beta}{2}$  of initial and final color charges.

### 4.1.2 Particular case: same initial and final color states

The other possibility is that the initial and final state are in the same *irrep*. In this case, we already know what is the color state that propagates in the medium (color triviality). However the cross section is now a sum of four, three and two-point correlators, which can be performed within the same kinematics 4.8 as before. As opposed to section 3.3.3, the pointlike limit vanishes this time. The sum  $\Sigma$  in 4.5 becomes

$$\Sigma \xrightarrow{\vec{x}_{12}=\vec{x}_{34}=\vec{0}} 0$$

Let's recall the expression 5.14 of the operator  $\mathcal{B}$ ,

$$\mathcal{B} = -\frac{1}{2} (C_{R_1} W_{34}^1 + C_{R_2} W_{34}^2 + C_{R_3} W_{12}^3 + C_{R_4} W_{12}^4) - \frac{1}{2} N_c (X_t + X_u) \mathcal{Q} \left( b = \frac{X_t - X_u}{X_t + X_u} \right) \quad (4.13)$$

and study this operator in the compact pair limit. Given the expression of  $\mathcal{Q}$  in 5.8,

$$\mathcal{Q} = \frac{1}{2N_c} [(T_t^2 + T_u^2) + b(T_t^2 - T_u^2)] \quad (4.14)$$

One identifies two parts: the  $b$ -dependent part, and the  $b$ -independent part that will be used to segment a bit the calculation of  $\Sigma$ . In general cases, both parts contain diagonal elements, as opposed to the previous section where we just had to deal with the  $b$ -dependent part of  $\mathcal{Q}$ .

Let's look at the  $b$ -dependent and  $b$ -independent parts of the calculation for the sum  $\Sigma$  (defined in 4.5). Some technicalities are present allowing to extract a general result valid for any parton *irreps* in a realistic process. In particular, the prefactor mixing the splitting variable  $z$  with color charges, see appendix E of [50], is derived in a compact form.

**The  $b$ -dependent part of  $\mathcal{B}$ .** Its contribution in  $\mathcal{B}$  solely originate from the  $\mathcal{Q}$  term, and reads

$$+ \frac{1}{4} \langle \alpha | T_t^2 - T_u^2 | \beta \rangle \underbrace{\left( \hat{\Gamma}_{23} + \hat{\Gamma}_{14} - \hat{\Gamma}_{13} - \hat{\Gamma}_{24} \right)}_X \quad (4.15)$$

In the sum  $\Sigma$ , we are looking at diagonal pieces proportional to  $b$ . The associated color structure is  $\langle \alpha | T_t^2 - T_u^2 | \alpha \rangle$ . Let us use the fact that three- and two-point correlators are limits of the four-point correlator.

- The first three point correlator is obtained from the four point one by the substitution

$$\vec{x}_{12} \rightarrow \vec{0}, \quad \vec{x}_{34} \rightarrow \vec{x}_{34}, \quad \vec{x}_{23} \rightarrow \vec{x}_{23} + z\vec{x}_{12}.$$

Applying this to  $X$ , one finds that  $X \rightarrow X_{3p} = 0$ . Hence there is no contribution proportional to  $\langle \alpha | T_t^2 - T_u^2 | \alpha \rangle$  in the first 3-point correlator. Performing the same for the second 3-point correlator:

$$\vec{x}_{12} \rightarrow \vec{x}_{12}, \quad \vec{x}_{34} \rightarrow \vec{0}, \quad \vec{x}_{23} \rightarrow \vec{x}_{23} + z\vec{x}_{34}.$$

yields the same result:  $X \rightarrow X_{3p'} = 0$ .

- The same procedure can be followed for the 2-point correlator.

$$\vec{x}_{12} \rightarrow \vec{0}, \quad \vec{x}_{34} \rightarrow \vec{0}, \quad \vec{x}_{23} \rightarrow \vec{x}_{23} + z\vec{x}_{12} + z\vec{x}_{34}.$$

and  $X \rightarrow X_{2p} = 0$ .

- Only in the four-point correlator the  $b$ -dependent part of  $\mathcal{Q}$  remains. This is a reminder that a color transition can only be realized by the four-point correlator. Using the previous section results for the compact pair limit (the value of  $X_{4p}$ ), one finds that 4.15 is given by

$$\frac{1}{4} \langle \alpha | T_t^2 - T_u^2 | \alpha \rangle \vec{x}_{12} \cdot H_{23} \cdot \vec{x}_{34} \quad (4.16)$$

One has to keep in mind that matrix elements of  $\langle \alpha | T_t^2 - T_u^2 | \alpha \rangle$  vanish if  $\mathbf{R}_1 \equiv \mathbf{R}_2$ .

### Remaining contribution on the diagonal of $\mathcal{Q}$ .

In 4.13, aside from the  $b$ -dependent part of  $\mathcal{Q}$ , all terms are diagonals. The contribution,  $\langle \alpha | T_t^2 + T_u^2 | \alpha \rangle$  from  $\mathcal{Q}$  can be traded in favor of

$$\langle \alpha | T_t^2 + T_u^2 | \alpha \rangle = \sum_{i=1}^4 C_{R_i} - C_\alpha \quad (4.17)$$

with  $\alpha$  labeling an **irrep** of the  $s$ -channel.  $W_{ij}^a$  in the following expression is defined as  $W_{ij}^a = \hat{\Gamma}_{ai} + \hat{\Gamma}_{aj} - \hat{\Gamma}_{ij}$ . In  $\mathcal{B}$ , combinations of  $W_{ij}^a$  that appear do not mix amplitude and conjugate amplitude indices between upper index  $a$  and the two lower indices  $ij$ . Each Casimir  $C_{R_i}$  are associated with a factor

$$C_{R_i} \left[ -\frac{1}{2} W^i - \frac{1}{4} (X_t + X_u) \right] \quad \forall i = 1, \dots, 4 \quad (4.18)$$

and the  $s$ -channel Casimir with

$$C_\alpha \left[ \frac{1}{4} (X_t + X_u) \right] \quad (4.19)$$

Let's expand  $\Sigma$ , at the leading order one has to consider the combination of  $\mathcal{B}$ :

$$\begin{aligned} \Sigma = e^{\mathcal{B}(\vec{x}_{23}; 0, 0)} & \left( \mathcal{B}(\vec{x}_{23}; \vec{x}_{12}, \vec{x}_{34}) - \mathcal{B}(\vec{x}_{23} + z\vec{x}_{12}; \vec{0}, \vec{x}_{34}) \right. \\ & \left. - \mathcal{B}(\vec{x}_{23} + z\vec{x}_{34}; \vec{x}_{12}, \vec{0}) + \mathcal{B}(\vec{x}_{23} + z\vec{x}_{12} + z\vec{x}_{34}; \vec{0}, \vec{0}) \right) + \dots \end{aligned} \quad (4.20)$$

All contributions proportional to  $\hat{\Gamma}_{12}$  in  $\mathcal{B}$  will vanish in this combination:

$$\underbrace{\hat{\Gamma}(\vec{x}_{12})}_{4 \text{ points}} - \underbrace{\hat{\Gamma}(\vec{0})}_{3 \text{ points}} - \underbrace{\hat{\Gamma}(\vec{x}_{12})}_{3 \text{ points}} + \underbrace{\hat{\Gamma}(\vec{0})}_{2 \text{ points}} = 0$$

The same is true for  $\hat{\Gamma}_{34}$ . The relevant contributions remaining in the diagonal are given by

$$-\frac{1}{4} (C_{R_1}, C_{R_2}, C_{R_3}, C_{R_4}, C_\alpha) \cdot M \cdot \left( \hat{\Gamma}_{13}, \hat{\Gamma}_{14}, \hat{\Gamma}_{23}, \hat{\Gamma}_{24} \right)^t$$

with  $M$  the  $4 \times 5$  matrix defined as

$$M = \begin{pmatrix} + & + & - & - \\ - & - & + & + \\ + & - & + & - \\ - & + & - & + \\ + & + & + & + \end{pmatrix}$$

To take care of the sum over the four correlators, let's translate “ $\hat{\Gamma}$ -vector” with respect to 4.5

$$\begin{pmatrix} \hat{\Gamma}_{13} \\ \hat{\Gamma}_{14} \\ \hat{\Gamma}_{23} \\ \hat{\Gamma}_{24} \end{pmatrix} \rightarrow \begin{pmatrix} \hat{\Gamma}_{13} & +\hat{\Gamma}(\vec{x}_{23} + z\vec{x}_{12} + z\vec{x}_{34}) & -\hat{\Gamma}(\vec{x}_{23} + z\vec{x}_{12}) & -\hat{\Gamma}(\vec{x}_{23} + z\vec{x}_{34} + \vec{x}_{12}) \\ \hat{\Gamma}_{14} & +\hat{\Gamma}(\vec{x}_{23} + z\vec{x}_{12} + z\vec{x}_{34}) & -\hat{\Gamma}(\vec{x}_{23} + z\vec{x}_{12} + \vec{x}_{34}) & -\hat{\Gamma}(\vec{x}_{23} + z\vec{x}_{34} + \vec{x}_{12}) \\ \hat{\Gamma}_{23} & +\hat{\Gamma}(\vec{x}_{23} + z\vec{x}_{12} + z\vec{x}_{34}) & -\hat{\Gamma}(\vec{x}_{23} + z\vec{x}_{12}) & -\hat{\Gamma}(\vec{x}_{23} + z\vec{x}_{34}) \\ \hat{\Gamma}_{24} & +\hat{\Gamma}(\vec{x}_{23} + z\vec{x}_{12} + z\vec{x}_{34}) & -\hat{\Gamma}(\vec{x}_{23} + z\vec{x}_{12} + \vec{x}_{34}) & -\hat{\Gamma}(\vec{x}_{23} + z\vec{x}_{34}) \end{pmatrix}$$

First of all, in the pointlike limit ( $\vec{x}_{12} = \vec{x}_{34} = \vec{0}$ ) this expression vanishes, and also the linear contribution in the expansion at small  $\vec{x}_{12}, \vec{x}_{34}$  vanishes. One has to push the expansion to the second order to get

$$\begin{pmatrix} \hat{\Gamma}_{13} \\ \hat{\Gamma}_{14} \\ \hat{\Gamma}_{23} \\ \hat{\Gamma}_{24} \end{pmatrix} \rightarrow \begin{pmatrix} z(z-1) \\ (z-1)^2 \\ z^2 \\ z(z-1) \end{pmatrix} \vec{x}_{12} \cdot H_{23} \cdot \vec{x}_{34} + \dots \quad (4.21)$$

We already obtained the contribution  $\vec{x}_{12} \cdot H_{23} \cdot \vec{x}_{34}$  in the previous section, and in the compact pair its value limit is given by 4.10. The associated color factor is given by

$$-\frac{1}{4} (C_{R_1}, C_{R_2}, C_{R_3}, C_{R_4}, C_\alpha) \cdot M \cdot \begin{pmatrix} z(z-1) \\ (z-1)^2 \\ z^2 \\ z(z-1) \end{pmatrix} = \mathcal{F} \quad (4.22)$$

For example, if we consider the splitting of a gluon into a digluon, the color structure of the vertex selects an anti-symmetric octet. Using 4.22 with  $C_{R_i} = N_c$  for all  $i$  and  $C_\alpha = N_c$  one find

$$\mathcal{F}(g \rightarrow gg) = -N_c \frac{(2z-1)^2}{4} \quad (4.23)$$

where that the overall minus sign simply arises from  $\vec{x}_{34} = -\vec{x}_{43}$ . One is able to identify the factor  $(1-2z)^2$  present at the end of the appendix E of [50]. Expression 4.22 can be used for any kind of parton splitting involved in this setup.

### 4.1.3 Result for broadening distribution

The two previous sections gave us the two kinds of contributions to the cross section  $\sigma_{\alpha \rightarrow \beta}$  for  $\alpha = \beta$  and  $\alpha \neq \beta$ . Namely,

$$\sigma_{\alpha \rightarrow \beta} = \alpha_s \Phi(z) \int_{\vec{x}_{12} \vec{x}_{23} \vec{x}_{34}} e^{i \vec{p}_1 (\vec{x}_{12} + \vec{x}_{34}) + i \vec{q} \vec{x}_{23}} \frac{\vec{x}_{12} \cdot \vec{x}_{43}}{\vec{x}_{12}^2 \vec{x}_{43}^2} \langle \alpha | \Sigma | \beta \rangle \sqrt{\frac{K_\beta}{K_\alpha}}$$

becomes in the compact pair limit

$$\begin{aligned} \sigma_{\alpha \rightarrow \beta} &\simeq \alpha_s \Phi(z) \int_{\vec{x}_{12} \vec{x}_{23} \vec{x}_{34}} e^{i \vec{p}_1 (\vec{x}_{12} + \vec{x}_{34}) + i \vec{q} \vec{x}_{23}} \frac{\vec{x}_{12} \cdot \vec{x}_{43}}{\vec{x}_{12}^2 \vec{x}_{43}^2} \\ &\times \sqrt{\frac{K_\beta}{K_\alpha}} \times F_{\alpha\beta} \int_0^1 d\delta e^{-C(\delta) \hat{\Gamma}_{23}} (\vec{x}_{12} \cdot H_{23} \cdot \vec{x}_{34}) \end{aligned} \quad (4.24)$$

where the factor  $F_{\alpha\beta}$  is given by

$$F_{\alpha\beta} = \begin{cases} \frac{1}{4} \langle \alpha | T_t^2 - T_u^2 | \beta \rangle & \text{for } \alpha \neq \beta \\ \mathcal{F} + \frac{1}{4} \langle \alpha | T_t^2 - T_u^2 | \alpha \rangle & \text{for } \alpha = \beta, \text{ with } \mathcal{F} \text{ defined in 4.22} \end{cases} \quad (4.25)$$

Following the lines of the end of section 4.1.1, the contribution  $\vec{x}_{12} \cdot H_{23} \cdot \vec{x}_{34}$  can be split an  $\vec{x}_{23}$ -dependent factor and a factor depending on  $\{\vec{x}_{12}, \vec{x}_{34}\}$ . As a result the cross section factorizes into: i) a suppression factor from  $d^2 \vec{x}_{12} d^2 \vec{x}_{34}$  integrals, and ii) a broadening distribution impacting the transverse momentum imbalance of the pair.

- The suppression factor corresponds to the production of two partons from a incoming single parton and depends on the transverse momentum  $\vec{p}$  as  $1/|\vec{p}|^4$ . Additionally, there is a factor  $\sqrt{K_\beta/K_\alpha} F_{\alpha\beta}$  that weighs possible transitions  $|\alpha\rangle \rightarrow |\beta\rangle$ .
- The broadening distribution results from the  $\vec{x}_{23}$ -integral. This distribution is a superposition of pointlike distributions associated with color charges  $C(\delta)$ .

## 4.2 Colorimetry

The idea to perform some “colorimetry” of a nuclear medium is not a new one, for example Ref. [64] proposed to study the  $D/\pi$  production ratio at  $p_t \sim 5 - 10 \text{ GeV}$  in nucleus-nucleus collisions and relate it to the density of color charge in the medium.

Here, I use the term “colorimetry” for similar topics. By definition an *irrep* is gauge invariant and should in principle be observable. This statement might be surprising at first, because there is confinement in QCD and only color singlet states are observed. However, in the toy-world discussed in chapter 3.2 of [39], one learns that our world could have been such that we would be able to see quarks in our detectors.

There are lots of topics to explore in both theory and phenomenology regarding the nuclear interaction, and I would like to underline a few where the previous study may give some insight.

### 4.2.1 Broadening distribution

Let’s simplify the result obtained in section 4.1.3 for the broadening distribution. At small values of  $\vec{x}_{23}$ , one can approximate the dipole cross section  $\hat{\Gamma}_{23}$  in the broadening distribution to obtain

$$e^{-C(\delta)\hat{\Gamma}_{23}} \rightarrow e^{-C(\delta)\frac{\bar{Q}_s^2}{4}x_{23}^2\log(1/\mu x)} \quad (4.26)$$

Within logarithmic accuracy  $\log(1/\mu x) \sim \mathcal{O}(1)$ , the Fourier transform of 4.26 gives a Gaussian distribution of width  $\sigma^2 \propto C(\delta)\bar{Q}_s^2$ . After averaging over the position  $\delta$  of the color rotation, the exact distribution is well approximated by a Gaussian of width  $\sigma^2 \propto \frac{C_\alpha + C_\beta}{2}\bar{Q}_s^2$ . The origin of this average is easy to understand. The probability for the color transition to occur is independent of the position in the medium, hence in average it will happen at  $z = L/2$ . It means that the pair will suffer a broadening as if it were a pointlike color charge  $C_\alpha$  during half of the path in the medium, and a pointlike color charge  $C_\beta$  for the other half.

The resulting  $q_t$ -distribution is a superposition of the distributions for the possible final color states  $\beta$ . In this simplified discussion, those distributions are approximately Gaussian distributions with a width proportional to the average color charge (between initial and final states) and a normalization  $\mathcal{N}_\beta$  proportional to the color factor  $F_{\alpha\beta}$ .

For a given range in  $q_t$ , one can use the interplay between  $F_{\alpha\beta_i}$  and the exponential falloff of the Gaussian distributions in order to identify regions where the total distribution is dominated by a few *irreps*. In this situation, the nuclear medium crossed by the parton pair effectively acts as an “*irrep* filter” for the final color state! This is interesting in itself because it gives us a handle on the final color state. This can then be used to study some important questions such as

- Does local parton hadron duality depend on the color state?
- Can we distinguish between different quarkonium production mechanism (e.g. color singlet model, color evaporation model, NRQCD...)?
- How does the radiative energy loss of coherent systems in a medium depend on the color state?

## 4.2.2 Daydreaming or actual applications?

Of course, we do not observe partons in detectors as in the toy world of Ref. [39] but hadronic  $p_t$ -distributions (in a given range) might be reminiscent from the color structure at the parton level.

### Local parton hadron duality in jet evolution

In the local parton hadron duality picture [15], a number of produced hadrons (observed but not computed) is related to a number of produced partons (not observed but computed).

From the parton side, one has to deal with evolution equations down to some lower virtuality scale  $Q_0$  producing more and more partons (e.g. DGLAP evolution equations). The scale  $Q_0$  corresponds to either how brave one is to deal with those equations and/or to how much one believes in the pQCD language. This scale  $Q_0$  is arbitrarily<sup>2</sup> chosen to separate the parton world from the hadron world. Ideally, one push down to  $Q_0 \sim \mathcal{O}(\Lambda_{QCD})$ .

After the evolution the number of produced partons is related to the number of hadrons produced via hadronization. In the local parton hadron duality approach, one can do phenomenology by relating the number of produced partons to the number of produced hadrons using some proportionality constant  $R$  depending on  $Q_0$ .

Here is a possibly interesting problem: on the one hand hadronization deals with *colorless objects* (hadrons are color singlet), and on the other hand hadronization deals with *colorful objects* (parton systems). There might be some dependence of the hadronization process on the color structure. Hence the question: “Is there a dependence of the factor  $R^{Q_0}$  on the color state of the parton system?”

In the study of dijet momentum imbalance, one can use the nuclear medium (*irrep-filter*) to answer this question. If one looks at an eventual dependence of the factor  $R^{Q_0}$  on the momentum imbalance  $|\vec{q}|$  of the parton pair, this dependence acts as a proxy for the dependence on  $R^{Q_0}$  on the *irrep*  $\beta$  of the pair.

### Quarkonium production mechanisms

It’s been more than 40 years since the discovery of the  $J/\psi$  [65, 66], and there is still no consensus on the dominant quarkonium production mechanism (see [67] and references therein for quarkonium production mechanism).

There are various approaches to quarkonium production. One may rely on the production of definite quantum number such as the early color singlet model where only the  $c\bar{c}$ -pairs produced with the right quantum numbers are considered, or the non-relativistic QCD effective theory where different quantum numbers are associated with different probabilities within a double expansion in  $\alpha_s$  and in the pair relative velocity  $v$ . In a more empirical model, the color evaporation model, the criterion for producing a quarkonium is to require a  $q\bar{q}$ -pair with an invariant mass between  $2m_q$  and the threshold for open heavy flavor hadron production, independently of the precise quantum numbers of the

<sup>2</sup>In principle the full theory containing the hadronization mechanism should not depend on this scale.

pair. The pair is supposed to be rotated from “wrong” quantum numbers (spin, color) into the quarkonium “right” quantum numbers by soft gluon emissions.

Instead of the dijet production discussed in this chapter, the same formalism is in principle usable for the production of two heavy quarks. The trick would be again to use the nuclear medium as a color filter to give a handle on the color state of the pair after crossing the medium. The quantum numbers of the pair after crossing the medium are correlated to the broadening of the pair in the medium (at least for the color part). Hence the broadening of the pair could give us some insight in order to constrain quarkonium production models.

### Energy loss of coherent systems

The radiation intensity associated to a given partonic process is expected to depend on the color state involved (e.g. [16]). The full treatment can be quite involved for a large number of partons involved in the process, however the conjecture in [68] states that the medium-induced radiation for a forward  $1 \rightarrow n$  process depends simply on the combination of color charges  $C_{in} + C_{out} - C_t$  when the transverse momentum  $\vec{K}_i$  of those partons are of the same order.

In order to prove this conjecture, the study of momentum imbalance of partonic systems produced in hard process may come in handy again. At some given range in the momentum imbalance, the medium acts as an *irrep* filter and selects a ratio of the possible  $C_{out}$  from the system of  $n$  partons. Event multiplicity being correlated to the radiation intensity, one would expect this multiplicity to evolve with the imbalance of the system through this simple change in the color charge  $C_{out}$ .

In this picture, the fact that it is the color charge  $C_{out}$  that contributes and not individual color charges of each parton, gives us some tangible information on the energy loss of coherent systems.

# CHAPTER 5

## A STUDY ON ANOMALOUS DIMENSION MATRICES

This chapter is dedicated to a study on soft anomalous dimension matrices. The first section is an introduction to the construction that can be found in [16] (referred to as DM). The second section is dedicated to some useful cases of this matrix in a QCD context: *how can those results be recovered using some birdtrack tricks?* The third section is an exploration of further cases of DM's construction involving irreps distinct from the  $SU(N_c)$  fundamental and adjoint: an algorithm to compute those matrices is detailed. Finally, the last section is a study of the symmetry of soft anomalous dimension matrices built from this algorithm with respect to the negative dimension theorem.

### 5.1 Soft anomalous dimension matrix

#### Double logarithmic approximation and associated physics

Let us consider a three-body process, for example

$$a + b \rightarrow c \quad (+X) \tag{5.1}$$

Parton momenta are  $p_i$  and irreps are  $R_i$  for  $i = \{a, b, c\}$ . Associated to such a process, consider an observable  $V$  (inclusive production rate for example) depending on the hard scale  $Q \gg \Lambda_{QCD}$  of the parton-parton interaction. At the hard scale  $Q$ , it is natural to expect additional soft gluon radiations to happen. If the observable  $V(Q)$  is in a kinematic region close to the Born-level kinematic region, it implies that:

- The additional radiation of gluons does not disturb the kinematics of the process. Alternatively, the radiation is considered to be soft regarding to the hard scale  $Q$ .
- There is a compensation for inclusive observables between virtual and real emissions.

Due to the bremsstrahlung law, large logarithms appear at each order in the  $\alpha_S$  perturbative expansion. A gluon emitted from a primary parton ( $a$ ,  $b$ , or  $c$ ) can be soft and/or collinear to the parent. Both cases produce a logarithmic contribution. Those logarithmic contributions appear at each order in the perturbative series in the form

$$\alpha_S^{Born} \times (\alpha_S \cdot [\log^2 + \mathcal{O}(\log)])^n \tag{5.2}$$



where  $n$  indicate the number of gluon (virtual or real) emissions. If those logarithms become large, they can compensate the smallness of the strong coupling such that

$$\alpha_S \cdot \log^2 \sim \mathcal{O}(1), \quad \alpha_S \ll 1 \quad (5.3)$$

spoil the predictive power of the perturbative series. Hence, those logarithms have to be resummed in order to recover the predictive power of the expansion. This resummation can be done in the **Double Logarithmic Approximation (DLA)** where one keeps only the leading logarithmic contributions. It will produce a form factor, that factorizes from the Born level cross section, encoding the physics of virtual-real emission and partial cancellation, called the Sudakov form factor. An important property of Sudakov form factors is that it is a “personal belonging” of each primary parton of the process (The mass  $m_i^2$  and color charge  $C_{R_i}$  are kept “private” for each parton  $\{a, b, c\}$ ).

Beyond the **DLA**, there are obviously other effects such as the “recoil” from secondary partons entering in the game, and also the single log contributions.

### Single logarithmic soft radiation

At the single logarithmic level, the radiation of secondary gluons from our three primary partons can be treated similarly. Group into independent Sudakov form factors each contribution that keeps color charge and mass “private”. This is possible because the color conservation  $T_a + T_b = T_c$  leads to

$$2T_a \cdot T_b = C_{R_c} - C_{R_a} - C_{R_b} \quad (5.4)$$

and similar relations for  $T_a \cdot T_c$  and  $T_b \cdot T_c$ .

The color structure becomes non-trivial when one choose to consider four partons instead of three:

$$a + b \longrightarrow c + d \quad (5.5)$$

In this case, color conservation reads  $T_a + T_b = T_c + T_d$  and there is no relation similar to 5.4. It is still possible to keep in four independent form factors the DL collinear and soft radiation and also the single log (SL) collinear radiation.

However, to complete the picture at the single logarithmic level, one has to also include soft radiation at large angles. Now, the color structure associated to this process cannot be formulated in terms of independent form factors, and it is encoded by introducing an extra form factor called the *cross-channel form factor*, or *fifth form factor* [16].

Both the Sudakov form factor and the cross channel form factor are the result of the resummation into an exponential of a given kernel. The kernel (of interest here) for the cross channel form factor is called the soft anomalous dimension matrix and is denoted by  $\mathcal{Q}$ .

### 5.1.1 Review of the Dokshitzer-Marchesini method

The technical point in the resummation of soft large angle radiation is to calculate the following operator that will be exponentiated into the fifth form factor.

$$\Gamma_{DM} = - (T_t^2 \cdot T + T_u^2 \cdot U) \quad (5.6)$$

$$= -N_c(T + U) \cdot \mathcal{Q}(b), \quad b \equiv \frac{T - U}{T + U} \quad (5.7)$$

with  $T_t^2 = (T_2 + T_3)^2 = (T_1 + T_4)^2$  and  $T_u^2 = (T_1 + T_3)^2 = (T_2 + T_4)^2$ . In 5.6,  $T$  and  $U$  are kinematical factors that depend on the physics considered<sup>1</sup>. The main interest of this section is to calculate the operator  $\mathcal{Q}$  involved in 5.6. After some simple algebra in 5.6, it can be shown to be

$$\mathcal{Q} = \frac{1}{2N_c} [(T_t^2 + T_u^2) + b(T_t^2 - T_u^2)] \quad (5.8)$$

**Remarks :**

- All partons are considered as outgoing, hence color conservation reads  $T_1 + T_2 + T_3 + T_4 = 0$ .
- The  $t$ -channel is  $1 + 4 \leftrightarrow 2 + 3$ , the  $u$ -channel is  $1 + 3 \leftrightarrow 2 + 4$  and the  $s$ -channel is  $1 + 2 \leftrightarrow 3 + 4$ .

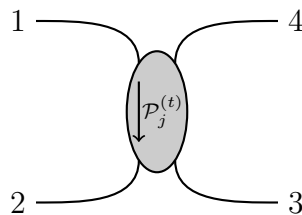
The two color operators  $T_t^2$  and  $T_u^2$  can be complicated objects in an arbitrary basis however they become simple in their respective projector-basis<sup>2</sup>. The matrix representation of  $T_t^2$  (resp.  $T_u^2$ ) is the diagonal matrix with  $t$ -channel (resp.  $u$ -channel) quadratic Casimirs. A compact formulation is

$$T_t^2 \cdot \mathcal{P}_i^{(t)} = C_i^{(t)} \mathcal{P}_i^{(t)} \quad (5.9)$$

where the superscript indicates the channel. Thus an essential element is the rotation matrix  $K_{st}$  that relates  $s$ -channel to  $t$ -channel projectors [16]

$$\mathcal{P}^{(s)} = K_{st} \cdot \mathcal{P}^{(t)} \quad (5.10)$$

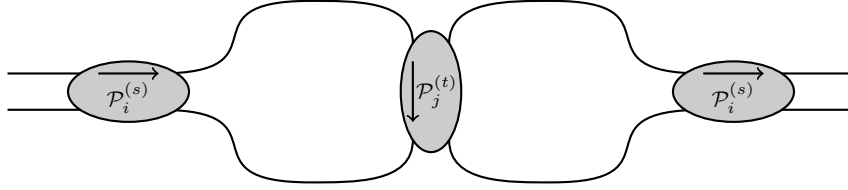
Let's see how one calculates the  $K_{st}$  matrix using birdtracks: consider a contribution to a Feynman diagram with a color tensor that is proportional in the  $t$ -channel to  $\mathcal{P}_j^{(t)}$



<sup>1</sup>For radiation resummation as in [16], it involves dipole antenna kinematic factors, and in the broadening case as in [50] it involves dipole scattering potentials.

<sup>2</sup>I assume for this discussion that the process is elastic, namely  $a + b \rightarrow a + b$ . Otherwise, one has to introduce instead of projector-basis a more general vector-basis. It is related to the discussion in section 3.1.3.

Then project this contribution into an  $s$ -channel projector



This color tensor is obviously proportional to  $\mathcal{P}_i^{(s)}$  and the proportionality constant is  $K_{st}(i, j)$ . Another way to see this is to use the notation from b.21 and trace:

$$K_{st}(i, j) \equiv \frac{1}{\alpha_i} \text{Tr} \left( \begin{array}{c} \alpha_i \\ \text{---} \\ \begin{array}{ccc} 1 & & 4 \\ \diagdown & & / \\ & \beta_j & \\ / & & \diagdown \\ 2 & & 3 \end{array} \\ \text{---} \\ \alpha_i \end{array} \right) \quad (5.11)$$

In the r.h.s., the birdtrack is a Wigner  $6 - j$  coefficient<sup>3</sup> (Wigner  $3n - j$  symbols are discussed in chapter five of [45]).

The calculation of  $\mathcal{Q}$  has two steps:

1. Calculate all projectors in all channels  $s, t, u$ .
2. Calculate the rotation matrices  $K_{st}$  and  $K_{su}$ .

This procedure is a nice training in *birdtracking* and getting accustomed to the color algebra, however there are some quicker ways to get the same result for relevant cases as we will see.

## 5.2 Relation to the broadening evolution kernel and calculation of $\mathcal{Q}$ for standard partons

In this section, I will relate the broadening kernel  $\mathcal{B}$  to the soft anomalous dimension matrix  $\mathcal{Q}$ . Then I will derive using birdtrack notations those operators for cases involving QCD partons. Finally I will mention a symmetry observed in [16] that will motivate the next section.

### 5.2.1 Evolution Kernel

The evolution operator  $\mathcal{B}$  in [50] is related to the soft anomalous dimension matrix in [16]. In order to see how, one starts with the relation of the evolution operator kernel for the broadening

$$\mathcal{B} = - \left( \hat{\Gamma}_{12} \mathcal{C}_{12} + \hat{\Gamma}_{34} \mathcal{C}_{34} + \hat{\Gamma}_{23} \mathcal{C}_{23} + \hat{\Gamma}_{14} \mathcal{C}_{14} + \hat{\Gamma}_{13} \mathcal{C}_{13} + \hat{\Gamma}_{24} \mathcal{C}_{24} \right) \quad (5.12)$$

<sup>3</sup>Up to some normalization involving  $3 - j$  and  $1 - j$  coefficients.

It is important to remark that each  $\mathcal{C}_{ij}$  takes a simple form in its own channel, as an illustration  $\mathcal{C}_{23}$  is

$$\mathcal{C}_{23} = \begin{array}{c} \text{---} 1 \\ \text{---} 2 \\ \text{---} 3 \\ \text{---} 4 \end{array} \begin{array}{c} \text{---} \\ \text{---} \\ \text{---} \\ \text{---} \end{array} = \sum_{\gamma_t} \begin{array}{c} \text{---} \\ \text{---} \\ \text{---} \\ \text{---} \end{array} \begin{array}{c} \text{---} \\ \text{---} \\ \text{---} \\ \text{---} \end{array} = \sum_{\gamma_t} \frac{C_{R_2} + C_{R_3} - C_{\gamma_t}}{2} \begin{array}{c} \text{---} \\ \text{---} \\ \text{---} \\ \text{---} \end{array} \quad (5.13)$$

where  $\gamma_t \subset \mathbf{R}_2 \otimes \mathbf{R}_3$  is an *irrep* of the  $t$ -channel<sup>4</sup>. The summation over  $\gamma_t$  comes from a completeness relation and the dashed inner diagram is the projection into the  $\gamma_t$  *irrep* as defined in b.21. From the six operators defined in 5.12, let's keep only  $t$ -channel and  $u$ -channel ones, and the  $s$ -channel operators  $\mathcal{C}_{12}$  and  $\mathcal{C}_{34}$  can be written

$$\begin{aligned} \mathcal{C}_{12} &= \frac{1}{2} (C_{R_1} + C_{R_2} - \mathcal{C}_{13} - \mathcal{C}_{14} - \mathcal{C}_{23} - \mathcal{C}_{24}) \\ \mathcal{C}_{34} &= \frac{1}{2} (C_{R_3} + C_{R_4} - \mathcal{C}_{13} - \mathcal{C}_{14} - \mathcal{C}_{23} - \mathcal{C}_{24}) \end{aligned}$$

with the shorthand notation that  $C_{R_i}$  represent  $C_{R_i}\mathbb{1}$  or the Casimir operator  $\hat{C}_i$ . The operator 5.12 becomes

$$\begin{aligned} \mathcal{B} &= -\frac{1}{2} (C_{R_1} W_{34}^1 + C_{R_2} W_{34}^2 + C_{R_3} W_{12}^3 + C_{R_4} W_{12}^4) - \sum_{\gamma_t} \frac{C_{\gamma_t}}{2} \mathcal{P}_{\gamma_t} X_t \\ &\quad - \sum_{\gamma_u} \frac{C_{\gamma_u}}{2} \mathcal{P}_{\gamma_u} X_u \end{aligned}$$

The first term is proportional to the identity in color space with  $W_{ab}^i = \hat{\Gamma}_{ia} + \hat{\Gamma}_{ib} - \hat{\Gamma}_{ab}$ . The two term are the non-trivial ones with respect to the color structure. The action on their respective basis ( $t$ - or  $u$ -channel projector basis) can be represented by a diagonal matrix of quadratic Casimir eigenvalues, that is  $T_t^2$  and  $T_u^2$  previously defined. The two associated factors are  $X_t = \hat{\Gamma}_{12} + \hat{\Gamma}_{34} - \hat{\Gamma}_{14} - \hat{\Gamma}_{23}$  and  $X_u = \hat{\Gamma}_{12} + \hat{\Gamma}_{34} - \hat{\Gamma}_{13} - \hat{\Gamma}_{24}$ . The soft anomalous dimension matrix corresponds to those two contributions in  $\mathcal{B}$

One can identify this result to the squared color current (2.8) of [16], up to the substitution of the dipole antenna  $\omega_{ij}$  by the dipole scattering cross section  $\hat{\Gamma}_{ij}$ . An alternative formulation is

$$\begin{aligned} \mathcal{B} &= -\frac{1}{2} (C_{R_1} W_{34}^1 + C_{R_2} W_{34}^2 + C_{R_3} W_{12}^3 + C_{R_4} W_{12}^4) \\ &\quad - \frac{1}{2} N_c (X_t + X_u) \mathcal{Q} \left( b = \frac{X_t - X_u}{X_t + X_u} \right) \end{aligned} \quad (5.14)$$

which relates  $\mathcal{B}$  to  $\mathcal{Q}$ .

It is also useful the define  $T_t^2$  and  $T_u^2$  in birdtrack notation as

$$T_t^2 = \sum_{\gamma_t} C_{\gamma_t} \cdot \mathcal{P}_{\gamma_t} = C_{R_2} + C_{R_3} - 2 \begin{array}{c} \text{---} \\ \text{---} \\ \text{---} \\ \text{---} \end{array} = C_{R_1} + C_{R_4} - 2 \begin{array}{c} \text{---} \\ \text{---} \\ \text{---} \\ \text{---} \end{array} \quad (5.15)$$

<sup>4</sup> The last birdtrack in the r.h.s. of 5.13 can be misleading. Regarding  $C_{R_2}$  and  $C_{R_3}$  it is indeed the identity operator for the vector space  $\mathbf{R}_1 \otimes \mathbf{R}_2 \otimes \mathbf{R}_3 \otimes \mathbf{R}_4$ . However regarding  $C_{\gamma_t}$ , it is the identity operator for the vector space  $\mathbf{R}_1 \otimes \mathbf{R}_4 \otimes \gamma_t$ , a subspace of the former vector space.



It leads to the simple result

$$\langle \alpha | T_t^2 | \beta \rangle = N_c \delta_{\alpha\beta} - \frac{\sqrt{K_\alpha K_\beta}}{K_{R_a}} \quad (5.20)$$

and finally

$$\langle \alpha | \mathcal{Q}(b) | \beta \rangle = \delta_{\alpha\beta} \left[ (1-b) \frac{2C_F + 2C_{R_a} - C_\alpha}{2N_c} + b \right] - b \frac{\sqrt{K_\alpha K_\beta}}{K_{R_a}} \quad (5.21)$$

This result naturally transposes to the case where  $q_2 \leftrightarrow \bar{q}_3$ .

$\mathfrak{g} + \mathfrak{g} \rightarrow \mathfrak{g} + \mathfrak{g}$ :

To compute  $\mathcal{Q}$  in this case, let's use the fact that all  $\mathbf{R}_i$  are in the adjoint irrep  $\mathbf{A}$ . The tedious part of  $\mathcal{Q}$  is the contribution  $T_t^2 - T_u^2$ , however in the form given by 5.15 and 5.16, one automatically gets

$$\langle \alpha | T_t^2 - T_u^2 | \beta \rangle = \frac{-2}{\sqrt{K_\alpha K_\beta}} \left( \text{Diagram 1} - \text{Diagram 2} \right) \quad (5.22)$$

where  $\alpha, \beta \in \mathbf{A} \otimes \mathbf{A}$ . The two contributions of 5.22 are related; one can flip the two upper lines of the right diagram to obtain the left one times a symmetry factor depending on  $\alpha$  and  $\beta$ . Let's call  $\sigma_\alpha$  and  $\sigma_\beta$  the eigenvalues of the projector  $\mathcal{P}_\alpha$  and  $\mathcal{P}_\beta$  under the permutation of the two in (or out) lines.

$$\text{Diagram 1} = \sigma_\alpha \sigma_\beta \text{Diagram 2} = \sigma_\alpha \sigma_\beta I_{\alpha\beta} \quad (5.23)$$

hence the operator  $T_t^2 - T_u^2$  becomes

$$\langle \alpha | T_t^2 - T_u^2 | \beta \rangle = \frac{-2}{\sqrt{K_\alpha K_\beta}} (1 - \sigma_\alpha \sigma_\beta) \text{Diagram 1} = \frac{-2}{\sqrt{K_\alpha K_\beta}} (1 - \sigma_\alpha \sigma_\beta) I_{\alpha\beta} \quad (5.24)$$

This operator is symmetric under the permutation  $\alpha \leftrightarrow \beta$ , hence it is only non-zero when the product  $\sigma_\alpha \sigma_\beta = -1$ . In other words,  $\alpha$  and  $\beta$  should have opposite symmetry under permutation. There are only two antisymmetric irreps in the decomposition of two gluons<sup>5</sup>

$$\mathbf{8} \otimes \mathbf{8} = \underbrace{\mathbf{1} \oplus \mathbf{8}_s \oplus \mathbf{27} \oplus \mathbf{0}}_{\text{Symmetric}} \oplus \underbrace{\mathbf{8}_a \oplus (\mathbf{10} \oplus \bar{\mathbf{10}})}_{\text{Antisymmetric}} \quad (5.25)$$

There are only two contributions to calculate:  $\alpha = \mathbf{8}_a$  or  $\alpha = \mathbf{10} + \bar{\mathbf{10}}$  (for all symmetric irreps  $\beta$ ).

<sup>5</sup> $\mathbf{10}, \bar{\mathbf{10}}$  are grouped together because they have the same symmetry and quadratic Casimir. They should have been properly separated if the cubic Casimir operator was involved in the construction of  $\mathcal{Q}$ .

**Case  $\alpha = \mathbf{8}_a$ :** the associated vector is

$$\langle \mathbf{8}_a | = \frac{1}{\sqrt{K_8}} \cdot \frac{1}{N_c} \text{ (diagram) }$$

where the first factor  $1/\sqrt{K_8}$  is the basis normalization and the second factor  $1/N_c$  is the normalization for projector  $\mathcal{P}_{\mathbf{8}_a} \cdot \mathcal{P}_{\mathbf{8}_a} = \mathcal{P}_{\mathbf{8}_a}$ . The factor  $I_{\mathbf{8}_a, \beta}$  reads

$$I_{\mathbf{8}_a, \beta} = \frac{1}{N_c} \text{ (diagram) } = \left( \frac{2N_c - C_\beta}{2} \right)^2 \frac{K_\beta}{N_c}, \quad (5.26)$$

where the two factors  $2N_c - C_\beta$  come from b.23.

**Case  $\alpha = \mathbf{10} + \bar{\mathbf{10}}$ .** To construct the associated projector, one just has to remark the following:

- The projection operator on the antisymmetric subspace of the tensor product  $\mathbf{A} \otimes \mathbf{A}$  is simply given in terms of  $\delta^{ab}$  tensor. It is a half of the identity minus the permutation.
- Aside from  $\mathbf{10} + \bar{\mathbf{10}}$  there is only  $\mathbf{8}_a$  that is an antisymmetric irrep. Subtracting from the antisymmetric projector the projector on the antisymmetric octet we get the projector on  $\mathbf{10} + \bar{\mathbf{10}}$ .

With those two remarks in mind, the sum of the two vectors associated to the  $\mathbf{10} + \bar{\mathbf{10}}$  subspace is given by

$$\langle \mathbf{10} | + \langle \bar{\mathbf{10}} | = \langle \mathbf{10} + \bar{\mathbf{10}} | = \frac{1}{\sqrt{K_{10}}} \left( \frac{1}{2} \left[ \text{(diagram)} - \text{(diagram)} \right] - \frac{1}{N_c} \text{(diagram)} \right) \quad (5.27)$$

Finally the scalar  $I_{\mathbf{10} + \bar{\mathbf{10}}, \beta}$  is given by

$$I_{\mathbf{10} + \bar{\mathbf{10}}, \beta} = \frac{1}{2} \left( \text{(diagram)} - \text{(diagram)} \right) - I_{\mathbf{8}_a, \beta} \quad (5.28)$$

$$= \frac{1}{2} \left( N_c K_\beta + \frac{2N_c - C_\beta}{2} \sigma_\beta K_\beta \right) - \left( \frac{2N_c - C_\beta}{2} \right)^2 \frac{K_\beta}{N_c} \quad (5.29)$$

$$= \frac{K_\beta}{4N_c} C_\beta (3N_c - C_\beta) \quad (5.30)$$

The eigenvalue  $\sigma_\beta$  of the permutation operator applied to  $\mathcal{P}_\beta$  is +1 because  $\alpha$  is set to be antisymmetric (and thus  $\beta$  must be symmetric for  $T_t^2 - T_u^2$  to be non vanishing).

**Result for  $\mathbf{Q}$  in the  $\mathbf{g} + \mathbf{g} \rightarrow \mathbf{g} + \mathbf{g}$  case.** In matrix representation  $T_t^2 - T_u^2$  is given by

$$\langle \alpha | T_t^2 - T_u^2 | \beta \rangle = \frac{-2(1 - \sigma_\alpha \sigma_\beta)}{\sqrt{K_\alpha K_\beta}} \times \left\{ \frac{K_\beta}{4N_c} \left[ \delta_\alpha^{\mathbf{8}_a} (2N_c - C_\beta)^2 + \delta_\alpha^{\mathbf{10} + \bar{\mathbf{10}}} C_\beta (3N_c - C_\beta) \right] + (\alpha \leftrightarrow \beta) \right\} \quad (5.31)$$

to be inserted in 5.8.

For completeness, the matrix representation of  $\frac{b}{2N_c} \langle \alpha | T_t^2 - T_u^2 | \beta \rangle$  is

$$-\frac{2b}{K_A} \begin{pmatrix} 0 & 0 & \sqrt{K_1 K_3} & \frac{\sqrt{K_1 K_4}}{4} & \frac{\sqrt{K_1 K_5}}{N^2} & \frac{\sqrt{K_1 K_6}}{N^2} \\ 0 & 0 & 0 & \frac{\sqrt{K_2 K_4}}{N^2-4} & \frac{(N+1)\sqrt{K_2 K_5}}{N^2(N+2)} & \frac{(N-1)\sqrt{K_2 K_6}}{N^2(N-2)} \\ \sqrt{K_1 K_3} & 0 & 0 & 0 & 0 & 0 \\ \frac{\sqrt{K_1 K_4}}{4} & \frac{\sqrt{K_2 K_4}}{N^2-4} & 0 & 0 & 0 & 0 \\ \frac{\sqrt{K_1 K_5}}{N^2} & \frac{(N+1)\sqrt{K_2 K_5}}{N^2(N+2)} & 0 & 0 & 0 & 0 \\ \frac{\sqrt{K_1 K_6}}{N^2} & \frac{(N-1)\sqrt{K_2 K_6}}{N^2(N-2)} & 0 & 0 & 0 & 0 \end{pmatrix} \quad (5.32)$$

where  $K_i$  is the dimension of the irrep with index  $i \equiv \{8_a, 10 + \bar{10}, 1, 8_s, 27, 0\}$ . And the diagonal in  $Q$  is given by

$$\text{Diag} \left( \frac{3}{2}, 1, 2, \frac{3}{2}, \frac{N_c - 1}{N_c}, \frac{N_c + 1}{N_c} \right) \quad (5.33)$$

**Some properties** of the soft anomalous dimension matrix  $Q$ . From the two previous class of cases, some generic properties of the soft anomalous dimension matrix can be underlined.

1. The ‘‘Block’’ organization for  $a + a \rightarrow a + a$  scatterings (valid for any QCD partons but also generalized partons in the following section).

- There are four blocks in  $Q$ . They correspond to the four possible combinations of symmetry ( $\sigma_\alpha = \pm 1$  and  $\sigma_\beta = \pm 1$ ).
- The  $b$ -dependent part is off the block diagonal and is given by  $\frac{b}{2N_c} \times (T_t^2 - T_u^2)$ . Those two parts are related by the exchange  $\alpha \leftrightarrow \beta$  (transposition).
- The  $b$ -independent part is diagonal and is given by  $\delta_{\alpha\beta} \frac{2N_c - C_\alpha}{2N_c}$ .
- As a consequence of previous point, within a given block in the block-diagonal, aside from the diagonal matrix elements of the soft anomalous dimension matrix vanishes.

2. Complex symmetric for  $a + b \rightarrow a + b$  scatterings

- The form of  $Q$  given here is symmetric<sup>6</sup> under  $\alpha \leftrightarrow \beta$ . This is a consequence of the basis choice used here and it is not restricted to only this case. In the DM case, only an orthogonal basis is used, hence the  $Q$  matrix obtained isn't symmetric.
- To recover a symmetric matrix with the basis choice of DM, one just add a factor  $\sqrt{K_\alpha/K_\beta}$ .

### 5.2.3 An unexpected symmetry

In their paper [16], DM have found an unexpected symmetry relating three (of six) eigenvalues of the matrix  $Q$  in the  $gg \rightarrow gg$  case. This symmetry relates an inner dof -the

<sup>6</sup>This symmetry of the soft anomalous dimension matrix under transposition was found in [69] and later explained in [70].



number of color  $N_c$ , and an external dof -the kinematic variable  $b$ , such that those eigenvalues  $\lambda(\{b, N_c\})$  are invariant under the exchange  $N_c \leftrightarrow b^{-1}$ . Due to the intricate calculation that is involved, they remark that “*such a symmetry being accidental looks improbable*” [16].

To explore if some other cases than  $gg \rightarrow gg$  have the same symmetry, one can first look at the relation 5.21 that encompasses three different cases:

$$qq \rightarrow qq \quad qg \rightarrow qg \quad q\bar{q} \rightarrow q\bar{q} \quad (5.34)$$

For  $qq \rightarrow qq$  the soft anomalous dimension matrix reads

$$\mathcal{Q}_{qq \rightarrow qq} \equiv \frac{1}{2N_c} \begin{pmatrix} N_c - 1 & -b\sqrt{N_c^2 - 1} \\ -b\sqrt{N_c^2 - 1} & N_c + 1 \end{pmatrix} \quad (5.35)$$

The two eigenvalues  $\lambda_{1,2}$  are solutions of

$$\lambda^2 - \lambda + \frac{1}{4}(1 - b^2)(1 - N_c^{-2}) = 0 \quad (5.36)$$

and are also invariant under  $b \leftrightarrow N_c^{-1}$  exchange.

The two remaining cases listed in 5.34 do not have this symmetry. This observation motivates the exploration of elastic processes with two identical generalized partons.

Indeed I already treated all standard QCD cases  $a + a \rightarrow a + a$  up to this point, since  $q\bar{q} \rightarrow q\bar{q}$  is trivially related to  $qq \rightarrow qq$ . One thus needs to consider partons in any irrep to further investigate if this symmetry appears systematically for those processes. *Generalized parton* are discussed in the next section.

## 5.3 Calculation of Q for generalized partons

In order to investigate the previous symmetry observed by DM, I will introduce the notion of generalized partons. Then I will come back to the  $qq \rightarrow qq$  case with a distinct approach from the previous section, in order to prepare the case of two symmetric diquarks. This will naturally lead to an algorithm for arbitrary  $2 \rightarrow 2$  processes involving arbitrary fully symmetric quark-systems. I will finally discuss this algorithm and the results obtained from it regarding to DM’s symmetry.

### 5.3.1 Generalized parton and soft anomalous dimension matrix

To further explore the soft anomalous dimension matrix  $\mathcal{Q}$ , I define a “*generalized parton*” as a pointlike system of an arbitrary number of  $SU(N_c)$  partons. With respect to the study of the color structure associated to the operator  $\mathcal{Q}$ , it means that one considers other irreps from the usual QCD ones:  $q, \bar{q}, g$ . Regarding to the broadening discussed in chapter 3, such a consideration does not add any extra complications. We already saw that a pointlike system is effectively a structureless color object regarding to the propagation in a medium.

The construction of the soft anomalous dimension matrix does not change, only **irreps** involved do, and let's recall

$$\mathcal{Q} = \frac{1}{2N_c} ([T_t^2 + T_u^2] + b [T_t^2 - T_u^2]) \quad (5.37)$$

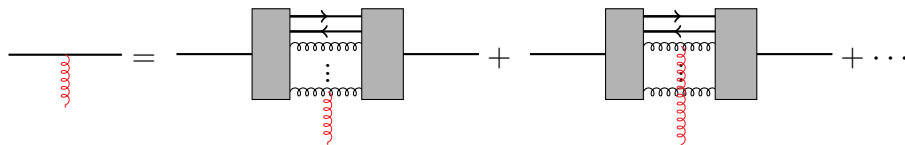
Does  $DM$ 's symmetry appears when working with those partons?

**Notation** A generalized parton in an **irrep**  $R$  is in birdtrack representation a **plain line**. It is



$$(5.38)$$

that relates usual  $q, \bar{q}, g$  (on the left of the box) projected into the **irrep**  $R$  (on the right of the box). The color generator of a generalized parton  $T_R^a$  can be represented using color conservation as the sum of constituents color generators  $t_i^a$ . In birdtrack notations, it reads



$$(5.39)$$

### 5.3.2 Quark-quark, again!

To set the bedrock of what will follow, let's review the  $qq \rightarrow qq$  case with a different approach. Using **YDs**, the decomposition of the tensor product “quark times quark”<sup>7</sup> is

$$\square \otimes \square = \square \oplus \square$$

In the r.h.s. one identifies the symmetric and antisymmetric **irreps**. In this part, scalars (dimensions, Casimir eigenvalues, ...) and operators (vector, projectors, ...) associated to the symmetric and antisymmetric **irreps** will be labelled by  $s$  and  $a$ . For example, dimensions read

$$K_{s,a} = \frac{1}{2} N_c (N_c \pm 1) \quad (5.40)$$

Remark that the dimension of the symmetric **irrep** is related to the dimension of the antisymmetric **irrep** by replacing  $N_c$  by  $-N_c$ . This is the first occurrence of the negative dimension theorem that will be discussed later on. Obviously, those dimensions verify

$$K_F^2 = K_s + K_a \quad (3 \times 3 = 6 + 3 \text{ with } N_c = 3). \quad (5.41)$$

The two quadratic Casimir eigenvalues are

$$C_{s,a} = \frac{(N_c \pm 2)(N_c \mp 1)}{N_c} \quad (5.42)$$

<sup>7</sup>The tensor product of two fundamental **irrep** of  $SU(N_c)$

and they are also related to each other by the substitution of  $N_c$  by  $-N_c$  however there is an overall minus sign. A relation to find the eigenvalue of the Quadratic Casimir operator for a given **irrep** with its **YD** is

$$C_R = \frac{1}{2} \left[ \rho \frac{N_c^2 - \rho}{N_c} + \sum_{i=1}^{row} a_i^2 - \sum_{j=1}^{col} b_j^2 \right] \quad (5.43)$$

where  $a_i$  is the number of boxes from line  $i$  and  $b_j$  is the number of boxes from column  $j$  in the **YD**. The pre-factor “1/2” is the trace normalization choice  $\text{Tr}(t^a t^b) = \delta^{ab}/2$ .

**The  $s$ -channel basis** can easily be found from the **YD** decomposition and it is constituted of the following two vectors

$$|s\rangle = \frac{1}{\sqrt{K_s}} \cdot \frac{1}{2} \left\{ \begin{array}{c} \text{---} \text{---} \text{---} \\ \text{---} \text{---} \end{array} \right\} + \begin{array}{c} \text{---} \text{---} \\ \text{---} \text{---} \end{array} \left. \vphantom{\begin{array}{c} \text{---} \text{---} \text{---} \\ \text{---} \text{---} \end{array}} \right\}, \quad |a\rangle = \frac{1}{\sqrt{K_a}} \cdot \frac{1}{2} \left\{ \begin{array}{c} \text{---} \text{---} \text{---} \\ \text{---} \text{---} \end{array} \right\} - \begin{array}{c} \text{---} \text{---} \\ \text{---} \text{---} \end{array} \left. \vphantom{\begin{array}{c} \text{---} \text{---} \text{---} \\ \text{---} \text{---} \end{array}} \right\}$$

### The $t$ -channel

Consider first the tensor decomposition of the  $t$ -channel using **YD**.

$$\bar{q} \otimes q = \begin{array}{c} \square \oplus \\ \vdots \\ \square \end{array} \quad (5.44)$$

with the r.h.s. being simply the adjoint and singlet **irreps**. Then let's choose the following tensor basis to build the  $t$ -channel projector basis elements

$$\mathcal{T}^0 = \begin{array}{c} \text{---} \\ \text{---} \end{array} \left[ \right], \quad \mathcal{T}^1 = \begin{array}{c} \text{---} \\ \text{---} \end{array} \left[ \text{---} \right] \quad (5.45)$$

The main advantage of such a basis is that when trying to rotate the  $t$ -channel back to the  $s$ -channel, one can use the following relation for  $\mathcal{T}^0$

$$\mathcal{T}^0 = \sum_{i=a,s} \sum_{j=a,s} \begin{array}{c} \text{---}^i \\ \text{---}^j \end{array} \left[ \begin{array}{c} \text{---} \\ \text{---} \end{array} \right] = \sum_{i=a,s} \begin{array}{c} \text{---} \\ \text{---} \end{array} \left[ \begin{array}{c} \text{---} \\ \text{---} \end{array} \right]^i \quad (5.46)$$

The tensor  $\mathcal{T}^0$  viewed from the  $t$ -channel is proportional to the singlet projector, viewed from the  $s$ -channel it is the identity (sum of projector from completeness relation). The same can be done for  $\mathcal{T}^1$  with

$$\mathcal{T}^1 = \sum_{i=a,s} \sum_{j=a,s} \begin{array}{c} \text{---}^i \\ \text{---}^j \end{array} \left[ \begin{array}{c} \text{---} \\ \text{---} \end{array} \right] \text{---} = \sum_{i=a,s} \frac{2C_F - C_i}{2} \begin{array}{c} \text{---} \\ \text{---} \end{array} \left[ \begin{array}{c} \text{---} \\ \text{---} \end{array} \right]^i \quad (5.47)$$

The red gluon exchange applied to an  $s$ -channel projector has an eigenvalue given by the combination of Casimir, it follows from **b.23**. **Those two relations fully determine the expression of the rotation matrix  $K_{ts}$  - the tedious part to compute in DM's approach.** Remark that one does not need the explicit expression of the  $s$ -channel projector to use **5.46** or **5.47**.

Using Fierz identity, one get the  $t$ -channel projector basis spanned by the adjoint  $|A\rangle$  and the singlet  $|1\rangle$

$$|1\rangle = \frac{1}{\sqrt{K_1}} \cdot \frac{1}{N_c} \left[ \begin{array}{c} \overline{\square} \\ \square \end{array} \right], \quad |A\rangle = \frac{1}{\sqrt{K_A}} \cdot (-2) \left[ \begin{array}{c} \overline{\square} \\ \square \end{array} \right] \quad (5.48)$$

I added for the adjoint projector two quark arrows, the relative orientation of those two arrows gives a  $-1$  factor from the “usual” Fierz identity (see b.11) and expressed in the  $s$ -channel

$$\begin{aligned} |1\rangle &= \frac{1}{\sqrt{K_1}} \frac{1}{N_c} \cdot \sum_{i=a,s} \sqrt{K_i} |i\rangle \\ |A\rangle &= \frac{-2}{\sqrt{K_A}} \cdot \sum_{i=a,s} \frac{2C_F - C_i}{2} \sqrt{K_i} |i\rangle \end{aligned}$$

The rotation matrix is given by<sup>8</sup>

$$K_{ts} = \begin{pmatrix} \frac{1}{N_c} \sqrt{K_s/K_1} & \frac{1}{N_c} \sqrt{K_a/K_1} \\ \frac{N_c-1}{N_c} \sqrt{K_s/K_A} & -\frac{N_c+1}{N_c} \sqrt{K_a/K_A} \end{pmatrix} \quad (5.49)$$

The contribution  $T_t^2$  is given in the  $s$ -channel by

$$T_t^2 = K_{st} C^{(t)} K_{ts} \quad (5.50)$$

where  $K_{st} = K_{ts}^{-1}$  and  $C^{(t)}$  is the diagonal matrix of the  $t$ -channel Casimir.

### $u$ -channel

As a consequence of our restricted choice of processes  $a+a \rightarrow a+a$ , both  $t$ - and  $u$ -channel are  $\bar{a}a \rightarrow \bar{a}a$ . This simplify a lot the calculation of the soft anomalous dimension matrix as one can almost get all the  $u$ -channel quantities for free from the  $t$ -channel ones!

*How does it happen?*

Let's consider a  $u$ -channel vector expressed in the  $s$ -channel basis

$$\begin{array}{c} \text{--- } s_1 \text{---} \\ \text{--- } s_2 \text{---} \end{array} \left[ \begin{array}{c} \text{--- } u \text{---} \\ \text{--- } u \text{---} \end{array} \right] = \delta_{s_1, s_2} \sigma_{s_2} \begin{array}{c} \text{--- } s_1 \text{---} \\ \text{--- } s_2 \text{---} \end{array} \left[ \begin{array}{c} \text{--- } u \text{---} \\ \text{--- } u \text{---} \end{array} \right]$$

here  $s_1$  is either the symmetric and antisymmetric **irrep** and by orthogonality  $s_1 = s_2$  for this vector to be non vanishing. Additionally, the permutation operator applied on the right of the lower Clebsch Gordan  $qq \rightarrow s_2$  can be substituted given an overall signum  $\sigma_{s_2}$  (eigenvalue of the permutation operator). One recognizes on the r.h.s. a  $t$ -channel vector projected into the  $s$ -channel basis affected by an overall signum  $\sigma_{s_2}$ . Let's define the diagonal matrix of the  $s$ -channel signum  $\sigma = \text{Diag}(+, -)$ . The operator  $T_u^2$  reads

$$T_u^2 = \sigma K_{st} C^{(u)} K_{ts} \sigma = \sigma T_t^2 \sigma \quad (5.51)$$

and obviously  $C^{(u)}$  being the diagonal matrix of the  $u$ -channel Casimir is equal to  $C^{(t)}$ .

<sup>8</sup>Remember that the basis choice is orthonormal by opposition to DM's basis that is only orthogonal. The ratio of square root of dimensions originate from the orthonormalization condition used here. To compare with their paper, remove the square root factor.

The soft anomalous dimension matrix is given by 5.37. It becomes

$$\mathcal{Q} = \left[ K_{st} \frac{C^{(t)}}{2N_c} K_{ts} + \sigma K_{st} \frac{C^{(u)}}{2N_c} K_{ts} \sigma \right] + b \left[ K_{st} \frac{C^{(t)}}{2N_c} K_{ts} - \sigma K_{st} \frac{C^{(u)}}{2N_c} K_{ts} \sigma \right] \quad (5.52)$$

and one recovers the expression found in 5.21.

### 5.3.3 The story of two symmetric diquarks

In this section, I will use the previous method to derive the soft anomalous dimension matrix for two symmetric diquark scatterings:  $\varphi\varphi \rightarrow \varphi\varphi$ . Using YD, the  $s$ -channel decomposition is

$$\varphi \otimes \varphi = \square\square \otimes \square\square = \square\square\square\square \oplus \square\square\square \oplus \square\square \quad (5.53)$$

Then let's give them label 0, 1, 2 from the left to the right<sup>9</sup>. Dimensions are given by the method of hook length

$$\begin{aligned} K_0 &= N_c(N_c + 1)(N_c + 2)(N_c + 3)/24 \\ K_1 &= (N_c - 1)N_c(N_c + 1)(N_c + 2)/8 \\ K_2 &= (N_c - 1)N_c^2(N_c + 1)/12 \end{aligned}$$

and Casimirs are

$$\begin{aligned} C_0 &= 2(N_c + 4)(N_c - 1)/N_c \\ C_1 &= 2(N_c^2 + N_c - 4)/N_c \\ C_2 &= 2(N_c + 2)(N_c - 2)/N_c \end{aligned}$$

In this section, **plain lines are associated to  $\varphi$**  (with an arrow if there is an eventual ambiguity).

**The  $t$ -channel contribution.** The decomposition  $\bar{\varphi} \otimes \varphi$  contains the singlet, adjoint and an additional irrep noted 27 (motivated by the dimension for  $N_c = 3$ ). The dimension can be found using the completeness relation knowing the singlet and adjoint dimensions.

$$K_{27} = K_\varphi^2 - K_A - K_\bullet = \frac{N_c^2(N_c + 3)(N_c - 2)}{4} \quad (5.54)$$

Its Casimir can be found with the following trick. The Generator  $t_\varphi^a$  is traceless, hence

$$\text{Tr}(t_\varphi^a) \text{Tr}(t_\varphi^b) \delta_{ab} = 0$$

In birdtrack notation this equation is

$$\begin{aligned} 0 &= \text{Diagram 1} = \sum_{i=\bullet, A, 27} \text{Diagram 2} = \sum_{i=\bullet, A, 27} \frac{2C_\varphi - C_\alpha}{2} K_\alpha \\ &= C_\varphi K_\varphi^2 - \frac{1}{2}(C_A K_A + C_{27} K_{27}) \end{aligned}$$

<sup>9</sup>Those are motivated by the Dynkin's notation of YD: **0** correspond to  $[4, 0, \dots]$ , **1** correspond to  $[2, 1, \dots]$ , and so on and so forth.

Leading to

$$C_{27} = \frac{2C_\varphi K_\varphi - C_A K_A}{K_{27}} = 2(N_c + 1) \quad (5.55)$$

Let's introduce the tensor basis  $\{\mathcal{T}^i\}$  for  $i = 0, 1, 2$  defined as

$$\mathcal{T}^0 = \begin{array}{|c|} \hline \square \\ \hline \end{array}, \quad \mathcal{T}^1 = \begin{array}{|c|} \hline \square \text{---} \text{---} \text{---} \\ \hline \end{array}, \quad \mathcal{T}^2 = \begin{array}{|c|} \hline \square \text{---} \text{---} \text{---} \text{---} \\ \hline \end{array} \quad (5.56)$$

This basis serves the same purpose as in the quark-quark case,  $\mathcal{T}^{\{0,1,2\}}$  are easily expressed in the  $s$ -channel.

The first two vectors of the  $t$ -channel are easily found to be

$$\sqrt{K_\bullet} |\bullet\rangle = \frac{1}{K_\varphi} \begin{array}{|c|} \hline \square \\ \hline \end{array} \quad (5.57)$$

$$\sqrt{K_A} |A\rangle = -\frac{1}{\tilde{a}} \begin{array}{|c|} \hline \square \text{---} \text{---} \text{---} \text{---} \\ \hline \end{array} \quad (5.58)$$

where  $\tilde{a}$  is the trace normalization of  $\varphi$ :  $\text{Tr}(t_\varphi^a t_\varphi^b) = \tilde{a} \delta^{ab}$ , or in birdtrack notations

$$\tilde{a} K_A = \text{---} \circ \text{---} = C_\varphi K_\varphi \quad (5.59)$$

The missing vector can be found using

- $\mathcal{P}_{27} = n_0 \mathcal{T}^0 + n_1 \mathcal{T}^1 + n_2 \mathcal{T}^2$ .
- Require orthogonality with  $\mathcal{P}_\bullet$  and  $\mathcal{P}_A$ .
- Fix the normalization to be  $\text{Tr}(\mathcal{P}_{27}) = K_{27}$ .

This leads to the following system to solve

$$\underbrace{\begin{pmatrix} \mathcal{C}_0 & \mathcal{C}_1 & \mathcal{C}_2 \\ \mathcal{C}_1 & \mathcal{C}_2 & \mathcal{C}_3 \\ \mathcal{B}_0 & \mathcal{B}_1 & \mathcal{B}_2 \end{pmatrix}}_A \cdot \underbrace{\begin{pmatrix} n_0 \\ n_1 \\ n_2 \end{pmatrix}}_n = \underbrace{\begin{pmatrix} 0 \\ 0 \\ K_{27} \end{pmatrix}}_R \quad (5.60)$$

The scalar  $\mathcal{C}_i$  and  $\mathcal{B}_i$  are

$$\mathcal{C}_i = \left( \begin{array}{|c|} \hline \text{---} \text{---} \text{---} \text{---} \\ \vdots \\ \text{---} \text{---} \text{---} \text{---} \\ \hline \end{array} \right), \quad \mathcal{B}_i = \left( \begin{array}{|c|} \hline \text{---} \text{---} \text{---} \text{---} \\ \vdots \\ \text{---} \text{---} \text{---} \text{---} \\ \hline \end{array} \right) \quad (5.61)$$

Those scalars are easy to obtain:

- $\mathcal{C}_0$  is just the dimension  $K_\varphi^2$ , and  $\mathcal{C}_1$  is the trace of the generator - that is zero. All higher  $\mathcal{C}_i$ 's are obtained using the previous trick to find  $C_{27}$  and one find that

$$\mathcal{C}_i = \sum_\alpha \left( \frac{C_\varphi - C_\alpha}{2} \right)^i K_\alpha \quad (5.62)$$

with  $\alpha$  is over each **irrep** label of  $\varphi \otimes \varphi$ .

- the same trick can be done for  $\mathcal{B}_i$ 's using in addition the *signum* (eigenvalue of the permutation operator) of the  $s$ -channel projectors:

$$\mathcal{B}_i = \sum_{\alpha} \left( \frac{C_{\varphi} - C_{\alpha}}{2} \right)^i \sigma_{\alpha} K_{\alpha} \quad (5.63)$$

With all those tools, one just pick its preferred mathematical toolkit to solve 5.60.

### Rotation matrix and soft anomalous dimension matrix

The  $t$ -channel vectors are in the  $s$ -channel basis given by

$$\begin{aligned} \mathcal{P}_{\bullet}^{(t)} &= \frac{1}{K_{\varphi}} \sum_{\alpha=0,1,2} \left( C_{\varphi} - \frac{C_{\alpha}}{2} \right)^0 \mathcal{P}_{\alpha}^{(s)} = \frac{1}{K_{\varphi}} \left( \mathcal{P}_0^{(s)} + \mathcal{P}_1^{(s)} + \mathcal{P}_2^{(s)} \right) \\ \mathcal{P}_A^{(t)} &= \frac{1}{-\tilde{a}} \sum_{\alpha=0,1,2} \left( C_{\varphi} - \frac{C_{\alpha}}{2} \right)^1 \mathcal{P}_{\alpha}^{(s)}, \quad \tilde{a} = \frac{C_{\varphi} K_{\varphi}}{K_A} \\ \mathcal{P}_{27}^{(t)} &= \sum_{\alpha=0,1,2} \left[ \sum_{i=0}^2 n_i \left( C_{\varphi} - \frac{C_{\alpha}}{2} \right)^i \right] \mathcal{P}_{\alpha}^{(s)} \end{aligned}$$

Finally the  $K_{ts}$ -matrix is given by the coefficient before each  $s$ -channel projection operators in the expression of the  $t$ -channel projection operators. Recall that  $\mathcal{P}_i = \sqrt{K_i} |i\rangle$ . To find  $\mathcal{Q}$  just plug into

$$\mathcal{Q} = \left[ K_{st} \frac{C^{(t)}}{2N_c} K_{ts} + \sigma K_{st} C^{(u)} K_{ts} \sigma \right] + b \left[ K_{st} \frac{C^{(t)}}{2N_c} K_{ts} - \sigma K_{st} C^{(u)} K_{ts} \sigma \right] \quad (5.64)$$

and one find that

$$\mathcal{Q} = \begin{pmatrix} \frac{N_c-1}{N_c} & -b \frac{\sqrt{(N_c+3)(N_c-1)}}{\sqrt{3}N_c} & 0 \\ -b \frac{\sqrt{(N_c+3)(N_c-1)}}{\sqrt{3}N_c} & \frac{N_c+1}{N_c} & -b \frac{\sqrt{N_c(N_c+2)}}{\sqrt{3/2}N_c} \\ 0 & -b \frac{\sqrt{N_c(N_c+2)}}{\sqrt{3/2}N_c} & \frac{N_c+2}{N_c} \end{pmatrix} \quad (5.65)$$

### Discussion

In the case  $\varphi\varphi \rightarrow \varphi\varphi$ , the three eigenvalues of  $\mathcal{Q}$  does not have the symmetry observed by DM. The initial guess was to explore cases with two identical (generalized) partons. Here, we see that the assumption “DM’s symmetry appears for  $a+a \rightarrow a+a$  kind of processes” does not hold anymore. However, a reminiscence of this symmetry can still be found. When one compares the large  $N_c$  limit with the small  $b$  limit, namely

$$\begin{aligned} \lim_{N_c \rightarrow \infty} \{\lambda_1, \lambda_2, \lambda_3\} &= \{1+b, 1-b, 1\} \\ \lim_{b \rightarrow 0} \{\lambda_1, \lambda_2, \lambda_3\} &= \left\{ 1 + \frac{1}{N_c}, 1 - \frac{1}{N_c}, 1 + \frac{2}{N_c} \right\} \end{aligned}$$

a weaker form of this symmetry appears for two of three eigenvalues. Two of three eigenvalues sharing this weaker kind of symmetry is encouraging-enough to explore further

cases. A good point is that the transition from  $qq \rightarrow qq$  to  $\varphi\varphi \rightarrow \varphi\varphi$  is transparent and does not include any additional complications. Hence, one is able to formulate an algorithm to compute similar cases.

The following section discuss the formulation of such an algorithm. Its application for multiple cases will give us insight of this new question: “does this weaker-symmetry still appears for those cases?”

### 5.3.4 Algorithm

The two previous cases  $qq \rightarrow qq$  and  $\varphi\varphi \rightarrow \varphi\varphi$  are the basics to formulate an algorithm to compute any soft anomalous dimension matrix involving generalized partons  $\phi_\rho$  that are represented by fully symmetric **YD** of  $\rho$  boxes. This algorithm is based on the following steps:

1. Calculate dimensions and quadratic Casimir eigenvalues for the  $s$ -channel decomposition. There is  $\rho + 1$  distinct **irreps** and none of them have a multiplicity higher than one. This can be seen from the **YD** decomposition, where one start from **YD** with all  $2\rho$  boxes on the first line, then move one box at the time to the second line up to the point where the two initial lines of  $\rho$  boxes are on top of each others. I will again label **irreps** with the second Dynkin index (corresponding to the number of boxes in the second line of a given **YD**).

Those are used to compute all  $\mathcal{C}_i$  and  $\mathcal{B}_i$  scalars.

2. In the  $t$ -channel, decompose the product  $\bar{\phi}_\rho \otimes \phi_\rho$  using **YD** to find

$$\bar{\phi}_\rho \otimes \phi_\rho = \bullet \oplus Adj \oplus 27 \oplus 64 \oplus \dots = \bigoplus_{i=0}^{\rho} [i, 0, \dots, 0, i] \quad (5.66)$$

The bracket  $[ ]$  stands for Dynkin indices of a **YD**.

Introduce the  $\mathcal{T}^i$  tensor basis with  $i = 0, \dots, \rho$  (see paragraph “Tensor basis”).

Solve the system  $A \cdot n = K$  as in 5.60 for all **irrep** of **YD**  $[i, 0, \dots, i]$  with  $2 \leq i \leq \rho$ . This gives  $\rho - 1$  system to solve. However there are (hopefully) some simplifications to it (see paragraph “System to solve”).

3. With the  $t$ -channel projectors in hand, build the rotation matrix  $K_{ts}$ . Use the fact that in the  $s$ -channel,  $\{\mathcal{T}^i\}$  are given by

$$\mathcal{T}^i = \sum_{\alpha} \left( \frac{2C_{\phi_\rho} - C_{\alpha}}{2} \right)^i \mathcal{P}_{\alpha}^{(s)} \quad (5.67)$$

This automatically give  $K_{st}$  and  $K_{ts} = K_{st}^{-1}$ .

4. Find the signum  $\sigma_{\alpha}$  of  $s$ -channel projectors under permutations. This can be done by multiple means: using  $\mathcal{P}_{\alpha}^{(s)}$  expressions, or solving the diophantine equation

$$\mathcal{B}_0 = K_{\phi_\rho} = \sum_{\alpha} \sigma_{\alpha} K_{\alpha} \quad (5.68)$$



with  $\sigma$ 's being either  $+1$  or  $-1$ <sup>10</sup>. Another empiric way is to notice that  $R_i$  is symmetric for  $i$  even and antisymmetric for  $i$  odd.

5. Finally, plugging into 5.52 yields  $\mathcal{Q}$  expressed in the  $s$ -channel projector basis.

### Tensor basis used

“Are the  $\rho + 1$  tensors  $\{\mathcal{T}\}$  enough ?” We consider the channel where  $T_0$  is the identity operator (of  $\varphi \otimes \varphi \rightarrow \varphi \otimes \varphi$  linear map) given by the following birdtrack

$$\mathcal{T}_0 = \begin{array}{c} \text{---} \\ \text{---} \\ \text{---} \\ \text{---} \\ \text{---} \\ \text{---} \end{array} \begin{array}{c} \text{---} \\ \text{---} \\ \text{---} \\ \text{---} \\ \text{---} \\ \text{---} \end{array}$$

There is  $\rho$  quark lines in each symmetrizer and we omit arrows taken from left to right. We can always replace any gluon exchange by the use of Fierz identity:

$$\begin{array}{c} \text{---} \\ \text{---} \\ \text{---} \end{array} \begin{array}{c} \text{---} \\ \text{---} \\ \text{---} \end{array} = \frac{1}{2N} \begin{array}{c} \text{---} \\ \text{---} \\ \text{---} \end{array} \begin{array}{c} \text{---} \\ \text{---} \\ \text{---} \end{array} - \frac{1}{2} \begin{array}{c} \text{---} \\ \text{---} \\ \text{---} \end{array} \begin{array}{c} \text{---} \\ \text{---} \\ \text{---} \end{array} \quad (5.69)$$

Now, we assume a tensor  $\mathcal{T}_{j>\rho}$ , there is  $j$  gluons exchange between the  $\rho$  upper lines with the  $\rho$  lower lines, and we show that it depends linearly on  $\mathcal{T}_{j\leq\rho}$ 's.

Replace all gluons using Fierz identity in  $\mathcal{T}_{j>\rho}$ . The tensor becomes a linear combination over possible permutations of upper lines with lower lines.

$$\mathcal{T}_{j>\rho} = \sum \left\{ \frac{1}{2N}, -\frac{1}{2} \right\}^j \begin{array}{c} \text{---} \\ \text{---} \\ \text{---} \\ \text{---} \\ \text{---} \\ \text{---} \end{array} \text{Permut}' \begin{array}{c} \text{---} \\ \text{---} \\ \text{---} \\ \text{---} \\ \text{---} \\ \text{---} \end{array}$$

Due to the four symmetrizers, we only need to keep track of permutation with different pair of indices (i.e.,  $\sigma_{ij}\sigma_{kl}$  with  $i, j, k, l$  distinct indices). As an example for  $\rho = 2$ :

$$\begin{array}{c} \text{---} \\ \text{---} \\ \text{---} \\ \text{---} \end{array} \begin{array}{c} \text{---} \\ \text{---} \\ \text{---} \\ \text{---} \end{array} \rightarrow \begin{array}{c} \text{---} \\ \text{---} \\ \text{---} \\ \text{---} \end{array} \begin{array}{c} \text{---} \\ \text{---} \\ \text{---} \\ \text{---} \end{array}$$

At most, it will remain  $\rho$  “cross” in the center of the diagram, and it corresponds to the  $\rho$  gluon-exchange contribution by *inverse Fierzing* each permutations. Hence  $\mathcal{T}_{j>\rho}$  is a linear combination of  $\mathcal{T}_{j\leq\rho}$ 's.

“Why did we choose intermediate gluonic-states in the  $t$ -channel ?” The  $t$ -channel decomposition is the following

$$\bar{\phi}_\rho \otimes \phi_\rho = \mathbf{1} \oplus \mathbf{8} \oplus \mathbf{27} \oplus \mathbf{64} \oplus \dots \quad (5.70)$$

where bold number indicate the **irrep** noted by its dimension when  $N_c = 3$ . In fact, for  $\rho$  boxes, one has  $\{1^3, 2^3, 3^3, \dots, \rho^3\}$  being the dimension of the decomposition. Those **irreps**

<sup>10</sup>There are cases where this diophantine equation has several solutions (even with the restriction  $\sigma_i = \pm 1$ ), and only one of them gives the correct signum. Those cases require a more careful treatment. For example, writing down the  $s$ -channel projectors and apply the permutation operator.

also appear within the decomposition of  $A^{\otimes\rho}$ ,  $A$  being the adjoint.  $\mathcal{T}^i$  is the following mapping

$$\bar{\phi}_\rho \otimes \phi_\rho \rightarrow A^{\otimes i} \rightarrow \bar{\phi}_\rho \otimes \phi_\rho \quad (5.71)$$

In particular,  $A^{\otimes\rho}$  contains the “last” irrep  $\rho^3$  of  $\bar{\phi}_\rho \otimes \phi_\rho$ . With the fact that  $\{\mathcal{T}\}$  are linearly independents, this tensor basis choice has all the properties needed to span  $\bar{\phi}_\rho \otimes \phi_\rho$  and build the projectors.

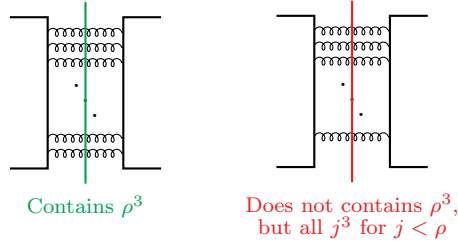
The cherry on top is the possibility to easily express  $\{\mathcal{T}\}$  in the  $s$ -channel, it is perfect for an algorithm!

**System to solve** Step 2 of the algorithm seems like a lot a work: solve  $\rho - 1$  times a  $\rho + 1 \times \rho + 1$  linear system to built the  $t$ -channel projectors...

Let’s consider the  $\rho^3$  irrep whose expression is given by

$$\mathcal{P}_\rho^{(t)} = \sum_{i=0}^{\rho} \mathcal{T}^i n_i \quad (5.72)$$

This irrep is not present in any  $j < \rho$  :  $A^{\otimes j}$  decomposition, it only appears for  $A^{\otimes\rho}$ . Hence the coefficient  $n_\rho$  cannot vanish, otherwise there will be no intermediate “gluonic-propagation” of the color charge for the irrep  $\rho^3$ . The remaining contribution to  $\mathcal{P}_\rho^{(t)}$  from  $j < \rho$  can be interpreted as “subtracting” all other irreps from the intermediate gluonic-state.



This means that the system to solve in order to find the projector into the  $\rho^3$ , is a  $\rho \times \rho$  one.

Now let’s consider the  $j^3$  irrep with  $j < \rho$ . Again it is given by

$$\mathcal{P}_j^{(t)} = \sum_{i=0}^{\rho} \mathcal{T}^i n_i \quad (5.73)$$

However, we already saw that for  $\rho$  gluon intermediate state  $\mathcal{T}^\rho$  tensor, there is a non vanishing  $\rho^3$  contribution propagating. Additionally, there is no tensor  $\mathcal{T}^{<\rho}$  available to remove this part. Hence the coefficient  $n_\rho$  in 5.73 has to be zero. This argument can be used again for  $\mathcal{T}^{\rho-1>j}$  leading to  $n_{\rho-1} = 0$ , and for all  $n_{>j} = 0$ . **The system to solve becomes just a  $j \times j$  one instead of a  $\rho \times \rho$  one.**

### 5.3.5 Application scope and results

This algorithm strongly relies on two properties:

1. There is no irrep appearing more than once in the  $s$ -channel decomposition.

2. The intermediate “gluonic-state” in the  $t$ -channel relates **irreps** to the number of gluons in the intermediate state. To clarify this statement, in the previous paragraph, we learned that  $\mathcal{P}_j^{(t)}$  contains  $\{\mathcal{T}^i\}$ 's up to  $i = j$ .

Those two properties are (of course) fulfilled in the  $\phi_\rho\phi_\rho \rightarrow \phi_\rho\phi_\rho$  case.

Additionally, this algorithm applies for a wider class of process  $a + b \rightarrow a + b$  where those two criterion have to be verified. Few examples are:

- The process  $\bar{q}q \rightarrow \bar{q}q$  can be treated with the same algorithm. This is easily understood because (i) the tensor basis  $\{\mathcal{T}\}$  naturally involves the singlet and octet **irreps** that can be related to the  $t$ -channel symmetrization and antisymmetrization by the use of Fierz identity, and (ii) crossing symmetry relates  $\bar{q}q \rightarrow \bar{q}q$  to  $qq \rightarrow qq$ .
- Consider  $\phi_\rho$  previously defined, and  $\phi_{\rho'}$  defined by the transposed **YD** of  $\phi_\rho$ . In the  $t$ -channel, the decomposition reads

$$\bar{\phi}_\rho \otimes \phi_{\rho'} = [0, \dots, 0, 1, \dots, \rho] \oplus [0, \dots, 1, 0, \dots, \rho - 1]$$

where the two Dynkin indices between dots are at positions  $\rho - 1$  and  $\rho$ . The first **irrep** appears only in the decomposition of  $j$  gluons for  $j \geq \rho$ , as opposed to the second **irrep** that appears for  $j \geq \rho - 1$ . We see that the distinction between  $\mathcal{T}^\rho$  and  $\mathcal{T}^{\rho-1}$  will discriminate between both **irreps** of the  $t$ -channel, hence, property “2” is verified. The first property is trivially verified as the  $s$ -channel contains only distinct **irreps**.

## Results from the Algorithm

I used Mathematica to apply this algorithm, and explore if DM's symmetry appears for some of the eigenvalues. As a matter of fact it does not (up to  $\rho = 20$ , the rest was not calculated due to computation time). However, the weaker form found in the symmetric diquark case (relating the small  $b$  limit to the large  $N_c$  limit) for two of three eigenvalues still appears for two out of  $\rho + 1$  eigenvalues. It is a bit disappointing that the initially two third only become a two out of  $\rho + 1$ , however, it is only a small set of all possible one that were “scanned” through this algorithm.

I think the two next steps to further study this symmetry would be: 1/ find an analytic expression for those matrices that may explain why this symmetry did not survive from two quarks to two generalized partons  $\phi_\rho$ , and 2/ consider a wider range of **YD** to see if the *weaker symmetry* survives. The first point can be done using the following method, first introduce the expression of hermitian projectors in the  $s$ -channel with only symmetrizers and antisymmetrizers, then replace the  $t$ -channel and  $u$ -channel gluons exchange by trace operators using Fierz identity, and finally use recurrence relation between symmetrizers (resp. antisymmetrizers) to simplify those expressions (see chapter 6 of [45]).

**A small note,** A surprising fact is the form of all matrices obtained. They all have non-vanishing elements only on  $(i, i)$ ,  $(i, i + 1)$ ,  $(i, i - 1)$ . This can be explained by a “zero counting” based on the following properties:

- The matrix can be put in a block form  $AA$ ,  $SS$ ,  $AS$  and  $SA$  based on the signum of the  $s$ -channel projector.
- From the  $SS$  and  $AA$  blocks there are only elements on the diagonal.
- From  $AS$  and  $SA$  blocks there is a non zero contribution only for adjacent **irrep** in the  $s$ -channel. Using as index for the  $s$ -channel the second Dynkin index of the decomposition,  $Q_{\alpha\beta} \neq 0$  for  $\alpha = \beta \pm 1$ .

## 5.4 Negative dimension Theorem and anomalous dimension matrices

### 5.4.1 Setup

Cvitanović and Kennedy stated an interesting theorem called the “Negative dimension theorem”. I refer to the chapter 13 of [45] for a list of observed manifestation of the theorem and it is beautifully done using birdtracks. The statement is the following:

**Theorem : Negative dimension:**

If  $\lambda$  stand for a Young Tableau (YT) with  $\rho$  boxes and  $\bar{\lambda}$  for the transposed tableau by flipping  $\lambda$  across the diagonal (i.e., exchanging symmetrizations and antisymmetrizations), then the dimensions of the corresponding  $SU(n)$  reps are related by

$$SU(n) : \quad d_{\lambda}(n) = (-1)^{\rho} d_{\bar{\lambda}}(-n) \quad (5.74)$$

### Reformulation - Notations

I will call even (resp. odd) any **irreps** associated to a **YD**  $\lambda$  that contains an even (resp. odd) number of boxes. The transformation  $\mathcal{N}$  changes the sign of  $N_c$ , namely

$$\mathcal{N}[f_{\lambda}(N_c)] = f_{\lambda}(-N_c) \quad (5.75)$$

Where  $f_{\lambda}$  is a scalar function of  $N_c$  depending on the **irrep** considered  $\lambda$  (i.e. dimension, eigenvalue of quadratic Casimir, ...) The primed **YD**  $\lambda'$  is the transposed of  $\lambda$  (This notation is preferred since  $\bar{\lambda}$  can be confused with the conjugate).

For two **YDs** transposed to each other  $\lambda$  and  $\lambda'$ , if

$$\mathcal{N}[f_{\lambda}(N_c)] = f_{\lambda}(-N_c) = (\pm)f_{\lambda'}(N_c) \quad (5.76)$$

I will qualify the pair  $\{f_{\lambda}, f_{\lambda'}\}$  to be  $\mathcal{N}$ -symmetric or  $\mathcal{N}$ -alternate depending of the sign in 5.76.

**Dimension** It was already stated in the initial theorem, however the demonstration can be easily understood using the hooklength formulation for the dimension. Consider  $\lambda$  a **YD** with  $\rho$  boxes. The dimension is given by the relation

$$d_{\lambda} = K_{\lambda} = \frac{Num}{Den} \quad (5.77)$$

A useful property between  $\lambda$  and  $\lambda'$  YD is that their hook number are equal. Hence, the denominator in their respective dimension is identical. The numerator is computed by the product  $\prod_{\lambda}(a + N_c)$  with  $a$  the distance to the diagonal (+1 to the right -1 to the bottom). For the transposed the numerator will be  $\prod_{\lambda'}(a + N_c) = (-1)^\rho \prod_{\lambda}(a - N_c)$ . For example :

$$\begin{array}{|c|c|} \hline 0 & +1 \\ \hline -1 & \\ \hline -2 & \\ \hline -3 & \\ \hline \end{array} \quad Num = (1 + N_c)N_c(-1 + N_c)(-2 + N_c)(-3 + N_c)$$

$$\begin{array}{|c|c|c|c|} \hline 0 & +1 & +2 & +3 \\ \hline -1 & & & \\ \hline \end{array} \quad \begin{aligned} Num &= (-1 + N_c)N_c(+1 + N_c)(+2 + N_c)(+3 + N_c) \\ &= -(1 - N_c)(-N_c)(-1 - N_c)(-2 - N_c)(-3 - N_c) \end{aligned}$$

The dimension of the two YD are a realization of the negative dimension theorem. In general, the pair  $\{K_\lambda, K_{\lambda'}\}$  is either  $\mathcal{N}$ -symmetric for an even number of boxes or  $\mathcal{N}$ -alternate for an odd number of boxes.

**Quadratic Casimir eigenvalues** To construct our anomalous dimension matrix  $\mathcal{Q}$ , one also need some information about Casimirs behavior under the same transformation. For a YD with  $\rho$  boxes, the following relation gives the quadratic Casimir

$$\frac{1}{2} \left( \rho \frac{N_c^2 - \rho}{N_c} + \sum_{line} a_i^2 - \sum_{col} b_i^2 \right) \quad (5.78)$$

YDs  $\lambda$  and  $\lambda'$  have the same number of boxes  $\rho$ , the first term is alternate under  $\mathcal{N}$ . The two sums left are also alternate under transposition of the YD. Hence, Casimirs between  $\lambda$  and  $\lambda'$  are related by  $\mathcal{N}$  with an alternate behavior.

$$C_\lambda(N_c) = - C_{\lambda'}(-N_c) \quad (5.79)$$

### 5.4.2 Fully symmetric times fully symmetric case

**Postulate** To summon the negative dimension theorem for soft anomalous dimension matrices, one has to show that

$$\mathcal{N}[\mathcal{Q}_{\lambda\lambda \rightarrow \lambda\lambda}(N_c)] = \mathcal{Q}_{\lambda\lambda \rightarrow \lambda\lambda}(-N_c) = \mathcal{Q}_{\lambda'\lambda' \rightarrow \lambda'\lambda'}(N_c) \quad (5.80)$$

In turn  $\mathcal{Q}$  is defined by

$$\mathcal{Q} \propto \frac{K_{st} C^{(t)} K_{ts} \pm K_{su} C^{(u)} K_{us}}{2N_c} \times [\text{kinematics not important here}]$$

Remember that the  $u$ -channel is simply related to the  $t$ -channel by the signum of the  $s$ -channel, let's just focus on asking:

$$\text{Is } K_{st} \frac{C^{(t)}}{N_c} K_{ts} \text{ } \mathcal{N}\text{-symmetric or } \mathcal{N}\text{-alternate ?}$$

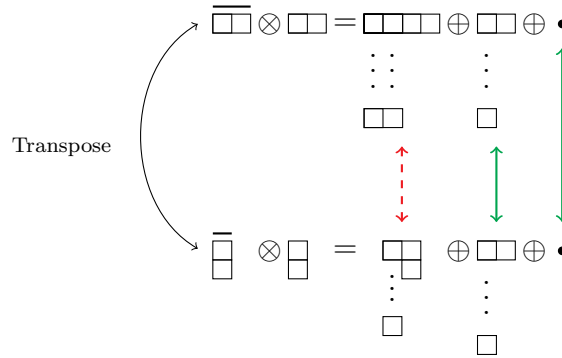
**Remark:** For the remaining of this section, I will use DM projector basis. The result obtained for  $\mathcal{Q}$  holds in other basis modulo trivial sign due to the ratio of  $s$ -channel dimensions. Basis independent quantities (e.g. eigenvalues) are free from such considerations. In particular, 5.35 seems to be in contradiction this section result, however this can easily be understood from the previous argument:

$$\left(\frac{K_s}{K_a}\right) [N_c] \xrightarrow{N_c \rightarrow -N_c} - \left(\frac{K_a}{K_s}\right) [N_c] \quad (5.81)$$

**First non-trivial case**

Let's start with  $\lambda = \square\square$ . The associated YD by negative dimension is  $\lambda' = \begin{smallmatrix} \square \\ \square \end{smallmatrix}$ .

$t$ -channel decomposition are given by



The  $t$ -channel decomposition is similar in  $\bar{\lambda} \otimes \lambda$  and  $\bar{\lambda}' \otimes \lambda'$ , they both contain the singlet and adjoint irreps and their respective dimension are  $\mathcal{N}$ -symmetric. The dimension of the tensor product  $\lambda \otimes \lambda$  verify

$$\mathcal{N}[K_{\lambda \otimes \lambda}(N_c)] = K_{\lambda}(-N_c) \cdot K_{\lambda}(-N_c) = K_{\lambda'}(N_c) \cdot K_{\lambda'}(N_c) \quad (5.82)$$

independently of  $\lambda$  being even or odd. In the previous figure, the red dashed arrow relate two YD: **27** and **0**. Those are not transpose to each other, however their respective dimension are

$$K_{27} = K_{\lambda}^2 - K_A - K_{\bullet} \quad (5.83)$$

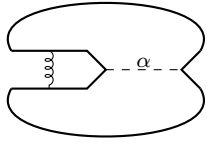
$$K_0 = K_{\lambda'}^2 - K_A - K_{\bullet} \quad (5.84)$$

In both equations  $K_{\bullet}$  and  $K_A$  are invariant under  $\mathcal{N}$  and we just saw that the pair  $\{K_{\lambda}^2, K_{\lambda'}^2\}$  is  $\mathcal{N}$ -symmetric. This implies that the pair  $\{K_{27}, K_0\}$  is  $\mathcal{N}$ -symmetric.

The quadratic Casimir pair  $\{C_{\lambda}, C_{\lambda'}\}$  is  $\mathcal{N}$ -alternate by construction (end of the previous subsection). Consider the following

$$0 = \begin{array}{c} \text{---} \\ \text{---} \end{array}$$

where lines correspond to the irrep  $\lambda$  (along the arrow). Using the completeness relation over the  $t$ -channel  $\bar{\lambda} \otimes \lambda$  yields to

$$0 = \sum_{\alpha=1,A,27} C_{\lambda} K_{\lambda}^2 - \sum_{\alpha=1,A,27} \frac{C_{\alpha} K_{\alpha}}{2}$$


and finally

$$C_{27} K_{27} = 2C_{\lambda} K_{\lambda}^2 - \sum_{\alpha=1,A} \frac{C_{\alpha} K_{\alpha}}{2} \quad (5.85)$$

However a similar relation can be obtained for  $\bar{\lambda}' \otimes \lambda'$

$$C_0 K_0 = 2C_{\lambda} K_{\lambda'}^2 - \sum_{\alpha=1,A} \frac{C_{\alpha} K_{\alpha}}{2} \quad (5.86)$$

From those two relations, one can conclude that  $\{C_{27}, C_0\}$  are  $\mathcal{N}$ -alternate.

There is a systematic here, and by iteration one can show that the elements of the decomposition  $\bar{\lambda} \otimes \lambda$  can be mapped (with a one to one correspondence) to those of the decomposition  $\bar{\lambda}' \otimes \lambda'$  by the transformation  $\mathcal{N}$ . Pair of dimensions are  $\mathcal{N}$ -symmetric and quadratic Casimir eigenvalues are  $\mathcal{N}$ -alternate. This leads to

$$\left\{ (C^{(t)}/N_c)_{\lambda\lambda \rightarrow \lambda\lambda}, (C^{(t)}/N_c)_{\lambda'\lambda' \rightarrow \lambda'\lambda'} \right\} \equiv \mathcal{N}\text{-symmetric}$$

also valid for the  $u$ -channel. This conclude all elements needed from the  $t$ -channel, aside from the rotation matrix  $K_{ts}$ . To study the properties of  $\mathcal{N}[K_{ts}]$  I need some elements from the  $s$ -channel.

**The  $s$ -channel** decomposition are given by

$$\begin{array}{c} \square\square \otimes \square\square = \square\square\square\square \oplus \begin{array}{|c|c|} \hline \square & \square \\ \hline \end{array} \oplus \begin{array}{|c|c|} \hline \square & \square \\ \hline \end{array} \\ \begin{array}{c} \uparrow \quad \quad \quad \uparrow \\ \text{green} \quad \quad \quad \text{blue} \\ \downarrow \quad \quad \quad \downarrow \end{array} \\ \begin{array}{c} \square \\ \square \end{array} \otimes \begin{array}{c} \square \\ \square \end{array} = \begin{array}{|c|c|} \hline \square & \square \\ \hline \end{array} \oplus \begin{array}{|c|c|} \hline \square & \square \\ \hline \end{array} \oplus \begin{array}{|c|} \hline \square \\ \hline \end{array} \\ \begin{array}{c} \uparrow \quad \quad \quad \uparrow \\ \text{red} \quad \quad \quad \text{blue} \\ \downarrow \quad \quad \quad \downarrow \end{array} \end{array} \quad (5.87)$$

Symmetry signum under permutation for both  $\lambda_1 \leftrightarrow \lambda_2$  and  $\lambda'_1 \leftrightarrow \lambda'_2$  are from the left to the right  $\sigma = \{+, -, +\}$ .

**Rotation matrix** Let's redefine the basis  $\{\mathcal{T}\}$ , and scalars in the  $A$  matrix used to compute  $t$ -channel projectors

$$\mathcal{T}^i \rightarrow \left( \frac{1}{N_c} \right)^i \mathcal{T}^i = \tilde{\mathcal{T}}^i, \quad C_i \rightarrow \frac{C_i}{N_c^i} = \tilde{C}_i, \quad \mathcal{B}_i \rightarrow \frac{\mathcal{B}_i}{N_c^i} = \tilde{\mathcal{B}}_i$$

A  $t$ -channel projector  $\mathcal{P}_\beta^{(t)}$  is now obtained by solving the system

$$\begin{pmatrix} \tilde{\mathcal{C}}_0 & \tilde{\mathcal{C}}_1 & \cdots \\ \tilde{\mathcal{C}}_1 & \tilde{\mathcal{C}}_2 & \cdots \\ \vdots & & \\ \tilde{\mathcal{B}}_0 & \tilde{\mathcal{B}}_1 & \cdots \end{pmatrix} \cdot \begin{pmatrix} \tilde{n}_0 \\ \tilde{n}_1 \\ \vdots \\ \tilde{n}_\rho \end{pmatrix} = \begin{pmatrix} 0 \\ 0 \\ \vdots \\ K_\beta \end{pmatrix}$$

where it is now important to remark that the whole matrix on the l.h.s. is  $\mathcal{N}$ -symmetric! In fact, all scalars in this matrix involve a product of  $s$ -channel dimensions ( $\mathcal{N}$ -symmetric) with ratio of Casimirs over  $N_c$  (thus  $\mathcal{N}$ -symmetric) for each  $s$ -channel projectors. The dimension  $K_\beta$  is also  $\mathcal{N}$ -symmetric, hence the solution  $\tilde{n}$  is  $\mathcal{N}$ -symmetric and this is valid for all  $\beta$ . In the  $s$ -channel projector basis a  $t$ -channel projector is expressed using the identity

$$\tilde{\mathcal{T}}^i = \sum_\alpha \left( \frac{2C_\lambda - C_\alpha}{2N_c} \right)^i \mathcal{P}_\alpha^{(s)} \quad (5.88)$$

where the bracket is again  $\mathcal{N}$ -symmetric. This concludes the fact that the matrix  $K_{ts}$  verifies:

$$\{(K_{ts})_{\lambda\lambda \rightarrow \lambda\lambda}, (K_{ts})_{\lambda'\lambda' \rightarrow \lambda'\lambda'}\} \equiv \mathcal{N}\text{-symmetric}$$

Following the initial postulate, the soft anomalous dimension matrix  $\mathcal{Q}_{\lambda\lambda \rightarrow \lambda\lambda}$  is thus simply related to the soft anomalous dimension matrix  $\mathcal{Q}_{\lambda'\lambda' \rightarrow \lambda'\lambda'}$  by the substitution  $N_c \rightarrow -N_c$ . One can obviously apply this theorem to any soft anomalous dimension matrices calculated from the previous algorithm with arbitrary fully symmetric **YD** and automatically obtain the case of fully antisymmetric **YD**. In particular, eigenvalues obtained follow the same pattern observed at the end of section 5.3.5.





## A.1 Young Diagrams and their use in QCD

In addition to birdtrack calculation, it is useful in pQCD calculations for YD to be within reach. For a given irrep, dimension, quadratic Casimir eigenvalue, cubic eigenvalue,... are often easily obtained from YD rather than from birdtracks. In this section, I will give some definitions and properties that are expected from YD, and some pocket formula with their demonstration.

### A.1.1 Permutation Group and Young diagrams

#### Definitions of Young Diagrams and Young Tableaux

In general, a YD is an arrangement of connected boxes such as:



However, our interest lie in a restricted set of all possible YD called the set of *regular Young Diagrams*. A regular Young Diagrams (or YD from hereon) is diagram where boxes are top left align. It means that there is a most as many boxes in a row  $i$  than in a row  $i - 1$ . An example of such diagram is



I will always note  $\rho$  to be the number of boxes in a YD. The YD denotes the shape used to arrange those  $\rho$  boxes. From a YD, one can build a YT by placing number within each box. Those numbers verifies two properties:

1. For a given row, they increase from left to right:  $a(i, j) \leq a(i, j + 1)$ .
2. For a given column, they strictly increase from top to bottom:  $a(i, j) < a(i + 1, j)$ .

Let's restrict the set of all possible **YT** to only those that have numbers 1 to  $\rho$  and each number appears once. This set is then called *standard Young Tableau* (**YT** from hereon, or I will specify otherwise if the **YT** is non-standard).

### Utility - Tensor product decomposition

A straightforward application of **YD** is the decomposition of a tensor product into a sum of **irreps**. In **QCD**, one will often meet for example the decomposition  $\mathbf{3} \otimes \bar{\mathbf{3}} = \mathbf{1} \oplus \mathbf{8}$  written in textbooks. This decomposition can easily be obtained from **YD** by following those few rules:

1. Place the two **YD** side by side (the most complex one on the left side preferably).
2. Label the right **YD** into a non-standard **YT** with: each rows have the same label, and labels increases from the top to the bottom.
3. Move the set of boxes with the first label into the left diagram in every possible ways such that the diagrams is still a *valid YD* (i.e. top left aligned).
4. Do the same for the next row of boxes, but keep only *distinct YT* with an acceptable *sequence*.

A sequence for a given **YT** is formed from the label read from right to left for each line from the top to the bottom. A sequence is acceptable if at any point in the sequence there is at least as many label  $i$  compared to  $i + 1$ ,  $i + 2$ , and so on. For example: acceptable sequence are  $(abc)$ ,  $(abac)$ , and rejected sequence are:  $(abb)$ , or  $(aacb)$ .

A small note: in the fourth item: by distinct **YT**, I means that if the same **YD** appears twice but with different labeling (i.e. distinct **YT**), one has to keep them both. Controversially, if a **YT** appears twice, one has to keep only one of them.

### Particularity of $SU(N_c)$ , and remark on “valid” Young Diagrams

The previous procedure applies for the permutation group  $S_n$ . However, if one is dealing with the **QCD** color gauge group  $SU(N_c)$  instead, one should recall that there is an additional primitive invariant to it (the *special S* of  $SU(N_c)$ ). Namely, there is the fully antisymmetric tensor of  $N_c$  indices in addition to the Kronecker delta tensor. This means that when  $N_c$  boxes appears in the same column, one simply remove such column and leave the rest of the diagram unchanged.

A consequence is that for  $SU(N_c)$ , a valid **YD** has at most  $N_c - 1$  boxes in each column, as opposed to the  $N_c$  for  $U(N_c)$ . This should be kept in mind for the third and fourth item of the previous procedure.

#### A.1.2 Pocket formula for Dimensions and Quadratic Casimir

Let's consider a **YD** associated to an **irrep R**. The knowledge of this **YD** is enough to find the dimension and quadratic Casimir eigenvalue associated to this **irrep**.

## Dimension

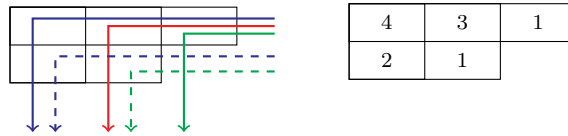
The dimension  $K_R$  reads

$$K_R = \frac{Num}{Den} \quad (\text{A.1})$$

The numerator is found using the following trick: place in the top-left box  $N_c$ , moving from left to right increase the value in the adjacent box by one, moving from the top to the bottom decrease the value in the adjacent box by one. For example,

$N_c$	$N_c + 1$	$N_c + 2$
$N_c - 1$	$N_c$	

The numerator is given by the product of the number within each box. In this example  $Num = N_c^2(N_c^2 - 1)(N_c + 2)$ . The denominator follows from the hook length formula. Move within every possible paths from the right to the bottom of the diagram with only one hook. The denominator is then given by the product of the length of each path (in the number of boxes crossed). In the previous example, one find



where on the left figure, the path along the YD are represented and in the right figure the path length is placed in the box where the hook occurs. The denominator of our example is then  $Den = 2 \times 3 \times 4$ .

## Quadratic Casimir eigenvalue

The quadratic Casimir eigenvalue for a given irrep will be noted  $C_2(\mathbf{R})$  in this section. We will soon see the cubic Casimir whose eigenvalue will be noted  $C_3(\mathbf{R})$ . In a way similar to the dimension, the quadratic Casimir eigenvalue can be obtained simply from

$$C_2(\mathbf{R}) = a \left\{ \rho \frac{N_c^2 - \rho}{N_c} + \sum_i a_i^2 - \sum_j b_j^2 \right\}, \quad a = 1/2 \quad (\text{A.2})$$

where  $a = 1/2$  is the usual trace normalization  $Tr(t^a t^b) = a \delta^{ab}$ . The first sum ( $i$ ) is over the rows of the YD, and the second sum ( $j$ ) is over the columns of the YD.  $a_i$  (resp  $b_j$ ) is the number of boxes within the row  $i$  (resp column  $j$ ) of the YD.

### A.1.3 Derivation using Young operator

The dimension formula can be demonstrated using Birdtrack and I refer to annexe B of [45] for such. Here, I will be interested in the demonstration of the formula for quadratic (and cubic) Casimir operators eigenvalues. In order to do so, one needs to introduce the Young Operator for a given YD.

### Young Operator

For a given **YD**, there is a unique way (up to overall sign) to define a Young Operator. This operator is not hermitian, however, it has all the properties needed for a projector: uniqueness, orthonormality, and completeness (see [45]). The procedure is the following:

1. Build the antisymmetrizer of  $\rho$  quark lines with respect to the **YD**. There is one antisymmetrizer for each column in the **YD** with respect to the number of boxes in each column. For example, the following **YD**  $\begin{matrix} \square & \square & \square \\ \square & \square & \square \end{matrix}$  has two antisymmetrizers with respect to two lines and one antisymmetrizer with respect to one lines. In birdtracks it gives (all quark arrows are from the left to the right)

$$A(\begin{matrix} \square & \square & \square \\ \square & \square & \square \end{matrix}) = \begin{matrix} \text{---} \blacksquare \text{---} \\ \text{---} \blacksquare \text{---} \\ \text{---} \end{matrix} \quad (\text{A.3})$$

2. In a similar fashion, build the symmetrizer of  $\rho$  quark lines with respect to the **YD**. The previous example gives

$$S(\begin{matrix} \square & \square & \square \\ \square & \square & \square \end{matrix}) = \begin{matrix} \text{---} \square \text{---} \\ \text{---} \square \text{---} \\ \text{---} \square \text{---} \end{matrix} \quad (\text{A.4})$$

3. Join quark lines between  $A$  and  $S$  such that the resulting birdtracks does not vanish. Two lines cannot go into the same symmetrizer and the same antisymmetrizer for a non-vanishing birdtrack. Because of the uniqueness of the Young operator, there is only one way to do such connection (up to an overall sign). In our example, one obtains

$$\begin{matrix} \text{---} \blacksquare \text{---} \\ \text{---} \blacksquare \text{---} \\ \text{---} \end{matrix} \begin{matrix} \text{---} \square \text{---} \\ \text{---} \square \text{---} \\ \text{---} \square \text{---} \end{matrix} \propto \text{YO}(\begin{matrix} \square & \square & \square \\ \square & \square & \square \end{matrix}) \quad (\text{A.5})$$

4. The normalization is found by requiring indempotence<sup>1</sup> of the Young operator.

For a given **YD**, in general there are several **YTs**. In this case the labeling of each lines matter. In our example, one might consider the **YT** with label 1, 2, 3 from the left to the right in the first row and 4, 5 in the next row. The Young operator associated is then given by

$$\begin{matrix} 1 & \text{---} \blacksquare \text{---} \\ 2 & \text{---} \blacksquare \text{---} \\ 3 & \text{---} \square \text{---} \\ 4 & \text{---} \square \text{---} \\ 5 & \text{---} \square \text{---} \end{matrix} \propto \text{YO}(\begin{matrix} \square & \square & \square \\ \square & \square & \square \end{matrix}) \quad (\text{A.6})$$

From the left to the right, one is basically telling: “ lines 1 and 4 go in the same antisymmetrizer, lines 2 and 5 go in the same antisymmetrizer, and line 3 is left alone. Then, lines 1 to 3 go in the same symmetrizer, and lines 3 and 4 go in the same symmetrizer.”

I will not need to use **YT** to find the quadratic (and cubic Casimir) eigenvalues. This is normal, as all **YT** associated to a **YD** have the same set of Casimir eigenvalues.

<sup>1</sup>If an operator have the same effect when applied one or several times, this operator has the property of indempotence. For a projection operator  $\mathcal{P}$ , it is the property that  $\mathcal{P} \cdot \mathcal{P} = \mathcal{P}$ .

### Quadratic Casimir - Setup

Let's consider a system of  $\rho$  quark lines. The identity acting on the space  $V^{\otimes\rho}$  with  $V$  the color space of the fundamental of  $SU(N_c)$ , is

$$\mathcal{I}_\rho = \begin{array}{c} \overrightarrow{\hspace{1cm}} \\ \overrightarrow{\hspace{1cm}} \\ \overrightarrow{\hspace{1cm}} \\ \vdots \\ \overrightarrow{\hspace{1cm}} \end{array}$$

In addition to the identity operator, the color generator  $\mathcal{G}_\rho^a$  for a system of  $\rho$  quark lines is defined as the sum over each lines  $i = 1, \dots, \rho$  of individual color generator  $t_i^a$  of each quark line

$$\mathcal{G}_\rho^a = \sum_{i=1}^{\rho} \begin{array}{c} \overrightarrow{\hspace{1cm}} \\ \overrightarrow{\hspace{1cm}} \\ \overrightarrow{\hspace{1cm}} \\ \vdots \\ \overrightarrow{\hspace{1cm}} \\ \overrightarrow{\hspace{1cm}} \end{array} \begin{array}{c} i \\ \text{---} \\ \text{---} \\ \text{---} \\ \text{---} \\ \text{---} \\ a \end{array}$$

and  $a$  is the color index of the generated gluon. The quadratic Casimir operator is defined as the operator

$$\hat{C}_2 = \mathcal{G}_\rho^a \cdot \mathcal{G}_\rho^b \delta_{ab} \quad (\text{A.7})$$

Notice the hat over  $C_2$  to indicate the operator, in contrast to eigenvalues that are given without the hat.

To single out eigenvalues of this operator (one for each possible **irrep** of  $V^{\otimes\rho}$ , one has to project into the desired **irrep**. Consider  $\mathbf{R}$  to be the desired **irrep**, and  $\mathcal{Y}_R$  its associated Young operator. Remember that the Casimir operator commute with the representation, and in particular with the **irrep**  $\mathbf{R}$ . One can write

$$\mathcal{Y}_R \cdot \hat{C}_2 = \hat{C}_2 \cdot \mathcal{Y}_R = C_2(\mathbf{R}) \mathcal{Y}_R \quad (\text{A.8})$$

Another way to remember this property is the color conservation. The operator  $\mathcal{G}_\rho^a$  commutes with any operator that map  $V^{\otimes\rho}$  into  $V^{\otimes\rho}$ . This is the main trick that I use to recover the pocket formula [A.2](#).

The Young operator is proportional to the action of the antisymmetrizer  $A_R$  then the symmetrizer  $S_R$ :

$$\mathcal{Y}_R \propto A_R \cdot S_R, \quad \text{read from the left to the right} \quad (\text{A.9})$$

Plugging this expression into the definition of the quadratic Casimir operator, one can write

$$C_2(\mathbf{R}) \mathcal{Y}_R \propto C_2(\mathbf{R}) A_R \cdot S_R = A_R \cdot (\mathcal{G}_\rho^a \cdot \mathcal{G}_\rho^b \delta_{ab}) \cdot S_R \quad (\text{A.10})$$

This relation is my starting point to recover [A.2](#). Remark that one does not need for the projection operator to be hermitian. This is an important point, as the derivation of hermitian projection operator can be quite involved when one use only the fundamental representation (see for example [\[71\]](#)).

### Quadratic Casimir - Simplifications and result

In the double sum over  $i = 1, \dots, \rho$  and  $j = 1, \dots, \rho$  introduced by the two color generators, there is a trivial contribution coming from the case where  $i = j$ . This contribution is shape-independent in the sense that it has not dependence in how the **YD** is shaped, but only on the number of boxes in the **YD**. For  $i = j$ , one can replace  $t_i^a t_i^b \delta_{ab}$  by simply the



with  $d_{abc}$  the traceless fully symmetric tensor defined in b.26. As in the case of the quadratic Casimir operator, one can write an analogue to A.10:

$$C_3(\mathbf{R})\mathcal{Y}_R \propto C_3(\mathbf{R}) A_R \cdot S_R = A_R \cdot (\mathcal{G}_\rho^a \cdot \mathcal{G}_\rho^b \cdot \mathcal{G}_\rho^c d_{abc}) \cdot S_R \quad (\text{A.17})$$

This expression is our starting point in order to derive the cubic Casimir eigenvalue of an irrep  $\mathbf{R}$ . In the triple sum over  $i, j, k$  from 1 to  $\rho$ , let's consider three cases: three equal indices, two out of three equal indices, three distinct indices.

- The simplest contribution is from  $i = j = k$ . This gives by definition the cubic Casimir eigenvalue of the fundamental irrep times the number of occurrences  $i = j = k$ .

$$\binom{\rho}{1} C_3(\mathbf{F}) = \rho \left( a \frac{N_c^2 - 4}{N_c} \right) C_2(\mathbf{F}) = \rho \left( a \frac{N_c^2 - 4}{N_c} \right) \left( a \frac{N_c^2 - 1}{N_c} \right) \quad (\text{A.18})$$

Let's remark the factor  $a^2$  associated to  $C_3(\mathbf{F})$  as opposed to  $a$  in  $C_2(\mathbf{F})$ .

- For two indices out of three equals: the operator  $\hat{C}_3$  is symmetric under any permutation of  $i, j, k$ , hence, one can factor out the symmetry factor  $3!$  and consider only  $i = j < k$  cases.

$$\sum_{i < j} t_i^a t_i^b t_k^c d_{abc} = \sum_{i < j} \overbrace{\quad}^{i \quad k} \star = \sum_{i < j} \left( \frac{C_3(\mathbf{F})}{C_2(\mathbf{F})} \right) \overbrace{\quad}^{i \quad k} \quad (\text{A.19})$$

and one recognize in the r.h.s. of this equation the birdtrack used in the quadratic Casimir case. This contribution to the cubic Casimir eigenvalue is then

$$\left( \frac{C_3(\mathbf{F})}{C_2(\mathbf{F})} \right) \times 3! a \left[ \sum_{i < j} \sigma^{(ik)} - \frac{1}{N_c} \frac{\rho(\rho - 1)}{2} \right] \quad (\text{A.20})$$

- Finally the last contribution, with  $i \neq j \neq k$ , can give some headache but is at the same time the most interesting one. In order to replace those gluons by a bunch of Kronecker delta tensors, one need a Fierz-like identity for the fully symmetric tensor  $d_{abc}$ . Using the trace representation of the fully symmetric tensor  $d_{abc}$  and *Fierzing* around, one finds

$$\overbrace{\quad}^{i \quad j \quad k} \star = 4a^2 \left[ \frac{1}{N_c} \overline{\quad} - \frac{1}{2N_c} (\overline{\quad} + \overline{\quad} + \overline{\quad}) + \frac{1}{4} (\overline{\quad} + \overline{\quad}) \right] \quad (\text{A.21})$$

In this relation, one can identify: (i) the identity tensor, (ii) permutations of two indices (previously seen), and (iii) transposition (cycle of two permutations).

- *Identity* - The contribution proportional to the identity yields a shape-independent contribution

$$3! \binom{\rho}{3} \frac{4a^2}{N_c^2} \quad (\text{A.22})$$



- *Permutation* - Let's use the same notation  $\sigma^{(ij)}$  for the permutation operator of two indices. The sum in first bracket of A.21 is

$$\hat{\sigma}_x^{(ijk)} = (\overline{\times} + \overline{\times} + \overline{\times}) = \hat{\sigma}^{(ij)} + \hat{\sigma}^{(ik)} + \hat{\sigma}^{(jk)} \quad (\text{A.23})$$

We already learned in the quadratic Casimir how to simplify  $\hat{\sigma}^{(ij)}$  operator. Eigenvalues of  $\hat{\sigma}_x^{(ijk)}$  are given by

$$\sigma_x^{(ijk)} = \begin{cases} \pm 3 & (ijk) \text{ in the same (anti)symmetrizer} \\ \pm 1 & (ijk) \text{ an off-hook (anti)symmetric} \\ 0 & \text{otherwise} \end{cases} \quad (\text{A.24})$$

I define an off-hook symmetric (resp antisymmetric) in a YD as the arrangement of  $(ijk)$  indices where only two indices are symmetric (resp antisymmetric) and the third index is neither.

For example, in  $\begin{array}{|c|c|c|} \hline 1 & 2 & 3 \\ \hline 4 & 5 & \\ \hline \end{array}$  there are only (135) and 234 symmetric off-hook, and no antisymmetric off-hook.

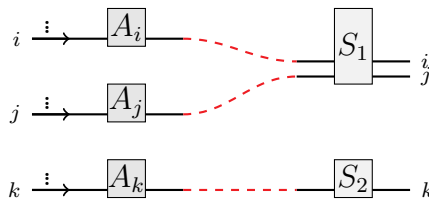
- *Transposition* - The last contribution depend on the two transposition defined by the operator

$$\hat{\sigma}_p^{(ijk)} = (\overline{\times} + \overline{\times}). \quad (\text{A.25})$$

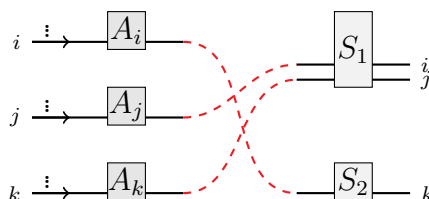
Let's consider a YD with an off-hook symmetric such as

$$\begin{array}{c} \square \cdots \boxed{i} \cdots \boxed{j} \\ \vdots \\ \vdots \\ \boxed{k} \end{array}$$

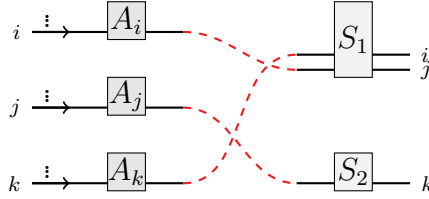
Indices  $ij$  pass through a symmetrizer  $S_1$  and index  $k$  through a symmetrizer  $S_2$ . Indices  $i, j, k$  pass through distinct antisymmetrizer  $A_i, A_j$ , and  $A_k$ . The associated Young operator consists of



By the uniqueness property, up to trivial permutations this is the **only** non vanishing birdtrack with the given set of symmetrizers and antisymmetrizers associated to the YD. Replacing the inner part in red by one of the two transpositions yields

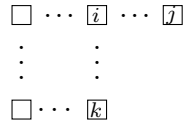


that vanish because there are missing links between  $A_i - S_1$  and  $A_k - S_2$ . The other contribution



also vanish because the link  $A_j - S_1$  and the link  $A_k - S_2$  are missing. The same can be done for an off-hook antisymmetric, and  $\sigma_p^{(ijk)}$  is vanishing for every off-hook.

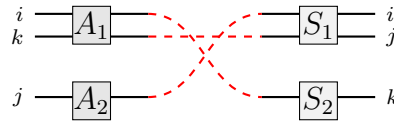
Now let's consider a "direct"-hook as a pattern of indices  $(ijk)$  that verify: two indices are symmetric and two indices are antisymmetric (at the same time). To visualize such triplet in a YD, look as the hook-length trick used in dimensions: a direct-hook consist of three indices forming an angle  $\pi/2$  in the YD:



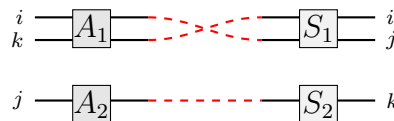
Introduce  $S_1$  as the symmetrizer of  $ij$ ,  $S_2$  as the symmetrizer of  $k$ ,  $A_1$  as the antisymmetrizer of  $ik$ , and  $A_2$  as the antisymmetrizer of  $j$ . The Young operator consists of



Replace the inner part in red by a transposition yields



This birdtrack is related to the previous one by a factor  $-1$ . The other transposition is



that vanish because two lines goes into the same symmetrizer and antisymmetrizer. The eigenvalue of  $\hat{\sigma}_p^{(ijk)}$  for a direct hook is then  $-1$ .

Considering all those contributions, the cubic Casimir eigenvalue for an irrep  $\mathbf{R}$  is given by:

$$\begin{aligned}
 C_3(\mathbf{R}) = & \binom{\rho}{1} C_3(\mathbf{F}) + \left( \frac{C_3(\mathbf{F})}{C_2(\mathbf{F})} \right) \times 3! a \left[ \sum_{i < j}^{\rho} \sigma^{(ik)} - \frac{1}{N_c} \binom{\rho}{2} \right] \\
 & + 3! \binom{\rho}{3} \frac{4a^2}{N_c^2} - 3! \frac{4a^2}{2N_c} \sum_{i < j < k}^{\rho} \sigma_x^{(ijk)} + \frac{3! 4a^2}{4} \sum_{i < j < k}^{\rho} \sigma_p^{(ijk)}. \quad (\text{A.26})
 \end{aligned}$$

with

	Symmetric	Antisymmetric	DirectHook	OffHook	Otherwise
$\sigma^{(ij)}$	+1	-1	$\emptyset$	$\emptyset$	0
$\sigma_x^{(ijk)}$	+3	-3	0	$\pm 1$	0
$\sigma_p^{(ijk)}$	+2	+2	-1	$\emptyset$	0

Finally, we usually set  $4a^2 = 1$  from the normalization of the trace of two fundamental generators  $Tr(t^a t^b) = a \delta^{ab} = \frac{1}{2} \delta^{ab}$

## A.2 Color triviality

Some elementary cases are often referred in the literature as *trivial* with respect to their color structure. In this section, I will underline what is referred as *color trivial* and implications for the couple { operator - basis choice }.

**Gauge group invariants** are a necessity in pQCD as  $SU(3)$  is expected to be an exact and preserved symmetry. Scalars with respect to color index are built as white constituents (i.e. color singlet states).

Here, we construct  $n$ -parton system projected into an overall singlet state that evolve in color space with respect to an arbitrary operator  $\mathcal{B}$ . A pre-requirement for  $\mathcal{B}$  is to be a linear map  $R_1 \otimes \cdots \otimes R_n \rightarrow R_1 \otimes \cdots \otimes R_n$ . When  $\mathcal{B}$  is projected on the left and right side into color singlet, it constructs a scalar invariant under gauge group rotations. I will write color evolution with increasing time from left to right and use a bracket notation to define initial and final color vectors.

$$\langle v_1^{(n)} | \mathcal{B} | v_2^{(n)} \rangle \equiv \text{Invariant} \quad (\text{A.27})$$

Obviously others invariants (between unmatching number of initial / final parton states) are possible but I will not consider them as, one can always study (at the cross section level) for the color structure a final parton as an initial anti-parton.

For the rest of this discussion  $\mathcal{B}$  is a linear map that conserve the number of partons.

**A basis choice** is to consider all possible singlet state of the system with  $n$  partons for a cross section. This is equivalent to look at each color state in the amplitude and complex amplitude then consider each case where the color state of the amplitude “match” the one in the complex amplitude (up to a trivial charge conjugate). By “match”, I mean that the Young diagram in the amplitude is the same as the conjugate Young diagram in the c-amplitude. In other words, amplitude and c-amplitude irreps are conjugated of each other. A distinction must be done between an irrep and the way irreps are labeled as an irrep can appear more than once in a given decomposition. This distinction is analogue to comparing two Young Diagrams versus comparing two Young Tableaux. One can think of different YT (with number in each boxes) with the same YD (only the shape).

$$\begin{aligned} |v^{(n)}\rangle &\equiv \text{Overall singlet of } n\text{-partons} \\ |u^{(n-j)}, w^{(j)}\rangle &\equiv \text{Irrep of } n-j \text{ partons match irrep of } j\text{-partons} \end{aligned}$$

There is no need to fix the normalization as only orthogonality is needed for this discussion, but an orthonormal basis would be the go-to choice for obvious reasons in practical computations. Note that a non-zero ket implies that  $R_{ampl} \equiv \bar{R}_{c-ampl}$  (here the “ $\equiv$ ” stands for same irrep with respect to their YD). We will only write non-zero ket and the equivalence is implied in the ket (resp bra) notation.

For practical purpose, if  $n - j = j$ , it is convenient to define a subset of all vectors that verifies  $R_{ampl} = \bar{R}_{c-ampl}$  (here the “ $=$ ” stands for same irrep and label with respect to their YT). I call this subset the *projector-basis*.

$$|u^{(j)}, u^{(j)}\rangle \equiv \text{An element of the projector-basis} \quad (\text{A.28})$$

**Color triviality for two partons** in a given irrep  $R_1$  and  $R_2$ . With respect to the two previous paragraphs, we are only looking at singlet states in the decomposition  $R_1 \otimes R_2$ . A birdtrack notation for a singlet is

$$|R_1, R_2\rangle = \begin{array}{c} R_1 \longrightarrow \\ \phantom{R_1} \phantom{\longrightarrow} \\ R_2 \dashrightarrow \end{array} \bullet \quad (\text{A.29})$$

where the bullet / vertex indicates, an arbitrary structure (can involved complicate loops, as long we have two external legs). The right side of the bullet have no leg at all, this is a color singlet. This is possible only if  $\bar{R}_2 \equiv R_1$ , using the arrow in opposite sign for conjugate, we have

$$|R_1, R_2\rangle = \begin{array}{c} R_1 \longrightarrow \\ \phantom{R_1} \phantom{\longrightarrow} \\ \bar{R}_1 \longleftarrow \end{array} \bullet \quad (\text{A.30})$$

The bullet is proportional to  $\delta_{R_1 \equiv \bar{R}_2}$  (that becomes  $\delta_{R_1 = \bar{R}_2}$  by orthogonality if we consider the bullet built from two Clebsch Gordan), hence the representation of a line for both (there is only one singlet in  $R \otimes \bar{R}$  for any irrep  $R$ ).

Without any information on the form of  $\mathcal{B}$ , we can express it as a polynomial of fully symmetrized trace of generators along a line of irrep  $R_1$ . Any traces of  $p > N$  generators can be related to lower traces of generators by the use of characteristic equation [45]. And those traces are related to  $N - 1$  independent Casimirs. This means that

$$\mathcal{B}|R_1, R_2\rangle = P_{\mathcal{B}}[C_R^{(2)}, C_R^{(3)}, \dots, C_R^{(N)}]|R_1, R_2\rangle \quad \forall R = R_1 = \bar{R}_2 \quad (\text{A.31})$$

That is  $\mathcal{B}$  can be replaced by a polynomial of independent Casimirs when applied to  $|R_1, R_2\rangle$ . This simple behaviors / substitution is called *color-triviality*.

**Assume** an operator  $\mathcal{B}$  that can be expressed as a polynomial  $P$  with

$$\mathcal{B} = P [T_i^a \cdot T_j^a \omega_{ij}] \quad (\text{A.32})$$

subscript  $i$  and  $j$  label the line associated to the generator. A sum over the color superscript  $a$  is implied. The  $\omega_{ij}$  term is over the field of  $\mathbb{R}, \mathbb{C}$  numbers and is often associated to the Lorentz structure of the underlying process.

→ For two partons, we have in birdtrack notation

$$\mathcal{B} = P \left[ \begin{array}{c} \text{---} \\ \text{---} \end{array} \begin{array}{c} \text{---} \\ \text{---} \end{array} \begin{array}{c} \text{---} \\ \text{---} \end{array} \right] \quad (\text{A.33})$$

The only singlet state is  $|R, \bar{R}\rangle$  and each diagrams in this expression have eigenvalue  $C_R$ . Hence

$$\begin{aligned} \mathcal{B}|R, \bar{R}\rangle &= P[C_R, C_R, C_R] \cdot |R, \bar{R}\rangle \\ &= b \cdot |R, \bar{R}\rangle \quad b \in P[\mathbb{C} \times C_R] \end{aligned}$$

→ Three partons : a sensitive difference from the two point case is that multiple singlets can be constructed this time. Each times  $\bar{R}_3$  appears in the  $R_1 \otimes R_2$  decomposition, there is an associated singlet<sup>2</sup>. The decomposition into *irreps* is

$$R_1 \otimes R_2 = \sum_i \alpha_i^{(2)} \quad (\text{A.34})$$

<sup>2</sup>The choice  $\bar{R}_3 \subset R_1 \otimes R_2$  is arbitrary and one can prefer  $R_1 \otimes R_3$  or  $R_2 \otimes R_3$  to construct a singlet basis.



**Assume** another operator  $\mathcal{B}$  that can be expressed as

$$\mathcal{B} = P_1 [T_i^a \cdot T_i^a \omega_{ii}] + P_2 [T_i^a T_i^b T_i^c d_{abc} \Omega_{ii}] + \dots \quad (\text{A.39})$$

In this case, color triviality is not restricted by the number of involved partons. We can replace  $T_i^a \cdot T_i^a$  by the quadratic Casimir  $C_i^{(2)}$  and  $T_i^a T_i^b T_i^c d_{abc}$  by the cubic Casimir  $C_i^{(3)}$ . This class of linear map is encountered for example in the Sudakov form factors, where we can attribute a contribution to each line with no “mixing”. In this case *Color triviality* holds for any number of partons.

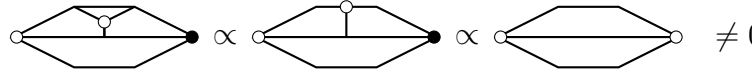
**Three partons and non color triviality** is also possible. This depends on the form of evolution operator  $\mathcal{B}$ . Consider  $\mathcal{B}$  similar to  $P_2$  in A.39 but with different attachments  $i, j, k$ .

$$\mathcal{B} \equiv \sum_{i,j,k} T_i^a T_j^b T_k^c d_{abc} \Omega_{ijk} \quad (\text{A.40})$$

with the sum over  $i, j, k$  left as free. As an illustration we will consider *ggg*-system. The vector basis consists of two elements as the adjoint appears two times in  $Adj \otimes Adj$  decomposition. An easy choice is to pick two elements proportional to  $f_{abc}$  and  $d_{abc}$ . We note  $|f\rangle$  and  $|d\rangle$  the two elements of the vector basis. Obviously, they are orthogonal vectors as  $\langle f|d\rangle \propto f_{abc} d^{abc} = 0$ . We have to consider some contributions outside of the diagonal, for example

$$\Omega_{112} \langle d| T_1^a T_1^b T_2^c d_{abc} |f\rangle \propto \Omega_{112} \langle d| T_1^a T_2^a |d\rangle \propto \Omega_{112} \langle d|d\rangle \neq 0 \quad (\text{A.41})$$

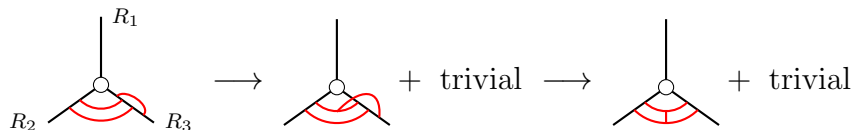
Easy to perform with birdtrack notations,



$$\text{Diagram 1} \propto \text{Diagram 2} \propto \text{Diagram 3} \neq 0 \quad (\text{A.42})$$

where lines are gluons, a white dot is a symmetric vertex and a black dot an anti-symmetric vertex. The fact that off-diagonal contributions are non-zero, show that for  $\mathcal{B}$  a linear map with the form A.40, color triviality does not hold even with three partons!

**Also** a three parton system with an operator  $\mathcal{B}$  that involves only two point interactions can be non-trivial.



$$\text{Diagram 1} \rightarrow \text{Diagram 2} + \text{trivial} \rightarrow \text{Diagram 3} + \text{trivial}$$

Each interactions (red lines) are two points interactions but they cannot be fully simplified using relation such as A.37 anymore. We do not have color triviality for those kind of contributions.

A way to compute this factor would be to pass in the channel

$$R_1 \otimes Adj \rightarrow \bar{R}_2 \otimes \bar{R}_3,$$

that is a four partons “inner process”. Compute relative weight  $w_\beta^{(v)}$  into each irrep  $\beta$  of the inner process, simplify the two emitted gluons between  $R_2$  and  $R_3$  lines by a factor  $(C_2 + C_3 - C_\beta)/2$  squared then the final gluon loop on  $R_3$  contributes to a factor  $C_3$ .

$$T_3^a (T_3^b T_2^b) (T_3^c T_2^c) T_3^a |v\rangle \equiv \sum_\beta w_\beta^{(v)} \left( \frac{C_2 + C_3 - C_\beta}{2} \right)^2 C_3 \cdot |v\rangle$$

due to the  $w_\beta^{(v)} \times (C_\beta^2 + 2C_\beta)$ , this is a non trivial contribution with off diagonal elements.

**Long story short,**

- $\mathcal{B}$  linear map  $R_1 \otimes \cdots \otimes R_n \rightarrow R_1 \otimes \cdots \otimes R_n$  that preserves the number of partons.  
If not : reformulate the problem to this one by switching in/out partons.
- A vector basis in a given channel  $|\alpha^{(n-j)}, \beta^{(j)}\rangle$ .

*“As long as  $\mathcal{B}$  does not necessitate to introduce re-projection into irreps of distinct multiple channels, the color structure can be considered as trivial.”*

The case that everyone loves :  $\mathcal{B} \equiv P [T_i^a T_j^a \omega_{ij}]$ , is color trivial up to three (non singlet) partons involved. One only need to know the Casimir of each partons to fully solve the problem.





## B.1 Phase

Starting from equation 3.59, introduce the short hand notation  $\vec{P}_m = \sum_{i=1}^m \vec{p}_i$ , then the initial phase  $\varphi_m$  in 3.46 reads

$$\varphi_m = \sum_{i=1}^{m-1} \vec{p}_i \cdot (\vec{x}_{im} - \vec{x}'_{im}) + \vec{P}_m \cdot (\vec{x}_m - \vec{x}'_m)$$

After the first  $\vec{p}_m$  integral the separation  $\vec{x}_m - \vec{x}'_m$  is set to zero, hence the remaining phase is

$$\begin{aligned} \sum_{i=1}^{m-1} \vec{p}_i \cdot (\vec{x}_{im} - \vec{x}'_{im}) &= \sum_{i=1}^{m-1} \vec{p}_i \cdot ((\vec{x}_{i,m-1} + \vec{x}_{m-1}) - (\vec{x}'_{i,m-1} + \vec{x}'_{m-1})) \\ &= \sum_{i=1}^{m-2} \vec{p}_i \cdot (\vec{x}_{i,m-1} - \vec{x}'_{i,m-1}) + \vec{P}_{m-1} \cdot (\vec{x}_{m-1} - \vec{x}'_{m-1}) \end{aligned}$$

that is by definition  $\varphi_{m-1}$  the phase that would be associated to the case of a  $m-1$  parton system. This procedure easily iterates, and after  $d^2 \vec{p}_m \cdots d^2 \vec{p}_{n+1}$  the remaining phase is simply  $\varphi_n$ .

The initial measure in 3.46

$$\prod_{i=1}^{m-1} \frac{d^2 \vec{x}_{im}}{(2\pi)^2} \frac{d^2 \vec{x}'_{im}}{(2\pi)^2} \cdot \frac{d^2 \Delta_m^-}{(2\pi)^2}$$

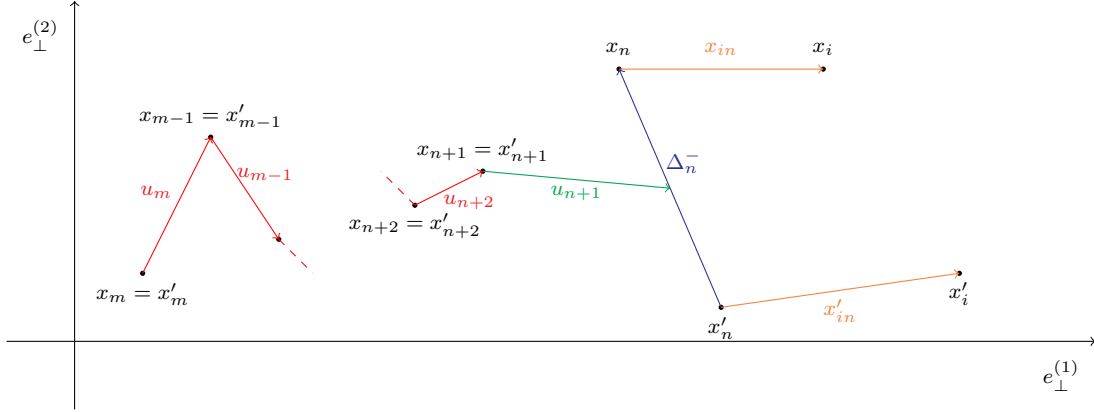
is now

$$\prod_{i=1}^{m-2} \frac{d^2 \vec{x}_{i,m-1}}{(2\pi)^2} \frac{d^2 \vec{x}'_{i,m-1}}{(2\pi)^2} \cdot \frac{d^2 \Delta_{m-1}^-}{(2\pi)^2} \cdot \frac{d^2 \vec{u}_m}{(2\pi)^2}$$

with  $\vec{u}_m = (\vec{x}_{m-1} + \vec{x}'_{m-1} - 2\vec{x}_m)/2$ . This procedure is iterated from  $m$  to  $n+1$  and the measure left is

$$\prod_{i=1}^n \frac{d^2 \vec{x}_{in}}{(2\pi)^2} \frac{d^2 \vec{x}'_{in}}{(2\pi)^2} \cdot \frac{d^2 \Delta_n^-}{(2\pi)^2} \cdot \prod_{j=n+1}^m \frac{d^2 \vec{u}_j}{(2\pi)^2} \quad (\text{B.1})$$

After all the  $d^2 \vec{p}_{n+1} \cdots d^2 \vec{p}_m$  momenta are integrated out, transverse positions are schematically given by this graph



It is now easy to follow the graph to express arguments of  $\psi$  as

$$\vec{x}_{\alpha,m} = \begin{cases} \vec{x}_{in} + \frac{\Delta_n^-}{2} + \sum_{k=n+1}^m \vec{u}_k & \text{if } \alpha \leq n \\ \sum_{k=\alpha+1}^m \vec{u}_k & \text{if } \alpha > n \end{cases}$$

In the conjugate amplitude,  $\psi^*$ 's arguments are obtained by the substitution  $\Delta_n^- \rightarrow -\Delta_n^-$ . Recall that the Fourier transform of the two wave functions  $\psi$  and  $\psi^*$  are

$$\psi(\{\vec{x}\}_m) = \int \left[ \prod_{j=1}^{m-1} d^2 \vec{r}_j e^{-i \vec{r}_j \cdot \vec{x}_{jm}} \right] \psi(\{\vec{r}\}_m) \quad (\text{B.2})$$

$$\psi^*(\{\vec{x}'\}_m) = \int \left[ \prod_{j=1}^{m-1} d^2 \vec{r}'_j e^{+i \vec{r}'_j \cdot \vec{x}'_{jm}} \right] \psi^*(\{\vec{r}'\}_m) \quad (\text{B.3})$$

in 3.46. As a summary, in the following table are the phases

	sign	$\vec{x}_{in}$	$\vec{x}'_{in}$	$\Delta_n^-$	$\vec{u}_m$	$\cdots$	$\vec{u}_{n+1}$
$\varphi_n$	+	$\vec{p}_i$	$-\vec{p}_i$	$\vec{P}_n$	$\emptyset$	$\cdots$	$\emptyset$
$\psi$	-	$\vec{r}_i$	$\emptyset$	$\vec{R}_n/2$	$\vec{R}_{m-1}$	$\cdots$	$\vec{R}_n$
$\psi^*$	+	$\emptyset$	$\vec{r}'_i$	$-\vec{R}_n/2$	$\vec{R}'_{m-1}$	$\cdots$	$\vec{R}'_n$

Due to the fact that  $\psi(\{\vec{r}\}_m)$ ,  $\psi^*(\{\vec{r}'\}_m)$  and  $e^{\mathcal{B}(n,n)}$  are independent of  $\vec{u}$ 's, integrals over  $d^2 \vec{u}_i$  for  $i = n+1, \dots, m$  set  $\vec{r}_i = \vec{r}'_i$  for  $i \leq n+1$  and yield a distribution  $\delta^{(2)}(\vec{R}_n - \vec{R}'_n)$ .

This leads to equation 3.60.

## B.2 Hessian matrix

Here are some complementary elements to recover 4.10.

Starting from the expression of  $\hat{\Gamma}$

$$\hat{\Gamma}(\vec{x}) = \frac{\bar{Q}_s^2}{2\mu^2} [1 - \mu x K_1(\mu x)] \quad (\text{B.4})$$

One can remark that the ascending series of  $x K_1(x)$  involves only power of  $x^{2n}$  (see 9.6.10 and 9.6.11 of [72]). This means that the function  $\hat{\Gamma}$  depends effectively on  $x^2$ . Using this fact,  $H_{23}$  can be decomposed into

$$(H_{23})_{ij} = \mathbb{1}_{ij} \cdot 2\tilde{\Gamma}'(x_{23}^2) + \left( e_{23}^{(i)} e_{23}^{(j)} \right)_{ij} \cdot x_{23}^2 4\tilde{\Gamma}''(x_{23}^2) \quad (\text{B.5})$$

with  $\tilde{\Gamma}(x^2) \equiv \hat{\Gamma}(\vec{x})$  in units of  $\mu$ :

$$\tilde{\Gamma}'(x^2) \xrightarrow{x^2 \ll 1} \frac{1}{4} \log(1/x^2) + \dots, \quad x^2 \tilde{\Gamma}''(x^2) \xrightarrow{x^2 \ll 1} \mathcal{O}(1)$$

In the small  $x_{23}$  region, one can neglect the second contribution of B.5. This yields 4.10

$$X \simeq \vec{x}_{12} \cdot \vec{x}_{34} \frac{\bar{Q}_s^2}{4} \log \left( \frac{1}{\mu^2 x_{23}^2} \right)$$



**Titre :** Effets nucléaires dans les collisions proton-noyau à haute énergie : élargissement de l'impulsion transverse des systèmes de partons énergétiques et matrices de dimension anormale.

**Mots clés :** pQCD, élargissement de l'impulsion transverse, matrice de dimension anormale.

Ce manuscrit regroupe les résultats obtenus dans le cadre de mes études doctorales sous la direction de Ginès Martínez et la supervision de Stéphane Peigné dans le groupe *théorie* du laboratoire SUBATECH entre octobre 2015 et septembre 2018.

Y est présenté une approche originale de la structure du groupe de couleur associée à la production de systèmes de partons énergétiques dans les collisions de type protons-noyaux. Dans un premier temps, le cas académique d'un système asymptotique passant au travers d'un milieu nucléaire et diffusant élastiquement est étudié afin de déterminer la distribution en impulsion transverse des partons de ce système. Cette étude se généralise ensuite à la production dans les collisions nucléaires. Dans un second temps, une étude sur la structure de couleur associée à ce problème y est détaillée. La structure de couleur associée aux rediffusions multiples est encodée dans un opérateur  $\mathcal{B}$ . Cet opérateur est formellement équivalent à la matrice de dimension anormale  $\mathcal{Q}$  qui resomme le rayonnement de gluons mous associé aux processus  $2 \rightarrow 2$ . Une étude sur ces opérateurs y est présentée.

Au sein du Modèle Standard de la physique des particules, la théorie décrivant l'interaction forte est la Chromodynamique Quantique (QCD). Cette théorie de jauge de groupe de symétrie  $SU(N_c)$  décrit les interactions entre des particules portant une charge de couleur: quarks, antiquarks, et gluons constituant les hadrons. La propriété de liberté asymptotique de QCD implique que la constante de couplage de la théorie  $\alpha_s$  décroît avec l'énergie. Ainsi à haute énergie, il est possible d'employer la QCD perturbative (pQCD) pour organiser des observables physiques en suite de paramètre  $\alpha_s$ . En vue d'applications en phénoménologie des collisions protons-noyaux dans les grands collisionneurs de hadrons (RHIC, LHC), il est possible d'utiliser la pQCD pour décrire des effets nucléaires. En particulier, cette thèse traite du phénomène d'élargissement de la distribution en impulsion transverse due à la présence d'un milieu nucléaire.

Pour un parton de haute énergie passant au travers d'un milieu nucléaire, il est possible d'utiliser une équation cinétique pour obtenir la distribution en impulsion transverse. Cette approche est décrite dans la section 3.2.1. Dans un premier temps, le potentiel de diffusion donné par 3.15 décrit l'échange d'impulsion transverse entre le parton et un nucléon. Cet échange est alors itéré en supposant que chaque interaction du parton avec un nucléon est indépendant de la position du nucléon dans le noyau. Il est alors possible d'écrire une équation cinétique pour la distribution en impulsion transverse, dont la solution est donnée par 3.23. L'expression obtenue 3.23 est bien connue et a été obtenue de nombreuses fois (e.g. [53, 43, 54]).

De façon semblable, il est possible de décrire l'évolution d'un système de  $n$  partons asymptotiques dans le formalisme des dipôles. Dans ce formalisme le système de  $n$  partons est décrit par un multipole de  $2n$  partons dans un singulet de couleur. L'équation 3.44 donne le résultat de cette évolution pour une paire asymptotique, et sa généralisation est donnée dans la section 3.2.4. Contrairement au cas d'un parton, l'étude de système de parton possède une richesse supplémentaire: la structure de couleur devient non-triviale. Cette richesse vient du fait que pour  $n \geq 2$ , il existe plusieurs singulets de couleur pour le système de  $2n$  partons. Pour chaque représentation irréductible (irrep) de la décomposition dans l'amplitude, il est possible de former un singulet avec son irrep conjuguée dans l'amplitude conjuguée. De plus, les interactions avec le milieu vont pouvoir permettre au système de  $2n$  partons de changer de singulet. La section 3.1 discute de cet espace de couleur au niveau de la section efficace.

Une façon économique de distinguer ces singulets est de suivre l'évolution de l'irrep du système de  $n$  partons au niveau de l'amplitude. Pendant l'évolution dans le milieu du multipole, l'irrep du système change de multiples fois. Cela traduit un processus de marche aléatoire dans l'espace de couleur. Cette marche aléatoire est encodée dans un opérateur de "broadening"  $\mathcal{B}$  qui une fois exponentié donne la distribution en impulsion transverse du système. Dans le cas de la paire,  $\mathcal{B}$  est donné par 3.43 qui se généralise sans difficultés au cas d'un système à  $n$  partons en suivant la section 3.2.4.

Il est intéressant en vue d'applications phénoménologiques, d'étudier deux limites de l'opérateur  $\mathcal{B}$  ainsi construit: (i) la limite ponctuelle, (ii) la limite compact. Dans la limite ponctuelle (i), discutée dans la section 3.2.4, plusieurs partons du système sont considérés être à la même position transverse. Cette contrainte simplifie drastiquement l'expression de  $\mathcal{B}$  pour  $n$  partons en la reliant à l'expression de  $\mathcal{B}$  pour  $j < n$  partons. Dans la seconde limite (ii), discutée dans la section 3.3, les partons du système sont proches les uns des autres comparés à la résolution du milieu donnée par l'échelle de saturation  $Q_s$ . Dans cette configuration, il est possible de compter le nombre de transitions entre les irreps du multipole et d'exprimer la distribution en impulsion transverse comme une série dans le nombre de transitions de couleur produite dans le milieu.

Muni de ces résultats pour les système de parton asymptotique, il est possible d'étudier la production réaliste de partons. Le chapitre 4 est consacré à la production d'une paire. À haute énergie, la production d'une paire provient de la fluctuation virtuelle d'un parton en deux partons. Cette fluctuation possède une longue durée de vie et se produit donc avant ou après le milieu. La section efficace est alors donnée par la somme de quatre contributions où la fluctuation se produit avant ou après dans l'amplitude et l'amplitude conjuguée.

Une irrep étant une quantité invariante de jauge, il est alors plausible de se demander

---

comment dépend la section efficace de production d'une paire (expérimentalement un dijet comme proxy pour la paire) en fonction de l'irrep initial et final du système. Pour ce faire, la limite (ii) est utilisée dans la région où les impulsions transverses des deux partons sont grandes  $p_t(1) \sim p_t(2) \gg Q_s$ . Pour une irrep initial distincte de l'irrep finale, uniquement le corrélateur à quatre points doit être considéré. Au premier ordre dans le développement en pair compact, la section efficace donne 4.11. Au même ordre et avec la même irrep dans l'état initial et finale, la section efficace est obtenue dans la section 4.1.2. Les deux résultats sont ensuite résumés dans la section 4.1.3 sous une forme compacte. Enfin, les applications de ces résultats sont discutées dans la section 4.2 où la possibilité d'utiliser le milieu nucléaire comme un filtre à couleur  $y$  est discutée et devrait apporter des pistes de réponse à des questions d'actualité en QCD tel que: discriminer parmi les mécanismes de production des quarkonias.

Pour ce faire, un outils puissant est l'utilisation de la représentation diagrammatique de la structure tensoriel de couleur ou "*birdtracks*". Cet outil est introduit dans l'interlude b, où les bases nécessaires pour dériver l'opérateur  $\mathcal{B}$   $y$  sont expliquées. L'avantage majeur des birdtracks est la suppression des indices muets (convention d'Einstein) qui permet d'avoir une visibilité accentuée des différents flux de couleurs présents dans ces calculs. De façon plus approfondie, le chapitre 5 est consacré au calcul de l'opérateur  $\mathcal{B}$  en utilisant les birdtracks.

Dans le chapitre 5, l'analogie formelle entre l'opérateur de broadening  $\mathcal{B}$  et la matrice de dimension anormale  $\mathcal{Q}$  est soulignée section 5.2.1. La matrice de dimension anormale a été dérivée dans le contexte de la resommation de gluons mous dans des processus  $2 \rightarrow 2$  dans [16]. L'aspect technique du calcul de  $\mathcal{Q}$  est d'exprimer des opérateurs dans le canal  $t$  et  $u$  dans le canal  $s$  du processus considéré. En effet,  $\mathcal{Q}$  est la somme de deux termes qui possèdent une expression simple dans respectivement le canal  $t$  ou dans le canal  $u$ . Pour ce faire, les birdtracks sont utilisées dans le chapitre 5. Il a été remarqué dans [16] une étonnante symétrie reliant l'échange d'un degré de liberté cinématique avec le nombre de couleur du groupe de symétrie dans certaines des valeurs propres de la matrice  $\mathcal{Q}$ . Cette symétrie (non expliquée) et la relation formelle entre  $\mathcal{Q}$  et  $\mathcal{B}$  motive l'étude des différents cas possibles afin de vérifier si cette symétrie est fortuite ou non. Pour des partons standards (quark, antiquark, gluon), la matrice de dimension anormale est calculée de façon économique dans la section 5.2.2 et l'étrange symétrie n'apparaît que pour les cas  $aa \rightarrow aa$  où  $a$  est un quark, antiquark ou gluon.

Cette dernière remarque motive l'utilisation de partons *généralisés* qui sont définis comme étant des partons dans une irrep différente de la fondamentale ou l'adjointe de  $SU(N_c)$ . La matrice  $\mathcal{Q}$  est étudiée dans les cas  $\varphi\varphi \rightarrow \varphi\varphi$  où  $\varphi$  est un tableau de Young complètement symétrique par le biais d'un algorithme détaillé dans la section 5.3.4. Parmi les cas étudiés, l'étonnante symétrie n'apparaît pas. Cependant, un reliquat reliant la limite de grand  $N_c$  à ce paramètre cinématique est apparent. La fin du chapitre 5 est dédié à l'application du théorème de dimension négative [45] au calcul de matrice de dimension anormale. Il est en effet possible de montrer qu'à partir de l'algorithme présenté, on peut obtenir l'ensemble des cas où  $\varphi$  est totalement antisymétrique uniquement par la substitution  $N_c \rightarrow -N_c$  dans l'expression de la matrice  $\mathcal{Q}$ .





## BIBLIOGRAPHY

- [1] Yuri L. Dokshitzer. QCD and hadron dynamics. *Phil. Trans. Roy. Soc. Lond.*, A359:309–324, 2001.
- [2] Michael E. Peskin and Daniel V. Schroeder. *An Introduction to quantum field theory*. Addison-Wesley, Reading, USA, 1995.
- [3] Andrei V. Smilga. *Lectures on quantum chromodynamics*. WSP, Singapore, 2001.
- [4] Yu. L. Dokshitzer. Gribov program of understanding confinement. *Sci. Cult. Ser.-Phys.*, 21:60–79, 2002.
- [5] Yuri L. Dokshitzer. QCD, theoretical issues. In *High-energy physics. Proceedings, International Europhysics Conference, Jerusalem, Israel, August 19-25, 1997*, pages 47–67, 1997.
- [6] John C. Collins, Davison E. Soper, and George F. Sterman. Factorization of Hard Processes in QCD. *Adv. Ser. Direct. High Energy Phys.*, 5:1–91, 1989.
- [7] Yuri L. Dokshitzer. Historical and futuristic perturbative and non-perturbative aspects of QCD jet physics. *Acta Phys. Polon.*, B36:361–380, 2005.
- [8] R. Baier, Yuri L. Dokshitzer, S. Peigne, and D. Schiff. Induced gluon radiation in a QCD medium. *Phys. Lett.*, B345:277–286, 1995.
- [9] Eugene Levin. The Pomeron: Yesterday, today and tomorrow. In *Proceedings, 3rd Gleb Wataghin School on High-energy Phenomenology: Campinas, Brasil, July 11-16 1994*, pages 0158–261, 1994.
- [10] Eugene Levin. Everything about Reggeons. Part 1: Reggeons in 'soft' interaction. 1997.
- [11] Quantal phase factors accompanying adiabatic changes. *Proceedings of the Royal Society of London A: Mathematical, Physical and Engineering Sciences*, 392(1802):45–57, 1984.
- [12] F. E. Low. Bremsstrahlung of Very Low-Energy Quanta in Elementary Particle Collisions. *Phys. Rev.*, 110:974–977, May 1958.

- [13] T. H. Burnett and Norman M. Kroll. Extension of the Low Soft-Photon Theorem. *Phys. Rev. Lett.*, 20:86–88, Jan 1968.
- [14] Yuri L. Dokshitzer. Perturbative QCD for beginners. In *3rd European School of High-energy Physics Dubna, Russia, August 27-September 9, 1995*, pages 59–120, 1995.
- [15] Yuri L. Dokshitzer, Valery A. Khoze, Alfred H. Mueller, and S. I. Troian. *Basics of perturbative QCD*. 1991.
- [16] Yu. L. Dokshitzer and G. Marchesini. Soft gluons at large angles in hadron collisions. *JHEP*, 01:007, 2006.
- [17] L.D. Landau. Fundamental problems. *Proc. Ninth Annual Conf. High Energy Phys. (Kiev 1959)*, page 95, Moscow 1962.
- [18] M.L. Goldberger. Interscience. in the quantum theory of fields. *The 12th Solway Conference Publisher*, New York 1961.
- [19] Geoffrey F. Chew. *S-Matrix Theory of Strong Interactions without Elementary Particles*. *Rev. Mod. Phys.*, 34:394–401, Jul 1962.
- [20] Murray Gell-Mann. The symmetry group of vector and axial vector currents. *Physique Fizika*, 1:63–75, Jul 1964.
- [21] Chen-Ning Yang and Robert L. Mills. Conservation of Isotopic Spin and Isotopic Gauge Invariance. *Phys. Rev.*, 96:191–195, 1954. [,150(1954)].
- [22] R. P. Feynman. Quantum theory of gravitation. *Acta Phys. Polon.*, 24:697–722, 1963. [,272(1963)].
- [23] S. L. Glashow. Partial Symmetries of Weak Interactions. *Nucl. Phys.*, 22:579–588, 1961.
- [24] Steven Weinberg. A Model of Leptons. *Phys. Rev. Lett.*, 19:1264–1266, 1967.
- [25] Abdus Salam and John Clive Ward. Electromagnetic and weak interactions. *Phys. Lett.*, 13:168–171, 1964.
- [26] Abdus Salam. Weak and Electromagnetic Interactions. *Conf. Proc.*, C680519:367–377, 1968.
- [27] F. Englert and R. Brout. Broken Symmetry and the Mass of Gauge Vector Mesons. *Phys. Rev. Lett.*, 13:321–323, 1964. [,157(1964)].
- [28] Peter W. Higgs. Broken Symmetries and the Masses of Gauge Bosons. *Phys. Rev. Lett.*, 13:508–509, 1964. [,160(1964)].
- [29] Murray Gell-Mann and M Levy. The axial vector current in beta decay. *Nuovo Cim.*, 16:705, 1960.
- [30] K. Symanzik. Renormalizable models with simple symmetry breaking. 1. Symmetry breaking by a source term. *Commun. Math. Phys.*, 16:48–80, 1970.

- 
- [31] Jean-Loup Gervais and B. W. Lee. Renormalization of the sigma-model (ii) fermion fields and regularization. *Nucl. Phys.*, B12:627–646, 1969.
- [32] Gerard 't Hooft. Renormalizable Lagrangians for Massive Yang-Mills Fields. *Nucl. Phys.*, B35:167–188, 1971. [,201(1971)].
- [33] M. Breidenbach, J. I. Friedman, H. W. Kendall, E. D. Bloom, D. H. Coward, H. DeStaebler, J. Drees, L. W. Mo, and R. E. Taylor. Observed Behavior of Highly Inelastic Electron-Proton Scattering. *Phys. Rev. Lett.*, 23:935–939, Oct 1969.
- [34] V. S. Vanyashin and M. V. Terentev. The Vacuum Polarization of a Charged Vector Field. *Zh. Eksp. Teor. Fiz.*, 48(2):565–573, 1965. [Sov. Phys. JETP21,no.2,375(1965)].
- [35] I. B. Khriplovich. Green's functions in theories with non-abelian gauge group. *Sov. J. Nucl. Phys.*, 10:235–242, 1969. [Yad. Fiz.10,409(1969)].
- [36] K. G. Wilson and John B. Kogut. The Renormalization group and the epsilon expansion. *Phys. Rept.*, 12:75–200, 1974.
- [37] Vladimir Gribov. QCD at large and short distances (annotated version). *Eur. Phys. J.*, C10:71–90, 1999. [,239(1998)].
- [38] V. N. Gribov. The Theory of quark confinement. *Eur. Phys. J.*, C10:91–105, 1999. [,259(1999)].
- [39] Howard Georgi. Weak interaction - an updated version of my old monograph, 2008.
- [40] Yuri L. Dokshitzer. Lesson 5: Hadron interactions, color and qcd partons at joliot curie, 2013.
- [41] Nestor Armesto. Nuclear shadowing. *J. Phys.*, G32:R367–R394, 2006.
- [42] Kari J. Eskola, Petja Paakkinen, Hannu Paukkunen, and Carlos A. Salgado. EPPS16: Nuclear parton distributions with LHC data. *Eur. Phys. J.*, C77(3):163, 2017.
- [43] Larry D. McLerran and Raju Venugopalan. Computing quark and gluon distribution functions for very large nuclei. *Phys. Rev.*, D49:2233–2241, 1994.
- [44] Javier L. Albacete and Cyrille Marquet. Gluon saturation and initial conditions for relativistic heavy ion collisions. *Prog. Part. Nucl. Phys.*, 76:1–42, 2014.
- [45] Predrag Cvitanovic. *Group theory: Birdtracks, Lie's and exceptional groups*. 2008.
- [46] F. J. Dyson. The Radiation theories of Tomonaga, Schwinger, and Feynman. *Phys. Rev.*, 75:486–502, 1949.
- [47] F. J. Dyson. The S matrix in quantum electrodynamics. *Phys. Rev.*, 75:1736–1755, 1949.
- [48] Stefan Keppeler and Malin Sjodahl. Orthogonal multiplet bases in  $SU(N_c)$  color space. *JHEP*, 09:124, 2012.
- [49] A. P. Yutsis, I. B. Levinson, and V. V. Vanagas. *Mathematical apparatus of the theory of angular momentum*. 1962.

- [50] Florian Cougoulic and Stéphane Peigné. Nuclear  $p_{\perp}$ -broadening of an energetic parton pair. *JHEP*, 05:203, 2018.
- [51] Alfred H. Mueller. Parton saturation: An Overview. In *QCD perspectives on hot and dense matter. Proceedings, NATO Advanced Study Institute, Summer School, Cargese, France, August 6-18, 2001*, pages 45–72, 2001.
- [52] Alfred H. Mueller. Parton saturation at small  $x$  and in large nuclei. *Nucl. Phys.*, B558:285–303, 1999.
- [53] R. Baier, Yuri L. Dokshitzer, Alfred H. Mueller, S. Peigne, and D. Schiff. Radiative energy loss and  $p(T)$  broadening of high-energy partons in nuclei. *Nucl. Phys.*, B484:265–282, 1997.
- [54] Larry D. McLerran and Raju Venugopalan. Fock space distributions, structure functions, higher twists and small  $x$ . *Phys. Rev.*, D59:094002, 1999.
- [55] L. P. Pitaevskii and E.M. Lifshitz. *Physical Kinetics: Volume 10 (Course of Theoretical Physics S)*. Butterworth-Heinemann, 1981.
- [56] B. G. Zakharov. Color randomization of fast gluon-gluon pairs in the quark-gluon plasma. 2018.
- [57] Guido Altarelli and G. Parisi. Asymptotic Freedom in Parton Language. *Nucl. Phys.*, B126:298–318, 1977.
- [58] N. N. Nikolaev, W. Schafer, and B. G. Zakharov. Nonuniversality aspects of nonlinear  $k$ -perpendicular-factorization for hard dijets. *Phys. Rev. Lett.*, 95:221803, 2005.
- [59] N. N. Nikolaev, W. Schafer, B. G. Zakharov, and V. R. Zoller. Nonlinear  $k$ -perpendicular-factorization for quark-gluon dijet production off nuclei. *Phys. Rev.*, D72:034033, 2005.
- [60] N. N. Nikolaev, W. Schafer, and B. G. Zakharov. Nonlinear  $k$ (perpendicular)-factorization for gluon-gluon dijets produced off nuclear targets. *Phys. Rev.*, D72:114018, 2005.
- [61] Cyrille Marquet. Forward inclusive dijet production and azimuthal correlations in  $p(A)$  collisions. *Nucl. Phys.*, A796:41–60, 2007.
- [62] Fabio Dominguez, Cyrille Marquet, Bo-Wen Xiao, and Feng Yuan. Universality of Unintegrated Gluon Distributions at small  $x$ . *Phys. Rev.*, D83:105005, 2011.
- [63] Edmond Iancu and Julien Laidet. Gluon splitting in a shockwave. *Nucl. Phys.*, A916:48–78, 2013.
- [64] Yuri L. Dokshitzer and D. E. Kharzeev. Heavy quark colorimetry of QCD matter. *Phys. Lett.*, B519:199–206, 2001.
- [65] J. J. Aubert, U. Becker, P. J. Biggs, J. Burger, M. Chen, G. Everhart, P. Goldhagen, J. Leong, T. McCorriston, T. G. Rhoades, M. Rohde, Samuel C. C. Ting, Sau Lan Wu, and Y. Y. Lee. Experimental Observation of a Heavy Particle *J. Phys. Rev. Lett.*, 33:1404–1406, Dec 1974.

- 
- [66] J. E. Augustin, A. M. Boyarski, M. Breidenbach, F. Bulos, J. T. Dakin, G. J. Feldman, G. E. Fischer, D. Fryberger, G. Hanson, B. Jean-Marie, R. R. Larsen, V. Lüth, H. L. Lynch, D. Lyon, C. C. Morehouse, J. M. Paterson, M. L. Perl, B. Richter, P. Rapidis, R. F. Schwitters, W. M. Tanenbaum, F. Vannucci, G. S. Abrams, D. Briggs, W. Chinowsky, C. E. Friedberg, G. Goldhaber, R. J. Hollebeek, J. A. Kadyk, B. Lulu, F. Pierre, G. H. Trilling, J. S. Whitaker, J. Wiss, and J. E. Zipse. Discovery of a Narrow Resonance in  $e^+e^-$  Annihilation. *Phys. Rev. Lett.*, 33:1406–1408, Dec 1974.
- [67] Elena G. Ferreira. Quarkonium: a theory overview. In *27th International Conference on Ultrarelativistic Nucleus-Nucleus Collisions (Quark Matter 2018) Venice, Italy, May 14-19, 2018*, 2018.
- [68] Stéphane Peigné and Rodion Kolevatov. Medium-induced soft gluon radiation in forward dijet production in relativistic proton-nucleus collisions. *JHEP*, 01:141, 2015.
- [69] Michael H. Seymour. Symmetry of anomalous dimension matrices for colour evolution of hard scattering processes. *JHEP*, 10:029, 2005.
- [70] Michael H. Seymour and Malin Sjödal. Symmetry of anomalous dimension matrices explained. *JHEP*, 12:066, 2008.
- [71] Judith Alcock-Zeilinger and Heribert Weigert. Compact Hermitian Young Projection Operators. *J. Math. Phys.*, 58(5):051702, 2017.
- [72] M. Abramowitz and I. A. Stegun, editors. *Handbook of Mathematical Functions*. Applied Mathematics Series 55. NBS, Washington, DC, 1964.



- CIS** Collinear and Infrared Safe. 5
- DIS** Deep Inelastic Scattering. 6, 7, 22, 30–32
- DLA** Double Logarithmic Approximation. 84
- dof** degrees of freedom. 1–3, 13, 23, 25, 27, 34, 65, 91
- HERA** Hadron-Electron Ring Accelerator. 7
- ir-frame** inertial reference frame. 1, 2
- irrep** Irreducible representation. 11, 12, 15–17, 20, 38, 40–42, 44, 45, 47–50, 52, 57, 63, 64, 68, 70, 73, 79, 83, 87–90, 92, 93, 95, 97, 98, 100–102, 104, 105, 111–117, 120
- LEP** Large Electron-Positron Collider. 7
- LHC** Large Hadron Collider. 7
- npQCD** non-perturbative QCD. 4, 16
- PDF** parton distribution function. 6, 30–32, 34
- pQCD** perturbative QCD. 4–7, 9, 12, 16, 30, 31, 107, 111
- PT** perturbation Theory. 4, 9, 27, 29, 31, 34
- QCD** Quantum ChromoDynamics. 3–7, 9, 11–13, 15, 17, 19, 22–27, 29–31, 33, 34, 36, 37, 41, 52, 56, 75, 82, 83, 86, 88, 91, 92, 112, 113
- QED** Quantum ElectroDynamics. 3, 4, 7, 15–17, 21–23, 35, 36
- QFT** Quantum Field Theory. 1–3, 21–23, 25
- QM** Quantum Mechanics. 56
- RHIC** Relativistic Heavy Ion Collider. 7



**SLAC** Stanford Linear Accelerator Center. 7, 22

**SMPP** Standard Model of Particule Physics. 1–3

**YD** Young Diagram. 76, 92, 93, 95, 98, 101–104, 106, 111–119

**YT** Young Tableau. 76, 112, 113, 115, 117



**Titre :** Effets nucléaires dans les collisions proton-noyau à haute énergie : élargissement de l'impulsion transverse des systèmes de partons énergétiques et matrices de dimension anormale.

**Mots clés :** pQCD, élargissement de l'impulsion transverse, matrice de dimension anormale.

**Résumé :** Dans le Modèle Standard de la physique des particules, la théorie de l'interaction forte, la chromodynamique quantique (QCD), est une théorie de jauge de groupe de symétrie  $SU(N_c)$  par rapport au nombre quantique de couleur. QCD obéit à la propriété de liberté asymptotique, permettant le calcul d'observables physiques à haute énergie en utilisant la QCD perturbative (pQCD). Cette thèse traite de la description en pQCD des taux de production de hadrons dans les collisions hadroniques à haute énergie, en vue d'applications à la phénoménologie des collisions proton-noyau et noyau-noyau dans les collisionneurs de hadrons (RHIC, LHC), où des effets nucléaires (shadowing, perte d'énergie partonique, élargissement de l'impulsion transverse) entrent en jeu.

Dans une première partie, j'étudie l'élargissement de l'impulsion transverse d'un système de partons énergétiques traversant un noyau, en mettant l'accent sur la structure de couleur du processus. Un cadre théorique basé sur le formalisme des dipôles est utilisé, et une équation cinétique est dérivée pour la distribution en

impulsion transverse de la paire de partons, en demandant que cette paire soit dans un état de couleur donné (représentation irréductible de  $SU(N_c)$ ) à la fois dans l'état initial et dans l'état final. La structure de couleur est codée dans un opérateur d'évolution de couleur, qui est obtenu pour tout type de paire de partons. Pour une paire compacte de petite taille, la dérivation donne une interprétation physique claire du processus d'élargissement de l'impulsion transverse.

Dans une deuxième partie, je discute la matrice de dimension anormale  $\mathcal{Q}$ , qui est formellement analogue à l'opérateur d'évolution précédent, et qui apparaît lors de l'étude du rayonnement de gluons mous associé à une diffusion partonique dure  $2 \rightarrow 2$ . Il a été remarqué que la matrice  $\mathcal{Q}$  associée à  $gg \rightarrow gg$  a une symétrie surprenante (reliant les degrés de liberté externe et interne). J'ai développé des outils pour dériver les matrices  $\mathcal{Q}$  associées à des diffusions  $2 \rightarrow 2$  impliquant des partons généralisés, afin d'explorer si la symétrie observée pour  $gg \rightarrow gg$  est fortuite ou non.

**Title:** Nuclear effects in high-energy proton-nucleus collisions: transverse momentum broadening of energetic parton systems and soft anomalous dimension matrices.

**Keywords:** pQCD, transverse momentum broadening, soft anomalous dimension matrix.

**Abstract:** In the Standard Model of particle physics, the theory of the strong interaction, Quantum Chromodynamics (QCD), is a gauge theory of symmetry group  $SU(N_c)$  with respect to the color quantum number. QCD obeys the property of asymptotic freedom, allowing the computation of high-energy physical observables using perturbative QCD (pQCD). This thesis deals with the pQCD description of hadron production rates in high-energy hadronic collisions, in view of applications to the phenomenology of proton-nucleus and nucleus-nucleus collisions at hadron colliders (RHIC, LHC), where so-called nuclear effects (shadowing, parton energy loss, transverse momentum broadening) come into play.

In a first part, I study the transverse broadening of an energetic parton system crossing a nucleus, putting emphasis on the color structure of the process. A theoretical setup based on the dipole formalism is used, and a kinetic equation is derived for the parton pair

transverse momentum distribution, requiring the parton pair to be in a given color state ( $SU(N_c)$  irreducible representation) both in the initial and final state. The color structure is encoded in a color evolution operator, which is obtained for any type of parton pair. For a small-size compact pair, the derivation yields a transparent physical interpretation of the pair transverse broadening process.

In a second part, I discuss the soft anomalous dimension matrix  $\mathcal{Q}$ , which is formally analogous to the previous evolution operator, and which appears when studying soft gluon radiation associated to  $2 \rightarrow 2$  hard parton scattering. It has been noticed that the  $\mathcal{Q}$ -matrix associated to  $gg \rightarrow gg$  has a surprising symmetry (relating external and internal degrees of freedom). I developed tools to derive the  $\mathcal{Q}$ -matrices associated to  $2 \rightarrow 2$  scatterings involving generalized partons, in order to explore if the symmetry observed for  $gg \rightarrow gg$  is fortuitous or not.